NATIONAL TECHNICAL UNIVERSITY OF ATHENS

SCHOOL OF CIVIL ENGINEERING

DEPARTMENT OF WATER RESOURCES AND ENVIRONMENTAL ENGINEERING

State-of-the-art approach for potential evapotranspiration assessment

Ph.D Thesis

Aristoteles Tegos

Athens, 2019

NATIONAL TECHNICAL UNIVERSITY OF ATHENS

SCHOOL OF CIVIL ENGINEERING

DEPARTMENT OF WATER RESOURCES AND ENVIRONMENTAL ENGINEERING

State-of-the-art approach for potential evapotranspiration assessment

Thesis submitted for the degree of Doctor of Engineering at the National Technical University of Athens

Aristoteles Tegos

Athens, 2019

THESIS COMMITEE

THESIS SUPERVISOR

Demetris Koutsoyiannis, Professor, N.T.U.A

ADVISORY COMMITTEE

1. Demetris Koutsoyiannis, Professor, N.T.U.A (Supervisor)
2. Nikos Mamassis- Associate Professor, N.T.U.A
3. Dr. Konstantine Georgakakos, Sc.D Hydrologic Research Center in San Diego, California- Adjunct Professor, Scripps Institution of Oceanography, University of California San Diego

EVALUATION COMMITTEE

1. Demetris Koutsoyiannis, Professor, N.T.U.A (Supervisor)
2. Nikos Mamassis, Associate Professor, N.T.U.A
3. Dr. Konstantine Georgakakos, Sc.D Hydrologic Research Center in San Diego, California- Adjunct Professor, Scripps Institution of Oceanography, University of California San Diego
4. Evanglelos Baltas, Professor, N.T.U.A
5. Athanasios Loukas, Associate Professor, A.U.Th
6. Stavros Alexandris, Associate Professor, Agricultural University of Athens
7. Nikolaos Malamos, Assistant Professor, University of Patras

Κάποτε υπό άλλη φυσική συνθήκη

και κάτω από άλλη φυσική κατάσταση

Θα συζητήσουμε τις ιδέες μας και θα γελάμε.

Προς το παρόν για σένα Πατέρα

Abstract

The aim of the Ph.D thesis is the foundation of a new temperature-based model since simplified PET estimation proves very useful in absence of a complete data set. In this respect, the Parametric model is presented based on a simplified formulation of the well-established Penman-Monteith expression, which only requires mean daily or monthly temperature data. The model was applied at both global and local regions and the outcomes of this new approach are very encouraging, as indicated by the substantially high validation scores of the proposed approach across all examined data sets. In general, the parametric model outperforms well-established methods of the everyday practice. A second analysis which was examined as part of this thesis is related to which spatial techniques is the optimal in order to transform the point scale estimate in regional. A thorough analysis of different geostatistical model was carried out (Kriging, IDW, NN, BSS) and it can be concluded that the IDW even is the most simplify geostatistical model, it can be produce consistent spatial PET results.

Another part of the thesis was the development of an R function for testing the trend significance of time series. The function calculates the trend significance using a modified Mann- Kendall test, which takes into account the well-known physical behavior of the Hurst-Kolmogorov dynamics. The function is tested in 10 stations in Greece, with approximately 50 years of PET data with the use of a recent parametric model.

Finally, a number of hydrological, agronomist and climatologist applications are presented for lighting the robustness of the new Parametric approach in multidiscipline areas.

Keywords: Potential evapotranspiration; Parametric model; Penman- Monteith method; large scale hydrology, Calibration, Remote Sensing; Spatial analysis; trend; Hurst; R-script; CLIMWAT; CIMIS

Περίληψη

Ο σκοπός της Διδακτορικής Διατριβής υπό τον τίτλο «Σύγχρονο Πλαίσιο Εκτίμησης της Εξατμοδιαπνοής – Αξιοποίηση Υδρολογικής Πληροφορίας και Μοντελοποίηση» είναι η θεμελίωση μιας νέας σχέσης θερμοκρασίας για την εκτίμηση της δυνητικής εξατμοδιαπνοής, καθώς τα απλοποιημένα μοντέλα εκτίμησης είναι εξαιρετικά χρήσιμα σε καθεστώς έλλειψης πρωτογενών δεδομένων. Σε αυτό το πλαίσιο, παρουσιάζεται το Παραμετρικό Μοντέλο που αποτελεί απλοποίηση του καταξιωμένου μοντέλου Penman-Monteith και το οποίο απαιτεί τη μέση ημερήσια θερμοκρασία ή τη μέση μηνιαία θερμοκρασία ως δεδομένο εισόδου. Το μοντέλο εφαρμόστηκε σε παγκόσμιο και σε τοπικό πεδίο και τα αποτελέσματα είναι πολύ ενθαρρυντικά, καθώς συνοδεύεται από μεγάλη αποδοτικότητα σε όλα τα πεδία εφαρμογής του. Γενικά, το παραμετρικό μοντέλο υπερισχύει όλων των εδραιωμένων μοντέλων ακτινοβολίας και διασφαλίζει τη βέλτιστη εκτίμηση της δυνητικής εξατμοδιαπνοής. Ένα δεύτερο επίπεδο μελέτης της παρούσας διατριβής σχετίζεται με το ποιο μοντέλο γεωστατιστικής είναι το βέλτιστο για τη μετατροπή της σημειακής πληροφορίας σε χωρική. Πραγματοποιήθηκε συστηματική μελέτη διαφορετικών τεχνικών γεωγραφικής ολοκλήρωσης και το αποτέλεσμα είναι ότι η μέθοδος Αντιστρόφου Σταθμισμένης Απόστασης είναι η βέλτιστη παρόλο που είναι η απλούστερη από όσες εφαρμόστηκαν.

Άλλο κομμάτι της διατριβής ήταν η ανάπτυξη ενός εργαλείου σε περιβάλλον R για την εκτίμηση των τάσεων σε χρονοσειρές. Η μεθοδολογία εκτιμά τις τάσεις με ένα τροποποιημένο στατιστικό έλεγχο Mann-Kendall λαμβάνοντας υπόψη τη φυσική συμπεριφορά της δυναμικής Hurst-Kolmogorov.

Τέλος, μέσω υδρολογικών, γεωπονικών και κλιματολογικών εφαρμογών αξιολογείται η χρησιμότητα του Παραμετρικού μοντέλου σε διαφορετικά επιστημονικά πεδία.

Keywords: Δυνητική Εξατμοδιαπνοή; Παραμετρικό Μοντέλο; Penman- Monteith μέθοδος; Υδρολογία Μεγάλης Κλίμακας, Βαθμονόμηση; Τηλεπισκόπηση; Χωρική Ανάλυση; Τάση; Hurst; R-script; CLIMWAT; CIMIS

Ευχαριστίες

μας σχέδια, στον Χρήστο Τύραλη για την στρατιωτικά αποδοτική του συνεργασία, στον Δρ. Παναγιώτη Δημητριάδη που είναι καλός αλλά δεν με ακούει ποτέ, στον Παναγιώτη Κοσσιέρη για την ομορφιά του και τον Δρ. Ιωάννη Τσουκαλά για την «ευγενική χορηγία της ευφυΐας του». Τέλος για τη φιλία τους και τη συνεργασία του το Γιάννη Μαρκόνη, το Σίμωνα Παπαλεξίου και το Φοίβο Σαργέντη.

Η εργασία δεν θα ολοκληρώνονταν αν δεν ζούσα στην Ιρλανδία που η καθολική ευγένεια του πληθυσμού της ακόμα και στις καθημερινές μετακινήσεις με το τρένο διαμορφώνουν ένα κατάλληλο περιβάλλον για να δουλέψεις και στις πλέον αντίξοες συνθήκες με την αναγκαία προσήλωση. Ευχαριστώ λοιπόν ανώνυμε Ιρλανδέ και Ιρλανδέζα! Σε αυτό το σημείο να ευχαριστήσω και επωνύμως τους Ιρλανδούς συναδέλφους κ.κ. Dr. Connie O'Driscoll, Dr. Maebh Grace, Dr. Tracey Lydon και Dr. Raymond Brendan για το πρώτο «σκανάρισμα» του διδακτορικού και τις εποικοδομητικές τους παρατηρήσεις.

Από τον επαγγελματικό χώρο των μηχανικών δεν θα ξεχάσω το Δρ. Παναγιώτη- Διονύσιο Παναγόπουλο που λόγω της καθημερινής μας τριβής παλιότερα, μου μετέφερε την αγάπη που πρέπει να έχει ο μηχανικός στην επιστήμη και το νέο. Ακόμη τον νεότερο συνάδερφο Αλέξανδρο Καρανάσιο που η επίβλεψη της διπλωματικής του εργασίας ήταν σημαντικό στοιχείο της παρούσας εργασίας.

Τέλος πολλές ευχαριστίες στην κ. Πηνελόπη Τσίρα για την υπομονή της, την περιποίηση και την αγάπη όλα αυτά τα χρόνια και φυσικά στα παιδιά μας Μαριλένα και Χρήστο που όταν θα έρθει η ώρα θα αποκωδικοποιήσουν με το δικό τους τρόπο τι προσπάθησε να τους κληροδοτήσει ο Πατέρας τους.

Ιρλανδία 2019,

Αριστοτέλης Τέγος

Contents

Table Captions

Figure Captions

1 Introduction

1.1 Overview

Evapotranspiration in all natural shapes (actual, potential) is a key component of the water balance strongly linked with numerous geosciences such as hydrology, agronomy, climatology. The accurate estimation in different time scale is a critical for the above mentioned scientific areas and numerous models have been developed for achieving this challenge.

The main aim of the Ph.D Thesis is the development of a new Parametric PET model. The thesis sections are organized as follows:

Chapter 2 presents an historical overview of the Potential Evapotranspiration definition, modeling principles and its applicability in the water/ geosciences practice.

Chapter 3 presents the global parametric model development including a thorough analysis of the PET key drivers, calibration of the parameters across the globe on calculated Penman-Monteith sample, analysis of the insufficient results of the new model, comparison of the new approach with the well known uncalibrated Hargreaves model and validation of the results in local PET Penman-Monteith samples.

Chapter 4 introduces the new parametric model in a denser agrometeorological network of CIMIS (California) and in meteorological stations of Spain and Germany. The parameters of the models are calibrated in a long sample of Penman- Monteith timeseries and the efficiency of the model for a calibration and validation period is tested. Moreover the comparison of the model with a number of radiation-based (Hargreaves 1975, Jensen-Haise, Mcguiness-Borne) and empirical models (Hargreaves- Samani 1985, Thornthwaite, Blaney- Criddle) was carried out for examining the efficiency of the new approach. Finally, a spatial analysis was made through different geostatististical methods for mapping the parameters, thus for transferring the PET information from local to spatial scale.

Chapter 5 introduces a first attempt for providing PET remote sensing global maps by incorporating the global parametric maps along with remote sensing aerial temperature data. The advantages of the new promising PET remote product is discussed together with some contrsuctive issues with regard to the reliability of the existing PET remote-sensing products.

Chapter 6 presents a R- script tool for quantifying the trend in annual PET series under the well-known scaling hypothesis which is more physically consistent than typical Mann- Kendall test. The usability of this tool is highlighted in hydrological timeseries analysis. It also presents the temperature and PET variability over Greece by using the parametric model for converting a large dataset of temperature in PET.

Chapter 7 introduces two interesting agrometerological applications in Arta Valley, by applying in practice the parametric model in monthly and daily scale and also by investigating alternative geostatistical techniques for the reliable mapping of the PET information.

Chapter 8 summarises the conclusion of the Ph.D thesis works its innovation for different disciplines, unresolved scientific issues and future objectives for further research.

In the **Appendix** the peer-review publications are listed along with detailed citations per article.

1.2   Scientific innovations of the thesis

The major innovative queries examined as part of this Ph.D thesis outlined below:

- Which are the key meteorological drivers for assessing the PET in large areas?

An extended global statistical analysis was carried out for investigating the relationship between PET, mean temperature, radiation, humidity and wind velocity. PET is strongly correlated with mean temperature and radiation but in some cases the humidity and velocity could improve the reliability of the PET estimate.

- Given the high data demanding dataset for estimating the reliability of PET, can we introduce parsimony and physical constraints for its quantification?

The major peer review publications as part of the thesis outcomes are available which represent: a) The global parametric model in a sample of 4088 FAO stations and b) The development of the parametric model in the CIMIS network in California.

- What is the main benefit of the new parametric model against the other radiation or temperature-based methods?

It is resulted that the performance of the new model is satisfactorily outperforming all the other radiation- based methods or temperature methods that have been applied. Specifically, the new parametric model is preferable to the most well-known temperature-based method which is the Hargeaves-Samani.

- Which is the optimal geostatistical model for transferring the local PET estimate in spatial scale?

A typical problem in engineering hydrology is the conversion of the points estimate to spatial information. Therefore a number of the geostatistical tools (IDW, Kriging, NN, BSS) were compared in order to find out the most applicable model in representing the PET in spatial scale. IDW the most simplistic, seems to be the optimal model.

- What are the changes of annual PET and how can we quantify the trend?

An R-script had been developed in order to investigate the annual PET trends under the scaling hypotheses which, given the ubiquitous presence in meteorological timeseries, have physical constraints.

- Which are the practical uses of a new PET model in the area of hydrological and agronomic engineering?

A number of innovative case studies have outlined the usability of the new parsimonious PET model. Specifically, the use of the model in the quick and reliable conversion of the mean temperature in PET estimates and the study of the long term changes and its usability in agronomic applications.

- What are the major incidental contributions and moderate innovations of this thesis?

During the development of the global parametric model in a limited number of areas, an influence of the humidity and/or the velocity had been detected and therefore more meteorological timeseries and more explanatory variables (humidity and/or velocity) are required for developing more robust PET expressions.

2 Overview of PET models

2.1   The potential evapotranspiration process

Potential evapotranspiration (PET) is key input in water resources, agricultural and environmental modelling. For many decades, numerous approaches have been proposed for the consistent estimation of PET at several time scales of interest. Accurate estimation of evapotranspiration has gained scientific interest due to high importance in hydrological modelling, irrigation planning and water resources management. According to Farquhar and Roderick (2007), changes in evaporative demand affect fresh water supplies and have impact on agriculture, the biggest consumer of fresh water.

Evaporation can be viewed both as energy (heat) exchange and an aerodynamic process. According to the energy balance approach, the net radiation at the Earth's surface Rn is mainly transformed to latent heat flux, Λ, and sensible heat flux to the air, H.

The evaporation rate, expressed in terms of mass per unit area and time (e.g. kg/m^2/d), is given by the ratio $E' := \Lambda / \lambda$, where λ is the latent heat of vaporization, with typical value 2460 kJ/kg. By ignoring fluxes of lower importance, such as soil heat flux, the heat balance equation is solved for evaporation, yielding:

$$E' = \frac{(Rn - H)}{\lambda} = \frac{Rn}{\lambda(1+b)} \qquad (1)$$

where b := H / Λ is the co-called Bowen ratio. The estimation of b requires the measurement of temperature at two levels (surface and atmosphere), as well as the measurement of humidity at the atmosphere. On the other hand, the estimation of the net radiation Rn is based on a radiance balance approach to determine the components Sn (Net short wave radiation) and Ln (Net long wave radiation). Typical input data required (in addition to latitude and time of the year), are solar radiation (direct and diffuse, or, in absence of them, sunshine duration data or cloud cover observations), temperature and relative humidity. The net radiation also depends of surface properties (i.e. albedo) and topographical characteristics, in terms of slope, aspect and shadowing. From the aerodynamic viewpoint, evaporation is a mass diffusion process. In this context, the rate of evaporation is related to the difference in the water vapor content of the air at two levels above the evaporating surface and a function of the wind speed F(u) in the diffusion equation. Theoretically, F(u) can be computed on the basis of elevation, wind velocity, aerodynamic resistance and temperature. Yet, for simplicity it is usually given by empirical formulas, derived through linear regression, for a standard measurement level of 2 meters. Penman (Penman, 1948) combined the energy balance with the mass transfer approaches, thus allowing the use of temperature, humidity and wind speed measurements at a single elevation. His classical formula for computing evaporation from an open water surface is written as:

$$E' = \frac{\Delta}{\Delta+\gamma} \frac{Rn}{\lambda} + \frac{\gamma}{\Delta+\gamma} F(u)D \qquad (2)$$

where Δ is the slope of saturated vapor pressure/temperature curve at equilibrium temperature (hPa/K), γ is a psychrometrcic coefficient, with typical value 0.67 hPa/K, and D is the vapor pressure deficit of the air (hPa), defined as the difference between the saturation vapor pressure es and the actual vapor pressure ea, which are functions of temperature and relative humidity. We remind that estimates the evaporation rate (mass per unit area per day), which is expressed in terms of equivalent evaporation of water by dividing by the water density ρ (1000 kg/m³).

Penman's method was extended to cropped surfaces, by accounting for various resistance factors, aerodynamic and surface. As mentioned in the introduction, Monteith introduced the concept of the so-called "bulk" surface resistance that describes the resistance of vapor flow through the transpiring crop and evaporating soil surface.

It is therefore the Penman-Monteith formula (Monteith 1965, Monteith 1981) most recognized globally, which is yet difficult to apply in data-scarce areas, since it requires simultaneous observations of four meteorological variables (temperature, net duration, relative humidity, wind velocity). For this reason, parsimonious models with minimum input data requirements are strongly preferred. Typically, these have been developed and tested for specific hydroclimatic conditions, but when they are applied in different regimes they provide much less reliable (and in some cases misleading) estimates. Therefore, it is essential to develop generic methods that remain parsimonious, in terms of input data and parameterization and this is part of this Ph.D thesis.

2.2 Historical overview of PET modelling

2.2.1 General

The accurate estimation of evapotranspiration has a great importance in hydrological modeling, irrigation planning and water resources management.

Figure 1 presents the historical milestones in developing evapotraspiration definition and physical modelling focusing in the two last centuries.
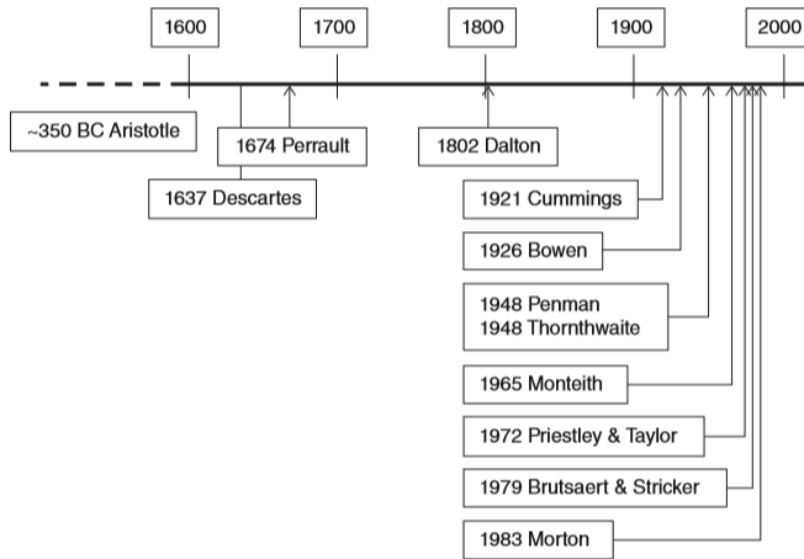
Figure 1. PET definitions milestones as presented in McMahon *et al.* 2016

The starting point was the first "common-sense" definitions introducing by Aristotle (Koutsoyiannis *et al.* 2007). His views in this fundamental work "Meterologika" encompasses a clear understanding for the phase change of water and the energy exchange. He referred that "… the sun causes the moisture to rise; this is similar to what happens when water is heated by fire" (Meteorologica, II.2, 355a 15). "… the vapour that is cooled, because of lack of heat in the area where it lies, condenses and turns from air into water; and after the water has formed in this way it falls down again to the earth" (ibid., I.9, 346b 30). Later Perrault (1611–1680) is credited with having made the first experimental measurement of evaporation, though in fact what he measured was sublimation by recording the loss of weight of a block of ice through time. The first direct measurement of the evaporation of liquid water was carried out by Edmund Halley in 1686 when he measured the loss of water from a heated pan. Surprisingly, Halley appears not to understand that the temperature is good predictor and key driver of evaporation loss as shown in Figure 2.
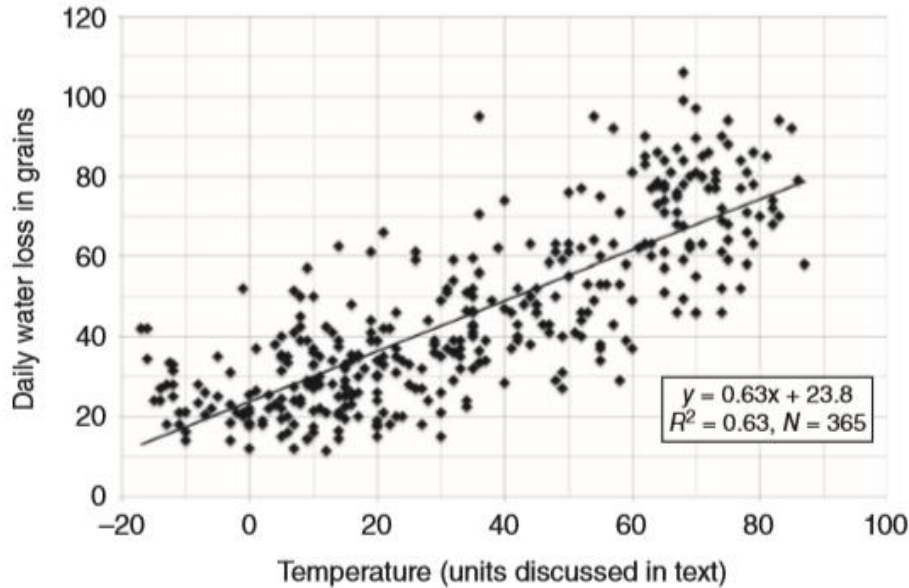
Figure 2. Evaporation vs temperature plot from Halley's experiment (source McMahon *et al.* 2016)

Dalton has become universally recognized as one of the foreseen scientist in the development of evaporation theory since he referred that "*the evaporating force must be universally equal to that of the temperature of the water, diminished by that already existing in the atmosphere".* The water existing in the atmosphere he refers to as the *'force of the vapour,'* effectively relative humidity. After Dalton's contribution in explaining evaporation as a physical phenomenon, Penman and Monteith later introduced the most recognized physical approaches until nowadays and more informatios are presented later herein.

More than 50 important evapotranspiration models can be found in literature (Lu *et al.*, 2005, McMahon *et al.* 2013) which can be grouped into seven categories: (i) empirical, (ii) water budget (iii) energy budget, (iv) mass transfer, (v) combination, (vi) radiation and (vii) measurement (Xu and Singh, 2000).

The recently review work by McMahon *et al.* 2016 has identified a total number of 166 models categorizing into six classes (Table 1): potential evaporation, reference evaporation, actual evaporation in terrestrial environments, open-water evaporation, deep lakes, and pan evaporation. The models therein are further typed into the following 10 classes: models based on mass-transfer (so-called Dalton equation), temperature models, radiation-temperature models, energy balance methods, single-source (vegetation, soil, or water) combination methods, multisource combination methods, multivariate models, models based on the Complementary Relationship, Budyko-like models, and miscellaneous models.

Table 1. Distribution and types of applications of 166 PET models (source: McMahon *et al.* 2016)

Model type	Application						Percentage of Total Models
	Potential	Reference crop	Actual	Open-water	Lakes/Storage	Pan	
Mass-transfer	0	0	1	55	0	2	34.9
Temperature	5	2	0	1	0	0	4.8
Radiation-temperature	7	8	2	5	0	1	13.9
Energy balance	0	0	0	0	3	0	1.8
Combination-single source	7	9	7	4	6	2	21.1
Combination-multisource	0	0	8	0	0	0	4.8
Multivariate	0	1	1	0	0	3	3.0
Models based on CR	0	0	7	1	1	0	5.4
Budyko-like	0	0	7	0	0	0	4.2
Miscellaneous	3	0	1	4	1	1	6.0
Percentage of total models	13.3	12.0	20.5	42.2	6.6	5.4	100

The variety of models and frameworks is related to the complexity of the natural phenomenon and depends on the wide range of input climate data and local climate conditions. The Penman-Monteith formulation (Monteith, 1981) for computing potential ET proposed from FAO as standardized method (Allen *et al.*, 1998) That method had numerous successful applications in the fields of hydrology and agrometeorology and in a variety of hydroclimatic regimes (Wang and Georgakakos, 2007). Basic disadvantage of Penman–Monteith model is the simultaneous requirement of several meteorological data as temperature, wind speed, relative humidity and sunshine measures. Such measurements are not always easily available or accessible to researchers due to the sparse hydrometeorological stations networks in several regions, e.g. Africa, as well as the instability in the records of radiation and relative humidity (Samani, 2000).

The interdependence of these meteorological parameters and their variability in space and time, lead in difficulties to formulate an equation that can be used to estimate ET from various crops under different climate conditions (Temesgen *et al.*, 2005). Notably, the difficulties due the sparse hydrometeorological networks in several regions like Africa and the instability in the records of radiation and relative humidity (Samani, 2000) reveals the demand of new simplifies models. Therefore, the demand of new simplified models in several time scales (Alexandris and Kerkides 2003, Oudin *et al.* 2005, Valiantzas, 2013,) like radiation-based and temperature-based models (Valiantzas 2006, Valiantzas, 2013), is justified.

2.2.2 Radiation-based models

As already clarified above, the complexity of the Penman–Monteith method stimulated many researchers to seek for alternative, simplified expressions, based on limited and easily accessible meteorological data. Given that the main sources of variability in evapotranspiration are temperature and solar radiation, the two variables are introduced in a number of such models, typically referred as radiation-based. It is noted that from numerous publications Tabari (2010) and Samaras *et al.* (2014) demonstrated that radiation-based methods are more powerful models for the ET estimation.

A well-known simplification is the Priestley–Taylor formula which is expressed in terms of equivalent depth, i.e. mm/d:

$$E = a_e \frac{\Delta}{\Delta+\gamma} \frac{R_n}{\lambda\rho} \qquad\qquad (3)$$

Where a_e is a numerical coefficient, with values from 1.26 to 1.28. In the original model, the energy term of the Penman–Monteith equation is increased by about 30%, in order to skip over the aerodynamic term. This assumption allows for omitting the usage of wind velocity and surface resistance in evapotranspiration calculations.

Another radiation-based models have been identified within the literature are the Hargreaves (Hargeaves 1985), Turc (Turc 1961), Jensen–Haise (Jensen and Haise 1963), Stephens– Stewart-P (Stephens and Stewart 1693) , Priestley–Taylor (Priestly and Taylor 1972), Makkink–Hansen (Hanses 1984) and Makkink (Makking 1957)

2.2.3 The value of the calibrated radiation- based PET models

Many researchers suggest the need for further model calibration in the radation-based models (especially in the energy term of radiation) to improve the overall efficiency (Irmak et al. 2003, Zhai L. et al. 2010, Azhar and Perera 2010, Thepadia and Martinez 2012, Tabari and Talalee 2011, Drooger and Allen 2002).

Specifically, Tabari and Talalee (2011) calibrated Hargreaves and Priestley-Taylor models on the basis of the PMF-56 method in arid and cold climates of Iran using data from 12 stations during 1994–2005. After Hargreaves calibration model, the average value of the adjusted coefficient for arid climate was 0.0031, which is about 34% higher than the original value (0.0023). Similarly, the average value of the new Hargreaves coefficient for cold climate was 0.0028, which is about 22% higher than the original value. The results showed that the original Priestley-Taylor coefficient of 1.26 was very low for the climatic regions, and the new Priestley-Taylor coefficients of 1.82 and 2.14 have the best fit as compared with the PMF-56 method in cold and arid climates, respectively. Overall, calibration of the Hargreaves and Priestley-Taylor equations resulted in improvements of the equations by reducing the errors of the ETo estimates.

Drooger and Allen (2002) modified the original Hargreaves method to a Modified-Hargreaves(MH) method by including a rainfall term improved ET0 estimates significantly for arid regions globally.

Monthly values of ET0 using PM were compared to values obtained using HG. They showed that the annual average difference between PM and HG. HG tends to underestimate PM largely in the very dry regions and to overestimate PM in the very wet regions

2.2.4 PET impacts in hydrological modelling

The majority of rainfall-runoff models at a daily or monthly time step require as input an estimate of potential evapotranspiration in order to compute actual evapotranspiration (Mcmahon *et al*. 2013). The generic mathematical description in this regard is:

$$ET_{Act} = f(SM, ET_{PET}) \qquad (4)$$

Where ET_{Act} is the estimated actual daily evapotranspiration (mmday^{-1}), SM is a proxy soil moisture level for the given day (mm) and ET_{PET} is the daily potential evaporation (mmday^{-1}). Due to local climatic conditions especially in arid catchments actual evapotranspiration is limited by soil moisture with the potential evapotranspiration becoming more important in wet catchments where soil moisture is not limiting.

Seiller and Anctil (2016) were assessed the performance of the hydrological modeling under observed and projected climate conditions on natural catchments in Canada and Germany by using as input twenty-four potential evapotranspiration formulas (Penman, Penman-Monteith, FAO56 P-M, Priestley- Taylor, Kimberly-Penman, Thom-Oliver, Thornthwaite, Blaney and Criddley, Hamon, Romanenko, Linacre, MOHYSE, HSAMI, Kharrufa, Wendling – WASim, Turc, Jensen and Haise , McGuinness and Bordne, Hargreaves and Samani, Doorenbos and Pruit, Abtew, Makkink, Oudin, Baier and Robertson).

 The 24 PET formulas produced large dissimilarities in the estimated PET in terms of quantity and shape. Conclusively, the combinational formulas proposed very similar shape and quantity, temperature-based formulas produced the largest spectrum of quantity and the Radiation-based formulas fell somewhere in between the other two classes namely combinational and temperature-based. These differences affected in several ways the resulting simulated discharge time series. Overall, the authors concluded that it was difficult to identify an ultimate PET formula for a hydrological modelling point of view, but it could be recommended avoiding temperature-based Blaney and Criddley and MOHYSE.

Another one critical outcome was the results showed that spread of the hydrological response was smaller for the combinational formulas than for temperature-based and radiation-based equations, revealing a higher stability of these combinational formulas.

Birhanu *et al.* (2018) were applied five hydrological models of increasing complexity (GR4J, SIMHUD, CAT, TANK, SAC-SMA) by inputting 12 Potential Evapotranspiration (Abtew, Blaney-Criddle, Chapman Australian, Granger Gray, Hamon, Hargeaves-Samani, Makkink, Matt Shuttleworth, Penman, Penman- Monteith, Priestley-Taylor, Turc) estimation methods of different input-data requirements in order to assess their effect on model performance, optimized parameters and robustness. The study area located over a set of 10 catchments in South Korea.

The main outcomes of the study outlined below:

- The hydrological models' performance was satisfactory for each PET input in the calibration and validation periods for all of the tested catchments.
- The hydrological models performances were found to be insensitive to the 12 PET.
- Identical behavioural similarities and Dimensionless Bias were observed in all of the tested catchments.
- For the hydrological models, lack of robustness and higher dimensionless Bias were found for high and low flow as well as for the Hamon PET input.

10

- The complexity of the hydrological models structure and the PET estimation methods did not necessarily enhance model performance and robustness.
- The model performance and robustness were found to be mainly dependent on extreme hydrological conditions, including high and low flow, rather than complexity;
- The simplest hydrological model and PET estimation method could perform better if reliable hydro-meteorological datasets are applied.

2.2.5 Outstanding issues

According to the fundamental work by Mcmahon *et al.* 2013 a number of issues regarding the evapotranspiration are still outstanding and outlined below:

- Hard-wired potential evaporation estimates at AWSs; The authors stated that: *"Some commercially available AWSs, in addition to providing values of the standard climate variables, output an estimate of Penman evaporation or Penman–Monteith evaporation. For practitioners, this will probably be the data of choice rather than recomputing Penman or Penman–Monteith evaporation estimates from basic principles. However, users need to understand the methodology adopted and check the values of the parameters and functions (e.g. albedo, wind function, ra and rs) used in the AWS evaporation computation"*
- Estimating evaporation without wind data; Authors mentioned that "*Many countries do not have access to historical wind data to compute potential evaporation*"
- Estimating evaporation without at-site data; The authors mentioned that "*Where at-site meteorological or pan evaporation data are unavailable, it is recommended that evaporation estimates be based on data from a nearby weather station that is considered to have similar climate and surrounding vegetation conditions to the site in question*".
- Dealing with a climate change environment: increasing annual air temperature but decreasing pan evaporation rates;
- Daily meteorological data average over 24h or day-light hours only; The authors stated that "*An issue that arose during this project relates to whether or not daily meteorological data used in evaporation equations should be averaged over a 24h daily period or averaged during daylight hours when evaporation is mainly, but not only*"
- Uncertainty in evaporation estimates. The authors refers that "*We describe several models for estimating actual and potential evaporation. These models vary in complexity and in data requirements. In selecting an appropriate model, analysts should consider the uncertainty in alternative methods.*"

In this PhD thesis the majority of the above mentioned critical points are considered in order to introduce new insights in the PET assessment.

3 Global Parametric model development

The need of parsimonious model structure is essential in several fields of water resources sciences (Koutsoyiannis, 2009; Koutsoyiannis, 2014). This refers both to the model structure and to the input data, which should be easily available. Most of simplified formulas fail to describe the phenomenon of evapotranspiration due to its high complexity and the varying local climate conditions. Thus, the idea of replacing some variables and constants used in the standard Penman-Monteith (PM) formula by a number of parameters which are regionally varying and estimated through calibration from a reference evapotranspiration sample, constitutes a new appealing strategy for evapotranspiration estimation.

3.1 Introduction

Evaporation, which is an overall term covering all processes in which liquid water is transferred as water vapour to the atmosphere—definition already provided by ancient Greek philosophers (Koutsoyiannis *et al*. 2007)—is crucial element of multiple disciplines and an essential input of hydrological modelling, water resources management, irrigation planning, and climatological studies. Numerous efforts are reported in the literature, presenting different expressions of evaporation (including actual, potential, reference crop, and pan evaporation), based on different types of data. McMahon *et al*. (2013, 2016) provide a major discussion of the background theory and definitions, as well as a critical assessment of the models developed so far.

Here, the concept of potential evapotranspiration, PET is highlighted, which is a theoretical quantity considered as "the rate at which evapotranspiration would occur from a large area completely and uniformly covered with growing vegetation, which has access to an unlimited supply of soil water, and without advection or heating effects" (Dingman, 1994). Since PET depends on soil properties, a better defined term is the so-called reference crop evapotranspiration, introduced by Doorenbos and Pruitt (1977), and typically denoted as ET_0, which refers to the evapotranspiration from a standardized vegetated surface (i.e., actively growing and completely shading grass of 0.12 m height, surface resistance 70 s m^{-1}, and albedo = 0.23). The globally accepted method for consistent estimation of PET is the Penman-Monteith (herein referred to as PM) equation, as formalized by the Food and Agriculture Organization (FAO), which is physically-based, and is therefore used as standard for comparisons with other, more simple approaches (Allen *et al.* 1989). The major drawback for the generalized application of the PM method worldwide is the need of simultaneous measurements of four meteorological variables (air temperature, wind speed, relative humidity, and net radiation or, alternatively, sunshine duration), at the desirable spatial and temporal resolution.

To overcome the data requirements of the PM formula, a number of alternative approaches have been developed, which are typically classified into temperature-based and radiation-based; the former use only temperature observations, which are dense and easily accessible, while the latter also use values of extraterrestrial radiation (which is, in fact, periodic function of latitude and day of

12

the year). For many decades, such approaches have been widely applied for PET modelling worldwide using the standard "literature" values of the parameters involved in their governing equations. However, since these have been developed for specific studies, locations, and climatic conditions (Xu and Singh, 2001), their applicability outside of these distinct conditions usually result in unreliable predictions, introducing significant bias in PET estimations. For this reason, and particularly in the last years, significant attention is payed to local calibrations of empirical PET models, either by using direct PET observations at the field scale (e.g., lysimeter measurements) and/or against simulated PET data, provided by the PM formula. One of the first attempts is reported by Allen and Pruit (1986), who calibrated and validated the Blaney-Criddle model against PM data, using local wind function and taking advantage of daily lysimeter measurements of alfalfa evapotranspiration. Similar calibration approaches were employed for all of the widespread PET formulas, such as the Thornthwaite, Blaney-Criddle and Priestley-Taylor (e.g., Amatya *et al.*, 1995; Mohawesh, 2010; Sentelhas *et al.*, 2010), and other empirical expressions as well (e.g., Oudin *et al.*, 2005). Many recent publications also focus on the re-evaluation of the sole parameter of the Hargreaves equation against regional data, for a range of climatic regimes (Gavilán et al., 2006; Fooladmand and Haghighat, 2007; Tabari and Talaee, 2011; Hu *et al.,* 2011; Haslinger and Bartsch, 2016).

Although the spatial resolution and accuracy of meteorological data over the extended areas of the globe is not sufficient, current advances in remote sensing technologies allowed quite reliable estimations of PET by combining satellite and ground information (Choudhury, 1997). Since gridded data of meteorological inputs and canopy characteristics is now easily accessible, several researchers employed PET estimations at large spatial scales, up to global (Allen *et al.*, 2007; 2011; Mu *et al.*, 2007; 2011), by employing scaling and interpolation techniques of varying physical complexity (Vinukollu *et al.* 2011).

Tegos et al. (2013; 2015) calibrated a simplified radiation-based expression of the PM formula, using monthly meteorological data from a large number of stations over Greece and California, respectively. In both areas, the proposed formula, which contains either three or two free parameters, clearly outperformed other widely used methods, such as Hargreaves and Samani (1985), Oudin *et al.* (2005), and Jensen and Haise (1963), as modified by McGuinness and Bordne (1972). Malamos *et al.* (2015) also employed the parametric model at the daily scale, in the context of PET mapping over the irrigated plain of Arta, Western Greece.

In the following chapters, the simplified (i.e. with two parameters) expression of the aforementioned model over the globe is presented, by inferring its parameters through calibration against given Penman-Monteith values (next referred to as reference PET or ET_0). The meteorological inputs and ET_0 data are retrieved by the FAO CLIMWAT database that provides monthly climatic information at 4300 locations worldwide. A preliminary analysis of these data allowed explaining the major drivers of PET over the globe and across seasons. An extended analysis of the model inputs and outputs was performed, including the production of global maps of optimized model parameters and associated performance metrics, as well as comparisons with a widely known formula by Hargreaves and Samani (1985). Finally, the interpolated values of the

optimized parameter values to validate the predictive capacity of the model against detailed meteorological data was used, in terms of monthly time series, at several stations worldwide. The results are very encouraging, since even with the use of abstract climatic information for its calibration, the model generally ensures very reliable PET estimations. However, we have detected few cases where the model systematically fails to reproduce the reference PET, particularly across tropical areas. Except for these specific areas, the parameter estimations through the derived maps can be directly employed within the proposed formula, at both point and regional scales.

3.1.1 Theoretical Background

The Penman-Monteith Equation

The Penman-Monteith equation for estimating potential evapotranspiration from a vegetated surface, as formalized by Allen et al. (1998), is:

$$\text{PET} = \frac{1}{\lambda} \frac{\Delta(R_n - G) + \rho_a c_a (v_a^* - v_a)/r_a}{\Delta + \gamma(1 + {r_s}/{r_a})} \tag{5}$$

where PET is the daily potential evapotranspiration (mm d^{-1}); R_n is the net incoming daily radiation at the vegetated surface (MJ m^{-2} d^{-1}); G is the soil heat flux (MJ m^{-2} d^{-1}); ρ_a is the mean air density at constant pressure (kg m^{-3}); c_a is the specific heat of the air (MJ kg^{-1} °C^{-1}); r_a is an aerodynamic or atmospheric resistance to water vapour transport for neutral conditions of stability (s m^{-1}); r_s is a surface resistance term (s m^{-1}); $v_a^* - v_a$ is the vapour pressure deficit of the air (kPa), defined as the difference between the saturation vapour pressure v_a^* and the actual vapour pressure v_a; λ is the latent heat of vaporization (MJ kg^{-1}); Δ is the slope of the saturation vapour pressure curve at specific air temperature (kPa °C^{-1}); and, γ is the psychrometric constant (kPa °C^{-1}). Given that the typical time scale of the PM equation is daily, all of the associated fluxes are expressed in daily or mean daily units.

The original Penman equation does not include the soil heat flux term, G, since Penman noted that, in his experiments, its impact in the energy balance was less than 2% (Ward and Robinson 1990). Nevertheless, evaporation estimations are sensitive to G only when there is a large difference between successive daily temperatures (McMahon *et al.*, 2013). In this respect, in most of practical applications this flux is not accounted for, thus leaving the net incoming daily radiation, R_n, as the sole energy term to be assessed; the latter is defined as the difference between incoming and outgoing radiation of short and long wavelengths.

Apart from the site location, expressed in terms of latitude, φ, the PM equation requires air temperature, relative humidity, solar radiation, and wind speed data for calculating the model's variables. FAO provides detailed guidelines for the cases of proxy or missing meteorological information. A typical example is the determination of solar radiation from measured duration of sunshine or cloud cover. Moreover, FAO suggests using average daily maximum and minimum air temperatures, instead of mean daily temperature, to represent more accurately the non-linearity of

the saturation vapour pressure – temperature relationship. If fact, the use of mean air temperature yields a lower saturation vapour pressure v_a^*, and hence a lower vapour pressure difference $v_a^* - v_a$, and lower reference evapotranspiration estimates (Allen *et al.*, 1998).

3.1.2 The Parametric Formula

The parametric model, initially proposed by Koutsoyiannis and Xanthopoulos (1999), and then formalized and implemented by Tegos *et al.* [2009; 2013; 2015a; 2015b], provides PET estimates through calibration based on given PET data. The model performance was satisfying as the proposed framework provides consistent monthly PET estimates at point and especially at the regional scale. The most recent application was the daily and monthly implementation of the model for the PET mapping in an irrigated plain of Greece (Malamos *et al.*, 2015) and the investigation of trend analysis in Greece through the development of an R-script tool (Tegos *et al.*, 2015).

The mathematical expression of the parametric model, which is applicable to different time scale from daily to monthly, is the following:

$$\text{PET} = \frac{aR_a + b}{1 - cT} \tag{6}$$

where PET is the potential evapotranspiration in mm, R_a (MJm^{-2}d^{-1}) is the extraterrestrial radiation, T (°C) is the mean air temperature, and a (kg kJ^{-1}), b (kg m^{-2}), and c (°C^{-1}) are model parameters that should be inferred through calibration, against "reference" PET data, either modelled or measured. From a macroscopic point-of-view, the above parameterization has some physical correspondence to the PM equation, since the product $a\,R_a$ represents the overall energy term (i.e., incoming minus outgoing solar radiation), parameter b represents the missing aerodynamic term, while quantity $(1 - c\,T)$ is an approximation of the denominator term of the PM formula (Tegos *et al.*, 2013).

The above equation uses two explanatory variables, namely extraterrestrial radiation, R_a, and temperature, T, and thus it belongs to the so-called radiation-based approaches. The extraterrestrial radiation, defined as the solar radiation received at the top of the Earth's atmosphere on a horizontal surface, is an astronomic variable, given by:

$$R_a = \frac{24(60)}{\pi} G_{\text{sc}} d_{\text{r}} [\omega_s \sin(\varphi) \sin(\delta) + \cos(\varphi) \cos(d) \sin(\omega_s)] \tag{7}$$

where G_{sc} is the solar constant, with typical value 82 kJ m^{-2} min^{-1}, d_{r} is the inverse relative distance of the Earth from the Sun, ω_s (rad) is the sunset hour angle, φ is the latitude (rad), and δ is the solar declination (rad). Variables d_{r} and δ are periodic functions of time, while ω_s is function of latitude and time. For details on computing the above astronomic variables, the reader may refer to the literature (e.g., McMahon *et al.*, 2016).

While for a given location the extraterrestrial radiation is a highly regular and fully predictable variable, thus only explaining the periodicity of PET, temperature exhibits quite irregular variability, thus explaining the fluctuations of PET, which is key component of the changing

hydrological cycle, at all temporal scales, from daily to annual and even larger ones, i.e. overannual (Koutsoyiannis, 2013). Following FAO recommendations, the advantage from minimum and maximum daily temperature data was taken, thus estimating the temperature term by the average:

$$T = (T_{\min} + T_{\max})/2 \tag{8}$$

This expression may be particularly useful in cases when records of mean daily temperature are missing, while average minimum ($T_{\min}$) and maximum temperature ($T_{\max}$) values are available.

3.1.3 Modified Parametric Model

It is well-known that the variability of daily and, even more, monthly PET is relatively small, if compared to other hydrometeorological variables, such as precipitation and runoff. For this reason, when attempting to estimate the model parameters *a, b*, and *c* through calibration, it is quite easy to achieve very high values of goodness-of-fitting criteria (e.g. efficiency), through combinations of parameter values that do not have physical sense. Additional uncertainty arises when the actual PET data is little informative to support the inference of the three parameters, e.g. due to limited length of associated meteorological data. In this respect, to avoid uncertainties due to "blind" calibration approaches or overfitting (Efstratiadis and Koutsoyiannis, 2010), we propose using the more parsimonious expression (also considering the minimum and maximum temperature, instead of the mean daily one):

$$\text{PET} = \frac{a'\, R_a}{1 - c'\, (T_{\min} + T_{\max})/2} \tag{9}$$

which contains two instead of three parameters (parameter *a′* in the numerator and parameter *c′* in the denominator). Apparently, in the context of a calibration exercise using alternative expressions (6) and (7), the optimized values of *c* and *c′* should be different.

The modified parameterization of the above equation resembles the well-known approach by Priestley and Taylor (1972), who developed a PET formula based on the original PM equation, but without the aerodynamic component; the latter was indirectly accounted by increasing the energy term by a factor of 1.26. For simplicity, this factor is generally considered as constant; however, several researchers have demonstrated that this exhibits quite significant seasonal and spatial variability (McMahon *et al*. 2013).

3.1.4 The CLIMWAT Database: Preliminary Analysis

Database Overview

The CLIMWAT 2.0 database is a joint initiative by the Water Development and Management Unit and the Climate Change and Bioenergy Unit of FAO (1993), which provides average monthly climatic data at 4300 stations (Figure 3, blue points), well-distributed worldwide. These data include monthly mean values of mean daily maximum and minimum temperature (°C), daily relative humidity (%), wind speed (km day^{-1}), daily sunshine duration (h), daily solar radiation

(MJ/m^2), monthly rainfall, gross and effective (mm), as well as mean monthly ET$_0$ estimations through the Penman-Monteith formula.

The exceptionally large sample of climatic data allows for extracting useful conclusions about the major drivers of PET over the globe. In this context, a comprehensive statistical analysis of reference PET data against the available meteorological variables, at both the annual and monthly scales was made.
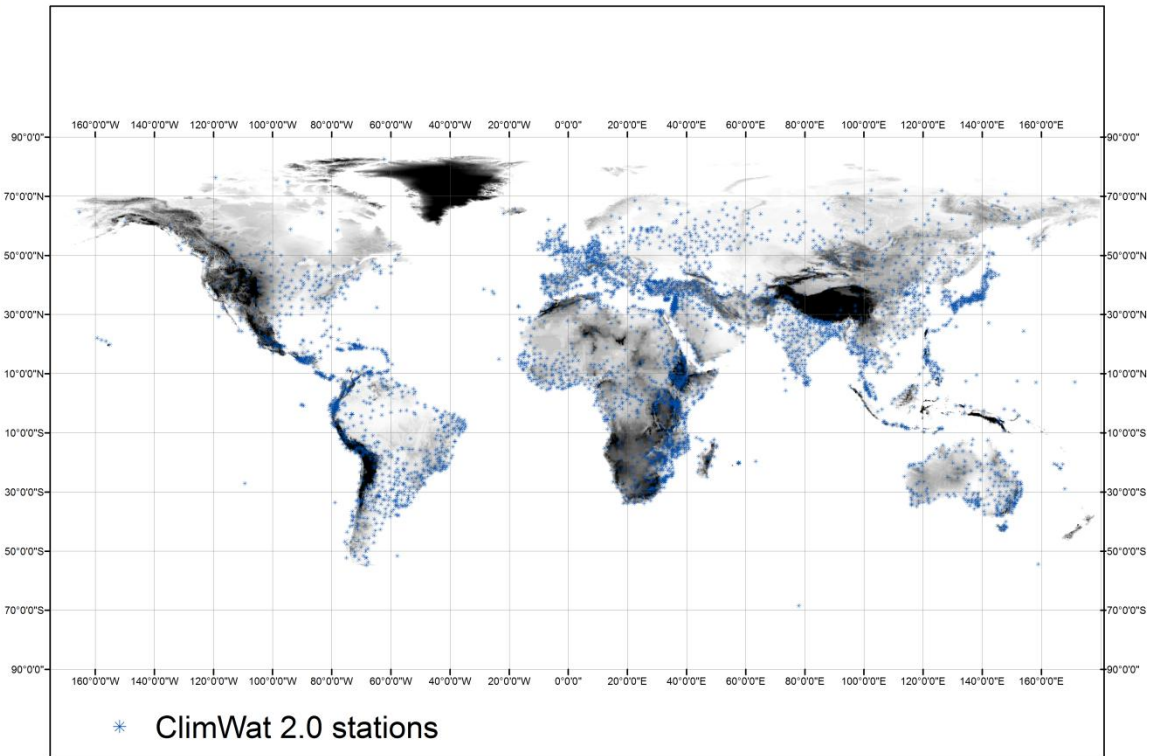
Figure 3. Food and Agriculture Organization (FAO CLIMWAT) hydrometeorological network (dark areas indicate high altitudes).

Which Meteorological Drivers Explain Mean Annual PET over the Globe?

In order to answer this question, the reference PET (i.e. ET$_0$) data against the four meteorological variables that are embedded in the Penman-Monteith equation was plotted, i.e. solar radiation, mean temperature estimated from Equation (7), relative humidity and wind speed, at the annual scale, and fitted the most suitable regression model.

Figure 4 illustrates that mean annual ET$_0$ over the globe is highly correlated with mean annual solar radiation and temperature, particularly when considering power-type or exponential regression functions. As expected, mean annual ET$_0$ is negatively correlated with mean relative humidity, while it seems uncorrelated to wind speed. It is worth mentioning that as the solar radiation and temperature increase, the variance of ET$_0$ increases significantly. Therefore, in order to reduce

17

heteroscedasticity effects, it is essential considering at least two explanatory variables in the context of empirical PET modelling.

Figure 4 also demonstrates the variability of mean annual ET_0 against mean annual sunshine duration and annual extraterrestrial radiation, which are typically used instead of solar radiation, in PET estimations (given that solar radiation observations are generally sparse, due to the cost of associated equipment, i.e. pyranometers, radiometers or solarimeters). Surprisingly, the mean annual sunshine duration is slightly less correlated with mean annual ET_0 than extraterrestrial radiation, although the former is expected to be better estimator of the actual solar energy received in the Earth's surface. This is a very important conclusion that confirms the suitability of radiation-based approaches, using both temperature and extraterrestrial radiation as explanatory variables of PET. However, it is essential remarking that the overall driver of PET and temperature as well is net solar radiation, which is a portion of the extraterrestrial one. Furthermore, the correlation between PET and temperature is so much significant only at coarse time scales, such as the annual one, while its correlation with the solar radiation remains significant, at all temporal scales (Lofgren *et al.*, 2011).
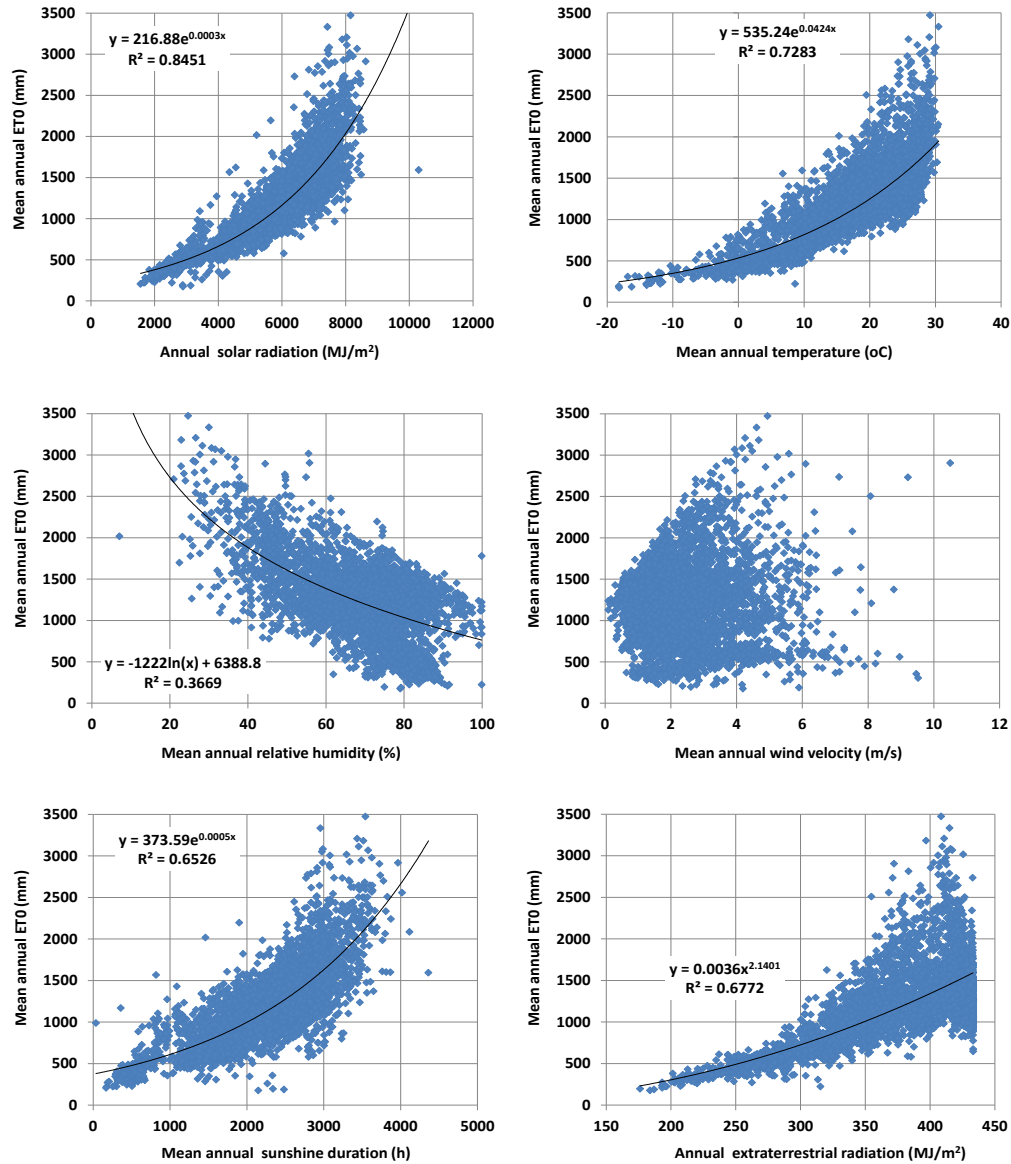
Figure 4. Scatter plot of mean annuals of (a) solar radiation, (b) temperature, (c) relative humidity, (d) wind speed, (e) sunshine duration, (f) extraterrestrial radiation vs. mean annual ET0.

How Well do Extraterrestrial Radiation and Temperature Explain the Seasonal Patterns of PET?

The key assumption of radiation-based models is that PET follows the seasonal patterns of extraterrestrial radiation, R_a, and temperature, T. In general, a loop-type shape exists between the mean monthly PET and the two aforementioned variables, due to the influence of thermal inertia, causing a delay in temperature changes against solar radiation changes across seasons. Apparently, due to the loop-shape relationship, the two pairs of variables are expected to be linearly correlated; actually, the more elongate the loop, the higher should be the correlation. In Figure 5, the relationships between monthly extraterrestrial radiation vs. mean monthly ET_0 and mean monthly temperature vs. ET_0 was estimated, at five characteristic stations in Australia, exhibiting different

19

hydroclimatic conditions, which confirm the above hypothesis. However, there are also cases where the shapes of T – ET_0 and R_a – ET_0 loops are irregular (nonconvex), thus resulting in very low, even negative, correlations. Such examples are shown in Figure 6, involving another set of stations in Australia.
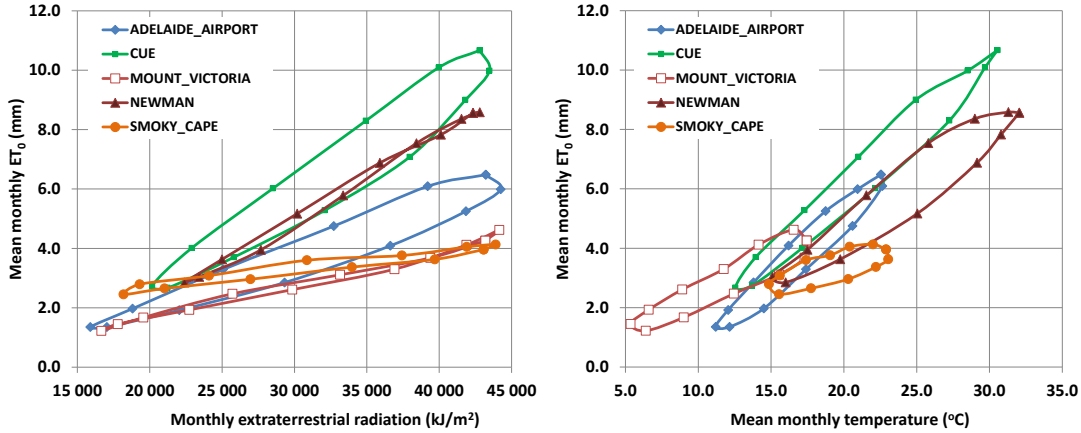
Figure 5. Scatter plots of monthly extraterrestrial radiation, Ra, vs. mean monthly ET0 (a) and mean monthly temperature, T, vs. ET0 (b) at five stations in Australia, exhibiting loop-type patterns.
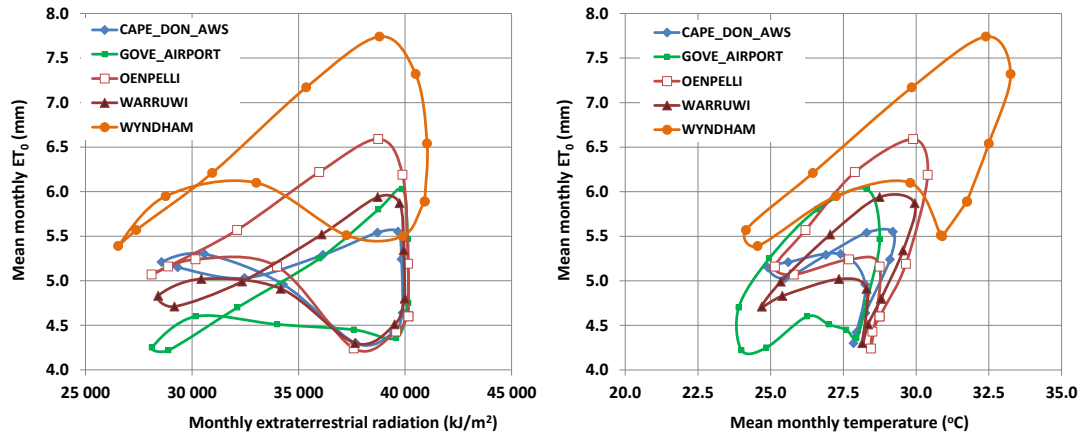
Figure 6. Scatter plots of monthly extraterrestrial radiation, Ra, vs. mean monthly ET0 (a) and mean monthly temperature, T, vs. ET0 (b) at five stations in Australia, exhibiting irregular patterns.

In order to investigate whether extraterrestrial radiation and temperature actually explain the seasonal patterns of ET_0 over the globe, we formulated the linear regression models of mean monthly ET_0 against the two variables and calculated the coefficient of determination, r^2 (i.e., square of Pearson correlation coefficient), at the full sample of 4300 CLIMWAT stations. Table 3 summarizes the results, by means of number of stations corresponding to ranges of r^2, from 0–10% up to 90–100%. It is shown that ET_0 exhibits very high linear correlation, by means of r^2 values greater than 0.90 against both extraterrestrial radiation and temperature at only 642 out of 4300 stations (14.9%). This percentage rises up to 49.7% (2135 stations) is we consider a wider acceptable range for r^2, i.e. upper than 0.80.

On the other hand, at 443 stations over the globe (10.3%), the coefficient of determination is less than 0.50 against both explanatory variables. Apparently, the particular hydroclimatic regime at these areas does not allow representing PET through simplified radiation-based approaches, thus requiring either more complex parameterizations or additional variables to explain the seasonal patterns of PET due to energy or water limitations, i.e. relative humidity and/or wind speed (McVicar *et al.*, 2012; Guo *et al.*, 2016). PET has been proven sensitive to potential changes in climate in regions with a lower temperature, less solar radiation, and greater relative humidity, while the influence of the wind velocity and relative humidity in its estimation is supported by several studies (McVicar *et al.*, 2012; Guo *et al.*, 2016; Rayner *et al.*, 2017; Roderick *et al.*, 2007; Roderick *et al.*, 2009; Wang *et al.*, 2012; Li *et al.*, 2013).

An interesting remark is that in 42 stations (1% of the sample), a linear regression function of temperature against ET_0 ensures r^2 greater than 0.90, while at the same stations, the correlation between ET_0 and R_a is negligible ($r^2 < 0.10$). The opposite case, i.e. very high correlation of PET with R_a, while very low with T appears only once, thus it is statistically negligible. In this vein, we can consider a linear regression model between mean monthly T and ET_0 as benchmark to evaluate the performance of any other empirical model, which parameters are identified through calibration.

Nevertheless, although a number of studies present alternatives to the PM formula (e.g., Pereira et *al.*, 2015; McMahon *et al.*, 2013), based on the sensitivity of potential evapotranspiration to temperature and/or solar radiation, the major advantage of our approach is the ability of point calibration of the involved parameters (Tegos *et al.*, 2015).

Table 2. Ranges of coefficient of determination, r2, between monthly ET0 and the two explanatory variables, R_a and T, across the full sample of 4300 CLIMWAT stations.

T vs. ET$_0$	R_a vs. ET$_0$										Total
	0–10%	10–20%	20–30%	30–40%	40–50%	50–60%	60–70%	70–80%	80–90%	90–100%	
0–10%	55	17	9	12	8	9	8	7	4	1	130
10–20%	38	11	7	4	11	8	3	3	5	3	93
20–30%	33	16	13	13	5	7	8	10	9	4	118
30–40%	36	14	24	10	7	5	12	12	8	15	143
40–50%	29	14	17	18	22	17	19	13	13	18	180
50–60%	34	10	17	16	17	28	26	21	26	31	226
60–70%	30	10	23	15	21	30	37	30	31	52	279
70–80%	45	11	15	19	28	20	44	48	77	135	442
80–90%	69	14	14	10	17	34	38	78	362	643	1279
90–100%	42	6	6	5	9	30	35	147	488	642	1410
Total	411	123	145	122	145	188	230	369	1023	1544	4300

Model Calibration and Evaluation Criteria

The large-scale PET information provided by FAO CLIMWAT database was used as reference data, for calibrating the parametric expression, thus providing local estimations of parameters a' and c' at all station sites. For the evaluation of the model performance against reference PET (i.e. ET$_0$) the following statistical criteria were used:

The coefficient of determination, most commonly referred to as efficiency or Nash-Sutcliffe efficiency:

$$\text{NSE} = 1 - \frac{\sum_{t=1}^{T}(\text{PET}_{\text{mod}}^t - \text{PET}_{\text{obs}}^t)^2}{\sum_{t=1}^{T}(\text{PET}_{\text{obs}}^t - \overline{\text{PET}_{\text{obs}}})^2} \tag{10}$$

1. The mean absolute error:

$$\text{MAE} = \frac{\sum_{t=1}^{T}|\text{PET}_{\text{obs}}^t - \text{PET}_{\text{mod}}^t|}{T} \tag{11}$$

2. The relative bias:

$$\text{BIAS} = \frac{\sum_{t=1}^{T}(\text{PET}_{\text{mod}}^t - \text{PET}_{\text{obs}}^t)}{\sum_{t=1}^{T}(\text{PET}_{\text{obs}}^t)} \tag{12}$$

where $\text{PET}_{\text{obs}}^t$ is the ET$_0$ value, estimated by the PM formula at time step t, $\text{PET}_{\text{mod}}^t$ is the modeled value at time step t, $\overline{\text{PET}_{\text{obs}}}$ is the monthly average value of the reference PET, and T is total number of time steps (in the particular case, T equals the number of months, i.e. Oudin *et al.*, 2005).

In calibrations, as performance measure the NSE was used, while the two other statistical metrics have been used for further evaluation. It is well-known that NSE ranges between $-\infty$ and 1, with NSE = 1 indicating perfect fitting of the modelled against the given reference values. Due to the generally high linear correlations of R_a and T against ET$_0$, we only consider values greater than 0.70 as satisfying, whereas positive values less than 0.50 are only marginally accepted. On the other hand, negative NSE values are definitely unacceptable, since they indicate that the mean observed value is a better predictor than the simulated value. The mean absolute error and the bias are quite

similar metrics, quantifying in absolute (i.e. mm/month) and relative (%) terms the deviation of the mean modelled ET_0 from the corresponding mean reference value, $\bar{Q}_{obs}$.

Optimization Procedure

At each station the associated global optimization problem was formulated, based on the given 12 monthly average values of ET_0, and using NSE as the objective function to maximize against parameters a' and c'. Within calibration, a quite extended feasible space was considered, by allowing a' and c' to vary within ranges [−0.02, 0.02] and [−5.0, 5.0], respectively. The global search was carried out with the evolutionary annealing-simplex algorithm, which is a heuristic technique that has been proved very effective on locating global optima in highly nonlinear spaces (Efstratiadis and Koutsoyiannis, 2002; Tsoukalas *et al.*, 2016).

Due to the exceptionally large number of calibration problems to be solved at the full sample of 4300 stations, the computational procedure was automatized in a MATLAB environment.

Assessment against Linear Regression Estimations

In order to assess the predictive capacity of the parametric model, the performance against two benchmarks by means of linear regression models of reference PET against T and R_a was compared. In Figure 7 the ranges of coefficients of determination is presented , r^2, achieved by the two linear regression models and the nonlinear parametric model, for the entire sample of 4300 stations. The parametric model ensures very satisfying efficiency (NSE > 0.90) in 58.8% of stations, while only 32.8% and 35.9% of stations exhibit such good performance, considering the linear regression models against T and R_a, respectively. In 2562 stations (59.6%), the parametric approach outperforms both regression models, while in 1327 stations (30.9%) it outperforms at least one model. Only in 411 stations (9.6%) the two benchmarks achieve a higher r^2 than the parametric approach. It should be remark that in linear regression theory, r^2 is mathematically equivalent to efficiency, which is the most widely used goodness-of-fitting measure for evaluating nonlinear models. However, while the coefficient of determination of a nonlinear model can take any value from −∞ to unity, in linear regression this metric is by definition non-negative (r^2). Moreover, linear regression models are by definition unbiased, given that the least-square line is forced to pass through the observed mean.

However, there are relatively few cases where the parametric model, even after calibration, does not ensure good predictive capacity. In particular, at 10.3% of stations, the model exhibits marginally accepted performance (0 < NSE < 0.50), while in 4.7% of stations the model predictions are definitely unacceptable (NSE < 0). In these cases, it is impossible to achieve acceptable predictions of mean monthly ET_0 through the parameterization implemented because of the irregular relationship of ET_0 vs. the two explanatory variables, or due to the influence of additional meteorological drivers (relative humidity and wind speed) as rationalized in previous Section.

23
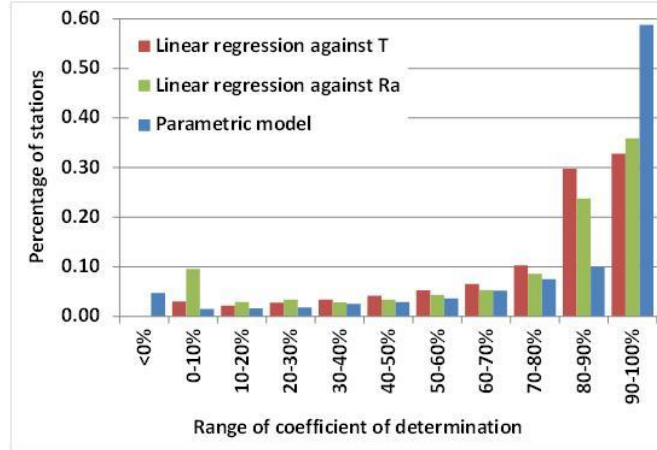
Figure 7. Ranges of coefficient of determination for the linear regression functions of monthly reference PET against Ra and T, and the nonlinear parametric model.

Assessment against Hargreaves-Samani Estimations

The substantial advantage of a parametric approach, allowing calibration, over an empirical formula with given numerical constants, is further highlighted by contrasting our predictions with the ones provided by the well-known Hargraves-Samani equation, given by:

$$ET_0 \ = \ 0.408 \times [0.0023 \times R_a(T + 17.8)]\,(T_{min} \ - \ T_{max})^2 \tag{13}$$

where *T* is the mean monthly temperature.

As shown in Table 3, providing abstract information on model efficiency in terms of quartiles, in the majority of stations the predictive capacity of Equation above is absolutely disappointing, mainly due to the existence of substantial bias in ET_0 estimations (Equation 13) across stations. This bias is actually embedded in the coefficients that are embedded in above Equation, which have been estimated on the basis of specific climatic regime, which cannot be representative of any conditions worldwide. On the other hand, Equation (9) with calibrated parameters ensures very satisfactory performance in an extended part of the station sample, since the model is adapted to local climatic conditions.

Table 3. NSE quartiles for the Hargraves-Samani against the parametric model.

Quartiles	Hargreaves-Samani	Parametric
Minimum value	−327.204	−5.997
1	−5.834	0.721
2	−0.971	0.947
3	0.245	0.984
4	0.980	0.999

Final Data Sample

Based on point calibration results, from further analysis the 4.7% of stations exhibiting negative efficiency were excludes, thus the final sample was restricted to 4088 stations. For convenience, we grouped them in five geographical zones, namely 908 stations in Africa, 352 in the wider region of

Oceania, 1854 in Eurasia, 369 in North America, and 605 in South America. As shown in Table 4, the majority of the stations (69.9%) are located in altitudes between 0 and 500 m, 21.6% of them are located between 500 and 1500 m, while only 8.5% of them are placed in altitudes greater than 1500 m. It can been seen that the stations located in Eurasia and in America follow a quite similar distribution, while in the case of Africa there is a larger percentage located in higher altitudes. On the other hand, in Oceania, the majority of stations are placed in altitudes up to 500 m.

Table 4. Altitude distribution (%) of the calibration set of CLIMWAT stations (4088 stations, in total).

Region	Altitude			
	< 500 m	500–1000 m	1000–1500 m	> 1500 m
Africa	53.6	14.5	16.2	15.7
Oceania	90.9	6.7	0.9	1.5
Eurasia	75.8	12.9	6.9	4.4
N. America	68.1	14	7.7	10.2
S. America	65.4	15.9	5.3	13.4
Total	69.9	13.3	8.3	8.5

Residuals Analysis for Stations with Negative NSE

In order to explain the poor performance of the model at the problematic 212 stations shown in Figure 8 (highlighted with blue points), the model residuals was investigated, i.e. the differences between model predictions and PM estimations. As shown in Figure 9, the residuals are approximately normally distributed, while as shown in Figure 10, they are uncorrelated. Therefore, the statistical behavior of the residuals is close to the desirable one (i.e. white noise), indicating absence of systematic errors (Kitanidis, 1997; Malamos and Koutsoyiannis, 2015). The negative NSE values are attributed to local overestimation during the warm months or underestimation during the cold months of the year, respectively, driven from the absence of relative humidity and wind speed from the parametric model formulation.
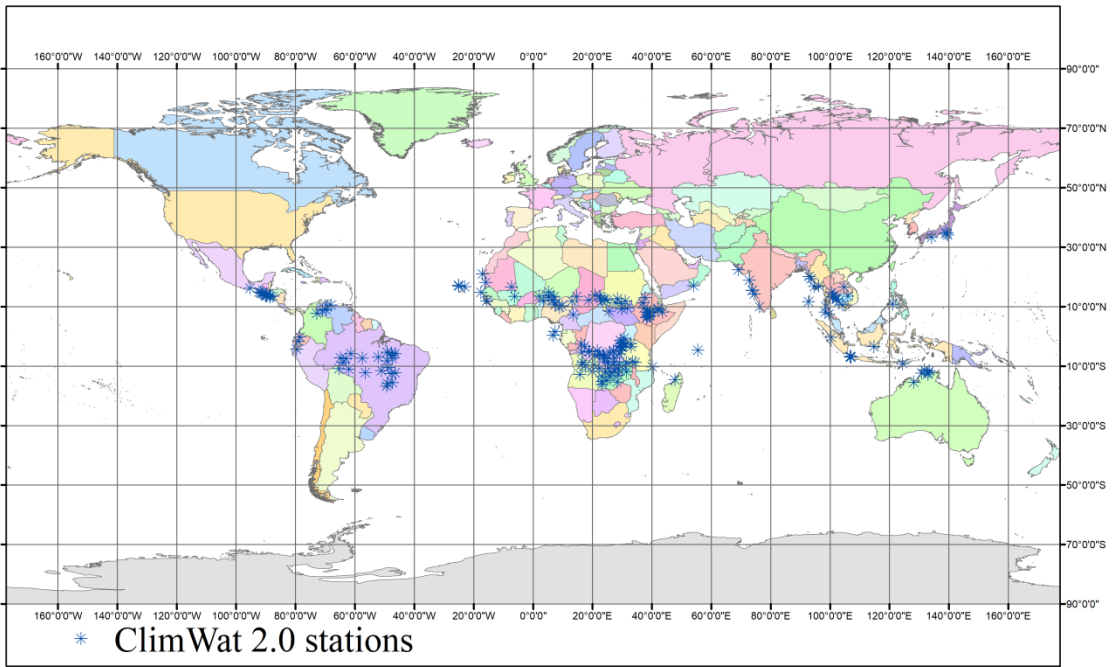
Figure 8. CLIMWAT stations with negative NSE.
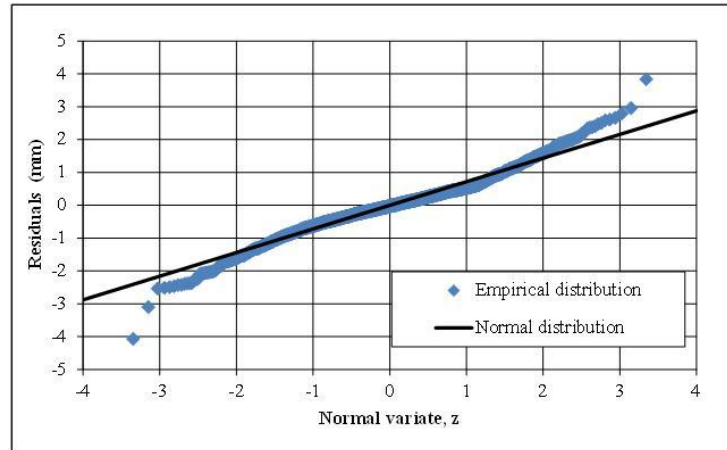
Figure 9. Normal probability plot of the empirical distribution function of the mode residuals using Weibull plotting positions against normal distribution function N (0, 0.7), for stations with negative NSE.
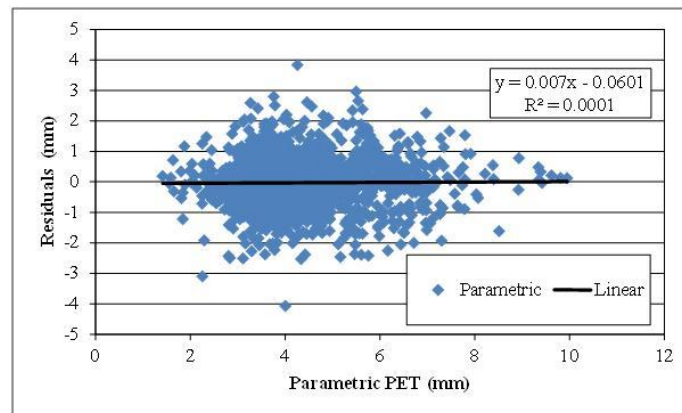
Figure 10. Residuals vs parametric PET for stations with negative NSE.

In order to further evaluate the effect of missing information of relative humidity and wind speed on the produced residuals, we plotted both of them along with the corresponding linear models, as presented in Figure 11. This illustrates that there is a significant linear correlation between the relative humidity and the estimation errors - residuals while the opposite seems to be the case for the wind speed. The absence of these two variables as explanatory input variables within the parametric model seem to be crucial in regions with seasonal variations of ET_0 due to energy or water limitations mainly in the tropical zone, as shown in Figure 8.

27
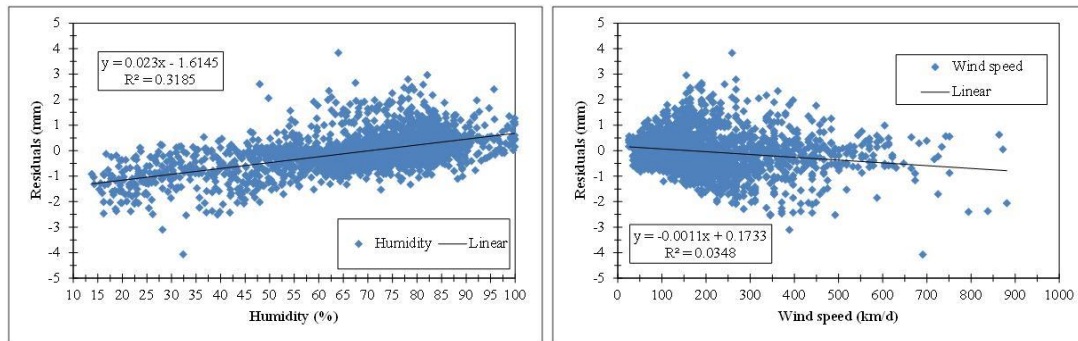
Figure 11. Residuals vs. humidity (a) and wind speed (b) for stations with negative NSE.

Evaluation of Model Performance across Geographical Zones

According to the acquired values of NSE (Table 5, Figure 12), the parametric model performs well in Eurasia, North America, and the wider region of Oceania, where 80%, 80%, and 77% of stations, respectively, present efficiency values more than 0.80. In South America, 66% of stations achieve a score greater than 0.80, while in Africa, this percentage falls to 50%. In particular, 22% of stations in Africa achieved NSE values below 0.50, which indicates a poor predictive capacity.

The mean absolute error of the parametric model in every geographical unit is small (Table 6). In South America, the MAE of the 95% of the stations is below 4 mm/month. This percentage is 88% for the wider region of Oceania, 79% for North America, 76% for Eurasia, and 72% for Africa.

Table 7 summarizes the values of the relative bias of the parametric model against the reference PET values, for all of the geographical units (Figure 12). It is obvious that the values are generally small, ranging from −0.122 to +0.062 proving that the results of the parametric model are almost unbiased for the majority of the stations. The differences between the biases across the geographical zones are not important, since the variation between the extreme values is similar.

The overall evaluation of the model across the different geographical areas is very satisfactory. All of the metrics prove that the predictive capacity of the model is very satisfying across Eurasia, North America, and the wider region of Oceania. On the other hand, in the equatorial regions of South America, Africa as well as the Indian and Indonesian Peninsula (Figure 8), the model performs poorly according to the NSE criterion, probably because it does not account for relative humidity and wind speed, which are key drivers of the evapotranspiration processes across these areas, influencing the net incoming solar radiation and the evaporation demand.

Table 5. Number of stations and associated NSE intervals across geographical zones.

Region	1.0–0.9	0.9–0.8	0.8–0.7	0.7–0.6	0.6–0.5	<0.5
Africa	34	16	12	9	7	22
Oceania	67	10	7	4	1	11
Eurasia	68	12	7	4	3	6
N. America	65	15	5	3	2	10
S. America	54	12	10	7	6	11

Table 6. Number of stations and associated intervals of monthly MAE across geographical zones.

Region	0–2 mm	2–4 mm	4–6 mm	6–8 mm	8–10 mm	>10 mm
Africa	36	36	15	6	3	4
Oceania	52	36	9	3	0	0
Eurasia	39	37	17	5	1	1
N. America	40	39	17	3	1	0
S. America	69	26	4	1	0	0

Table 7. Number of stations and associated intervals of BIAS across geographical zones.

Region	−0.122–0.000	0.000–0.001	0.001–0.062
Africa	65	14	21
Oceania	38	12	50
Eurasia	72	5	23
N. America	68	13	19
S. America	55	15	30
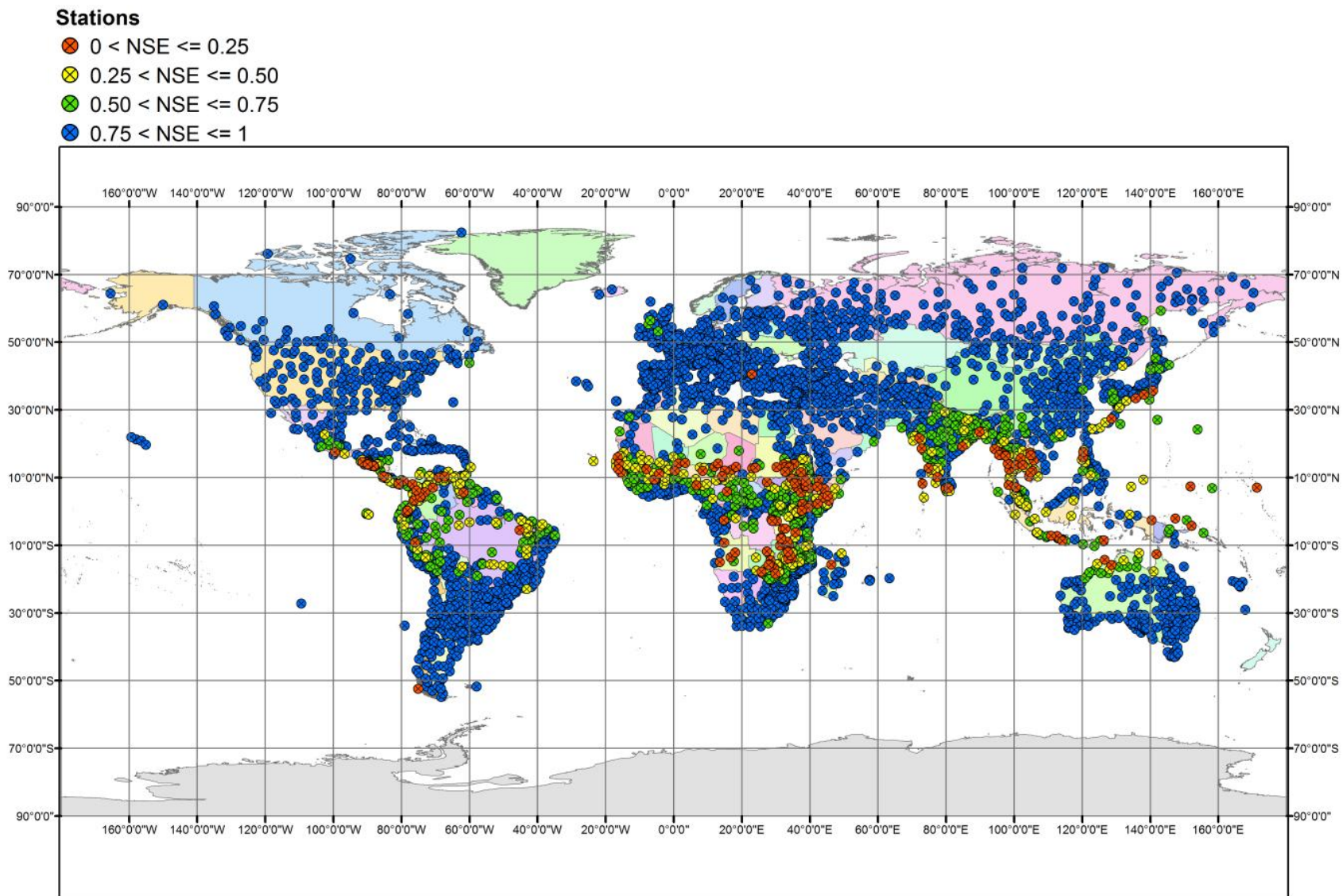
Figure 12. Distribution of NSE across CLIMWAT stations.
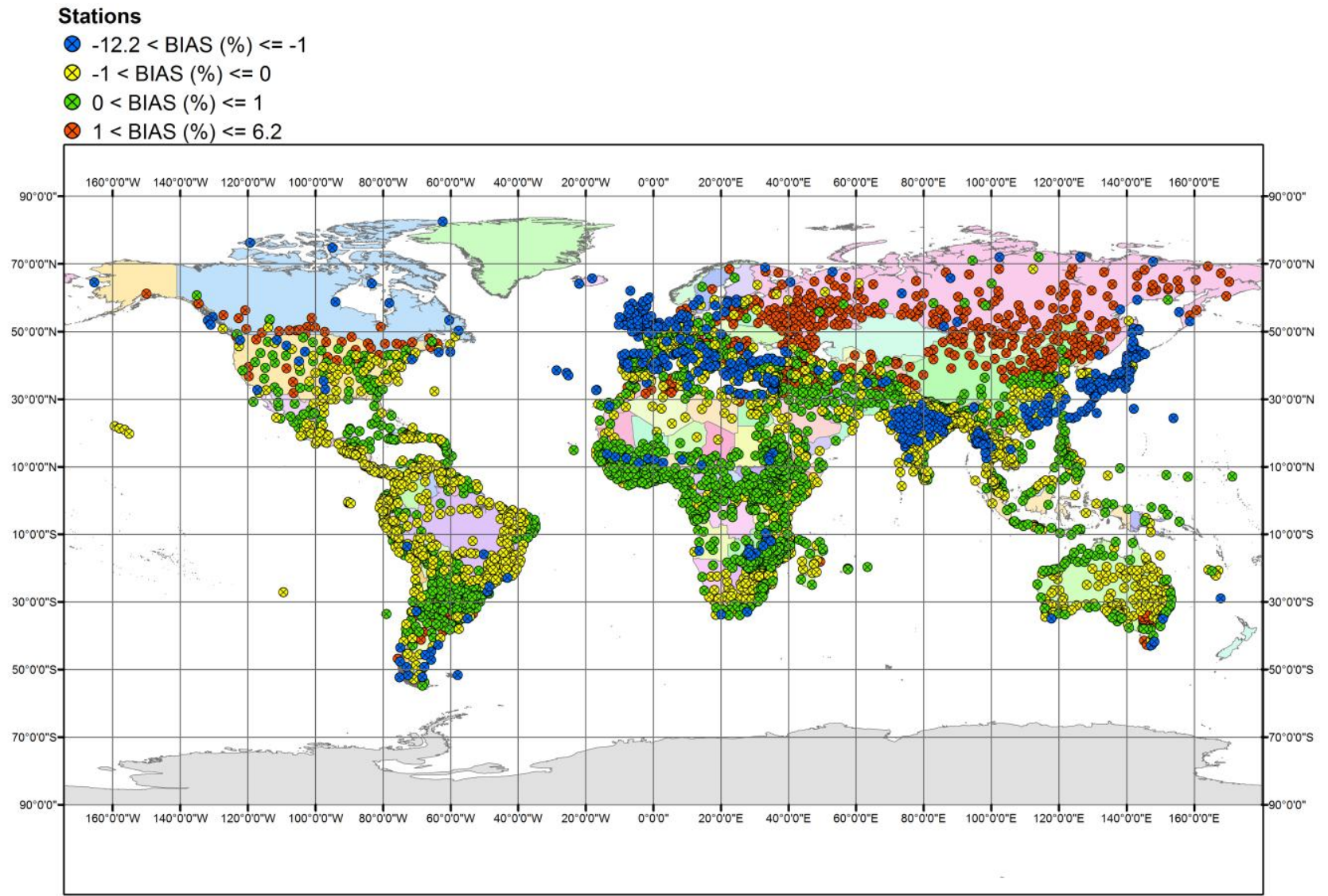
Figure 13. Distribution of BIAS across CLIMWAT stations.

Spatial Analysis and Model Validation

Spatial Interpolation of Optimized Parameters

Even though point PET estimates can be used for small-scale studies, it is the regionalisation of PET that is of great significance in hydrological science (Merz and Blöschl, 2004). A preliminary attempt in PET mapping was presented by Foyster (1973), and followed by several publications where different spatial interpolation methods have been applied (Dalezios *et al.*, 2002; Mardikis *et al.*, 2005; Vicente-Serrano *et al.*, 2007), with satisfying performance. In a recent study, Tegos *et al.* (2015) illustrated that the inverse distance method (IDW) was the most efficient than other interpolation techniques, i.e. Kriging, Bilinear Surface Smoothing and Natural Neighbours. Furthermore, IDW is a straightforward and computationally non-intensive method, which is capable to address the huge spatial extent of the study area, i.e. the entire globe.

Formally, the IDW method is used to estimate the unknown value $\hat{y}(S_0)$ in location S_0 given the observed *y* values at sampled locations S_i in the following manner:

$$\hat{y}(S_0) = \sum_{i=1}^{n} \lambda_i y(S_i) \tag{14}$$

Essentially, the estimated value in S_0 is a linear combination of the weights (λ_i) and observed y values in S_i, where λ_i is defined as:

$$\lambda_i = \frac{d_{0i}^{-a}}{\sum_{i=1}^{n} d_{0i}^{-a}} \tag{15}$$

with:

$$\sum_{i=1}^{n} \lambda_i = 1 \tag{16}$$

In the above Equation, the numerator is the inverse of distance d_{0i} between S_0 and S_i with a power α, and the denominator is the sum of all inverse-distance weights for all locations *i* (in the particular case, all stations exhibiting positive efficiency).

Spatial Distribution of Parameters

The approach allows for mapping the spatial distribution of the optimized model parameters a′ and c′, instead of its response, i.e. PET. This is a major advantage, since it allows implementing Equation (5) wherever in the globe, using interpolated values of the point (i.e., locally calibrated) parameters. It is interesting to note that the two parameters are negatively correlated (Figure 14), thus reflecting the significant correlation of the associated meteorological variables of the parametric formula (extraterrestrial radiation, in the numerator, and temperature, in the denominator).
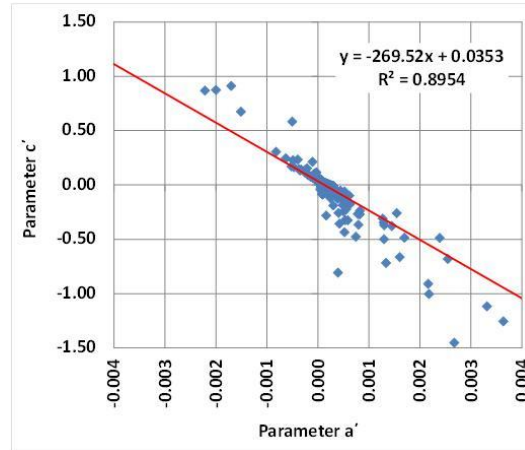
Figure 14. Scatter plot of optimized parameters through the final data sample of 4088 stations exhibiting positive NSE values.

In this context, based on the optimized parameters from the final data set of 4088 stations (as already explained, the rest of stations are not acceptable, and hence the corresponding parameter values will be unreliable), maps of spatially-interpolated parameters over the globe were created. The IDW method was employed in a GIS environment, considering for practical reasons (i.e., in order to avoid extreme computational burden), a relatively large grid size of 0.1 decimal degrees in WGS84 coordinate system and a variable search radius including the 12 nearest stations, in order to tackle the measurement of large distances across the globe.

Figure 15 illustrates the spatial distribution of parameter a'. The highest values are generally observed around the equatorial zone, while they are getting lower as we move away from it. This is a reasonable outcome since this parameter is associated with solar radiation. This means that around the equatorial zone, where the incoming solar radiation is higher, the values of parameter a' are to be higher while around the poles, where solar radiation is lower, the values of parameter a' were expected to be lower. Another observation is that in the case of two stations, one located at Brazil and one at the Democratic Republic of Congo, the calculated values for parameter a′ were low, creating "sinkholes" in the corresponding maps. This is explained from the fact that at those areas, the hydro-meteorological network is not dense enough, thus the influence of the specific stations extends, as a direct effect of the IDW implementation and also the tropical forest providing high humidity regime can be influenced. Apart from this, the spatial analysis of parameter a′ is normal and physically explained.

33
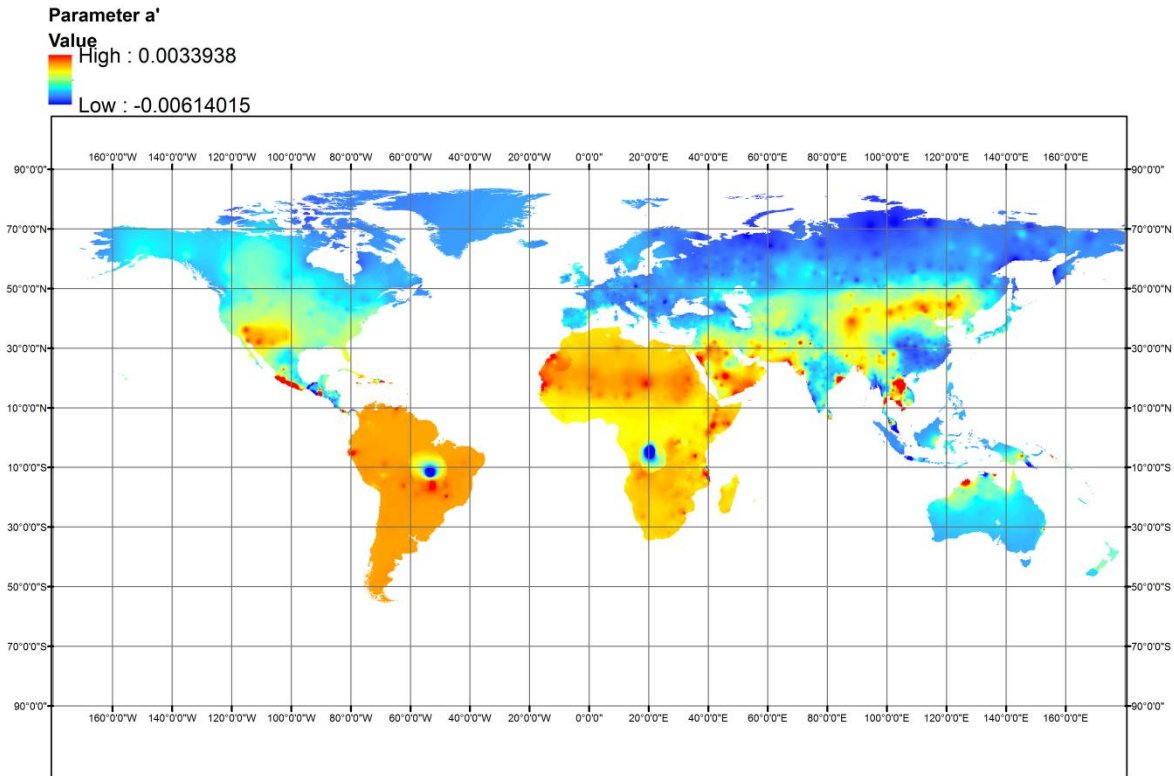
Figure 15. Spatial distribution of parameter a′ over the globe.

In contrast to parameter a', the spatial distribution of parameter c', depicted in Figure 16, the lowest values around the equatorial zone, while these are getting higher as we move away from the equator. Since c' is inversely proportional to temperature, it was expected that its values get higher as temperature is getting lower and vice versa. In the case of the above stations, i.e. one at Brazil and one at the Democratic Republic of Congo, the values of parameter c' were extremely high, contrariwise to parameter a'. The explanation for this phenomenon is the same as above, yet in this case the interpolation method resulted in a ridge-type distribution over the specific areas.

Conclusively, the model results can be considered reliable, since the spatial distribution of both parameters around the globe is physically explained, while minor irregularities are also attributed to physical reasons, i.e. inadequate representation of humidity and wind processes.
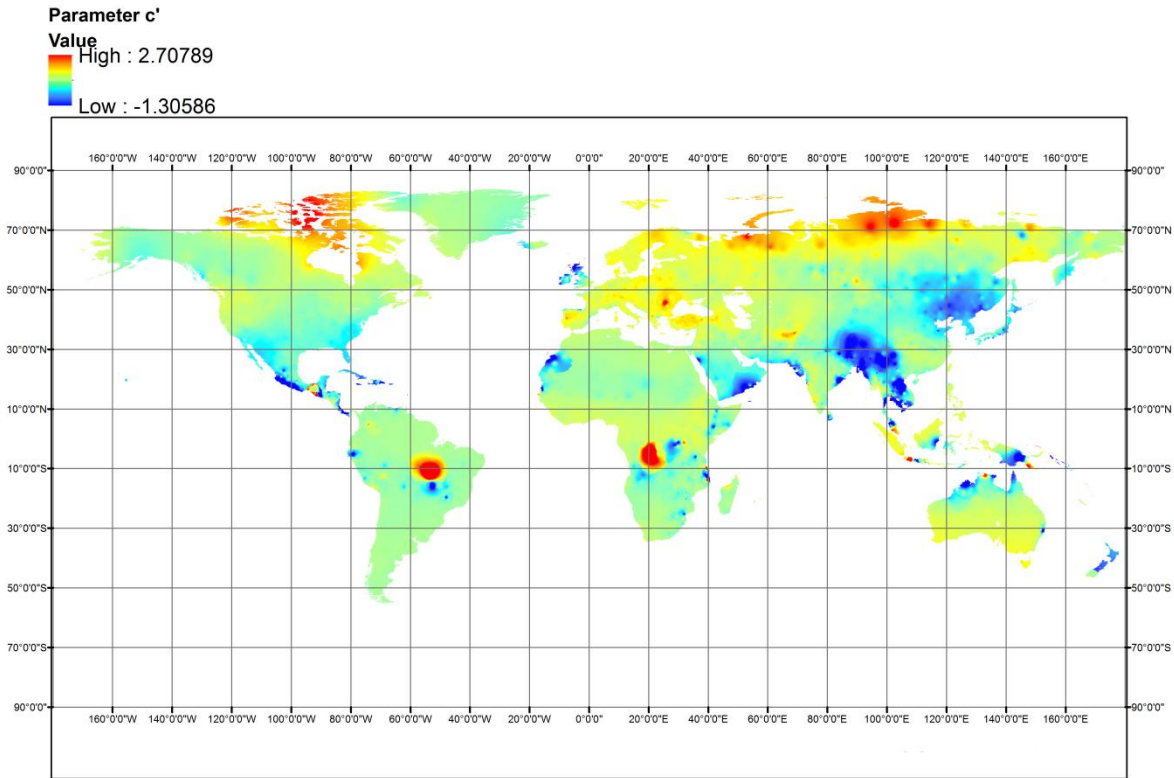
Figure 16. Spatial distribution of parameter c′ over the globe.

Model Validation

The validation of the model was performed by comparing monthly ET_0 predictions provided by the parametric formula using interpolated parameters against PM estimates in a number of independent stations. In particular, two validations sets was considered, a "local" and a "global" one. The former comprises 37 stations across California, for which monthly meteorological time series are available from the California Irrigation Management Information System (Hart *et al.*, 2009). The "global" set comprises 17 stations from countries with different hydroclimatic regimes (Spain, Germany, Ireland, Greece, Iran, and Australia), for which we obtained full time series of the required meteorological data, at the monthly scale, form various data sources.

For the local validation set (Table 8), the model predicts monthly ET_0 with significant accuracy, thus exhibiting an average efficiency up to 0.855, and an average bias of only −0.07. Except for three stations (Bishop, Castroville, De Laveaga), the NSE exceeds 0.70, while in 17 out of 37 stations it exceeds 0.90. This indicates an almost perfect performance, particularly when taking into account that the model has been calibrated using abstract (i.e. mean monthly) meteorological information over the entire globe, while the validation set comprises detailed data, both in terms of spatial extent and temporal resolution. Similarly satisfying are the outcomes from the global validation set, which are summarized in Table 9 (average efficiency 0.852, average bias 0.02), thus confirming the model predictive capacity across different climates.

Table 8. Statistical indices for the local validation dataset (CIMIS stations, California, USA).

a/a	Station	Validation period	NSE	MAE (mm)	BIAS
1	Five Points	6/1982–6/2013	0.880	20.4	−0.09
2	Davis	10/1982–6/2013	0.857	13.8	−0.01
3	Firebaugh/Telles	10/1982–6/2013	0.897	16.8	−0.09
4	Gerber	10/1982–6/2013	0.896	17.9	−0.10
5	Durham	10/1982–6/2013	0.870	19.7	−0.14
6	Carmino	11/1982–6/2013	0.952	11.3	−0.01
7	Stratford	11/1982–6/2013	0.913	17.2	−0.06
8	Castroville	12/1982–6/2013	0.442	23.7	−0.23
9	Kettleman	12/1982–6/2013	0.903	18.8	−0.10
10	Bishop	3/1983–6/2013	0.475	16.5	0.03
11	Parlier	6/1983–6/2013	0.858	22.1	−0.16
12	McArthur	12/1983–6/2013	0.940	11.5	0.01
13	U.C. Riverside	6/1985–6/2013	0.858	13.2	0.08
14	Brentwood	5/1986–10/2006	0.930	13.2	−0.06
15	San Luis Obispo	5/1986–6/2013	0.856	12.0	−0.08
16	Blackwells corner	5/1987–6/2013	0.939	13.7	−0.05
17	Los Banos	6/1988–6/2013	0.926	14.0	−0.06
18	Buntingville	5/1986–6/2013	0.953	11.1	0.03
19	Temecula	12/1986–6/2013	0.769	12.9	0.02
20	Santa Ynez	12/1986–6/2013	0.842	13.6	−0.10
21	Seeley	6/1987–6/2013	0.845	18.4	0.03
22	Manteca	12/1987–6/2013	0.796	25.2	−0.10
23	Modesto	10/1987–6/2013	0.922	14.7	−0.06
24	Irvine	11/1987–6/2013	0.803	13.2	−0.10
25	Oakville	10/1989–6/2013	0.930	13.3	−0.10
26	Pomona	4/1989–6/2013	0.701	19.0	−0.15
27	Fresno State	11/1988–6/2013	0.906	18.4	−0.12
28	Santa Rosa	1/1990–6/2013	0.894	11.5	−0.09
29	Browns Valley	5/1989–6/2013	0.856	22.3	−0.16
30	Lindcove	6/1989–6/2013	0.782	31.0	−0.22
31	Alturas	5/1989–6/2013	0.916	10.4	−0.02
32	Cuyama	10/1989–6/2013	0.950	11.5	0.05
33	Tulelake FS	5/1989–6/2013	0.922	11.9	0.05
34	Windsor	1/1991–6/2013	0.905	11.4	−0.09
35	De Laveaga	10/1990–6/2013	0.676	21.8	−0.19
36	Westlands	5/1992–6/2013	0.932	15.0	−0.03
37	Sanel Valley	2/1991–6/2013	0.939	11.0	−0.02
	Average		**0.855**	**16.0**	**−0.07**

Table 9. Statistical indexes for the global validation dataset.

a/a	Station	Country	Validation period	NSE	MAE (mm)	BIAS
1	Aachen	Germany	01/1951–5/2011	0.955	6.8	0.06
2	Bremen	Germany	01/1951–5/2011	0.954	5.5	0.03
3	Alicante	Spain	01/1980–09/2010	0.916	11.1	0.00
4	Badajoz	Spain	01/1961–05/2005	0.921	13.0	−0.09
5	Valencia	Spain	09/1954–08/1964	0.893	10.0	−0.06
6	Zaragoza	Spain	02/1974–01/1996	0.953	10.8	−0.01
7	Herakleion	Greece	01/1968–12/1989	0.947	10.2	−0.00
8	Kerkyra	Greece	01/1968–12/1989	0.936	9.8	−0.09
9	Kavala	Greece	01/1968–12/1989	0.835	13.5	0.04
10	Limnos	Greece	01/1968–12/1989	0.762	24.3	0.12
11	Athens	Greece	01/1968–12/1989	0.924	13.6	0.03
12	Melbourne	Australia	01/2009–1/2016	0.752	18.5	0.17
13	Dublin	Ireland	01/2013–6/2016	0.870	5.1	−0.09
14	Bandar-Anzali	Iran	1/1990–12/2005	0.875	13.9	−0.16
15	Ramsar	Iran	1/1990–12/2005	0.788	16.2	0.15
16	Khorram-Abad	Iran	1/1990–12/2005	0.400	38.3	0.37
17	Kashan	Iran	1/1990–12/2005	0.804	19.6	−0.13
	Average			**0.852**	**14.1**	**0.02**

3.1.5   Conclusions

 The concept of parametric PET modelling was thoroughly analyzed, by performing a global survey of its applicability. The model has a very simple structure and uses easily retrieved information, by means of air temperature and extraterrestrial radiation. Therefore, the model is simultaneously simple and parsimonious, in terms of both parameterization and data requirements.

Preliminary analysis of the extended climatic data at 4300 stations worldwide, provided by the FAO CLIMWAT database, allowed for justifying the use of temperature and extraterrestrial radiation as key explanatory variables of reference PET over the globe. However, it also indicated that in few cases the two variables exhibit irregular seasonal patterns, which cannot be adequately represented through simple modelling structures. The statistical analysis of the residuals, in these cases, showed that the model is consistent in terms of parameters estimation and model validation.

At all CLIMWAT stations, optimal estimations of model parameters c' and a' were provided, by calibrating them against given Penman-Monteith values at the mean monthly scale. Using typical goodness-of-fitting criteria (efficiency, mean absolute error, relative bias), the model performance was evaluated, which was generally very satisfying in a large portion of stations. However, in less than 10% of the data set the calibrated model exhibited negative efficiency. Further analysis across broader geographical regions showed that the model deviates from the Penman-Monteith PET

estimates in some locations, which is rather expected due to the significant influence of relative humidity and wind speed, which are not accounted for in the parametric model.

An important outcome of this research was the generation of spatially distributed maps of model parameters, by employing the IDW interpolation technique against their optimized values at 4088 out of 4300 stations, exhibiting non-negative efficiency. The spatial pattern of both parameters over the globe is fully reasonable, which is a strong indicator of their physical consistency. These maps can be straightforwardly used to provide suitable parameter values at both the local and regional scale, thus allowing for the direct use of the parametric model wherever in the world.

The validation procedure against PM estimates from detailed meteorological information (i.e. monthly time series) from 37 stations across California, as well as 17 independent stations across Europe, Asia, and Australia, proved that the application of the parametric model using spatially interpolated parameters provides reliable estimates, thus being a promising alternative of the widely recognized yet data demanding Penman-Monteith approach, when there is lack of the full data set that the latter requires.

4 Parametric model in CIMIS network

4.1 Introduction

The following chapters present the development of the Parametric model in the CIMIS network (California) along with some locals stations in Spain and Germany. The performance of the new model was compared with well-established radiation-based (Hargreaves, Jensen-Haise, Mcguiness-Bordne), temperature-based (Thorhwaite, Blaney Criddle) models. Finally, alternative spatial techniques were applied for identifying the optimal interpretation of the spatial PET information.

4.2 Parametric formula

Parsimonious modeling is essential in several water discipline fields (Koutsoyiannis 2009, Koutsoyiannis 2014). In this vein, the hydro model structure and the input should be easily available. Due to highly complexity of the P-M equation, most of simplified formulas fail to describe the phenomenon of evapotranspiration. Thus, the idea of replacing some variables and constants used in the standard Penman-Monteith (PM) formula by a number of parameters which are regionally varying and estimated through calibration from a reference evapotranspiration sample, constitutes a new appealing strategy for evapotranspiration estimation.

Koutsoyiannis and Xanthopoulos (1999), Tegos *et al.* (2009) and Tegos *et al.* (2013) examined the structure and the sensitivity of input data in PM model. They concluded that there is a direct relationship between potential evapotranspiration, extraterrestrial radiation and temperature. Furthermore, Mamassis *et al.* (2014) reached to the conclusion that the influence of every meteorological parameter in evaporation is almost linear, with temperature having the greater influence.

By dividing both the numerator and the denominator by Δ, the PM equation can be written in the form:

$$\text{PET} = \frac{1}{\lambda \rho} \frac{R_n + \gamma \lambda F(u) D}{1 + \gamma'/\Delta} \tag{17}$$

In the above expression, the numerator is the sum of a term related to solar radiation and a term related to the rest of meteorological variables, while the denominator is function of temperature.

Based on the previous analysis, a simplification of the Penman-Monteith formula, where the numerator is approximated by a linear function of extraterrestrial solar radiation, while a linear descending function of temperature approximates the denominator, can be described by the following formula:

$$\text{PET} = \frac{a R_a - b}{1 - c T_a} \tag{18}$$

where PET (mm) is the potential evapotranspiration, Ra (kJ m^{-2}) is the extraterrestrial shortwave radiation calculated without measurements and Ta (°C) is the air temperature.

Equation (18) contains three parameters, i.e. a (kg kJ^{-1}), b (kg m^{-2}) and c (°C^{-1}), to which a physical interpretation can be assigned. Since extraterrestrial solar radiation is the upper bound of net shortwave radiation, the dimensionless term a* = a / λρ represents the average percentage of the energy provided by the sun (in terms of Ra) and, after reaching the Earth's terrain, is transformed to latent heat, thus driving the evapotranspiration process. Parameter b lumps the missing information associated with aerodynamic processes, driven by the wind and the vapour deficit in the atmosphere. Finally, the expression 1 – cTa approximates the term: 1 + γ/Δ. We recall that γ′ is a function of the surface and aerodynamic resistance (equation 5) and Δ is the slope vapour pressure curve, which is a function of Ta.

4.3 Radiation-Based and temperature-based models

Another widely used approach is the temperature-based Hargreaves model (Hargeaves and Samani 1982) that estimates the reference evapotranspiration at monthly and daily scale. The method has received considerable attention because it can produce very acceptable results under diverse climates using only temperature and radiation measurements (Shahidian *et al.* 2013). According to several researchers (Samani 2000, Xu and Singh 2002) the method performs poorly in extreme humidity and wind conditions.

A recent study (Oudin *et al.* 2005), evaluated a number of evapotranspiration methods, on the basis of precipitation and streamflow data from a large sample of catchments in the USA, France and Australia. After extended analysis with the use of four hydrological models, the researchers modified the Jensen and McGuiness model and proposed a generalized radiation- based equation. Table 10 summarizes the expressions that estimate PET according to the above-mentioned methodologies:

Table 10. Radiation-based and temperature- based methods for potential evapotranspiration estimation.

Method	Jensen and Haise	Mcguiness and Bordne	Hargreaves	Oudin
PET expression	$\dfrac{R_a\,T_a}{40\,\lambda\,\rho}$	$\dfrac{R_a\,(T_a + 5)}{68\,\lambda\,\rho}$	$0.0023\dfrac{R_a}{\lambda}\,(T_\alpha + 17.8)\,(T_{max} - T_{min})^{0.5}$	$\dfrac{R_a\,(T_a + 5)}{100\,\lambda\,\rho}$

where PET (mm d^{-1}, equivalent to kg m^{-2} d^{-1} of the dimensionally consistent Penman- Monteith equations) is the potential evapotranspiration, R_a (kJ m^{-2}d^{-1}) is the extraterrestrial shortwave radiation, T_a (°C) is the air temperature, λ is the latent heat of vaporization (kJ kg^{-1}) and ρ is the water density (kg L^{-1}).

The Thornthwaite model (Thornthwaite, 1948) is the most simplified method and requires only temperature measurements. The model's form is:

$$PET = 1.6\, L_d \left(\frac{10\,T_a}{I}\right)^a \quad (19)$$

where PET is the potential evapotranspiration (mm/month), L_d is the daytime length, T_a is the mean monthly air temperature (°C), I is the annual heat index and a is an empirically determined parameter which is function of I.

The temperature-based Blaney-Criddle method (Blaney and Criddle, 1962) has received worldwide application for the estimation of irrigation demands. The model expression is:

$$\text{PET} \ = \ K\, p\, (0.46\, Ta \ + \ 8.13) \tag{20}$$

where PET is the potential evapotranspiration (mm/month), T_a the mean temperature (°C), K is the monthly consumptive use coefficient and p is the mean daily percentage of annual daytime hours.

4.4   Hydrometeorological data and computational tools

For exploration purposes, monthly meteorological data from 39 CIMIS stations were used, available at www.cimis.water.ca.gov, 10 stations from Germany and finally 4 stations from Spain (Table 11). The European data are freely available in the European Climate Assessment dataset (http://eca.knmi.nl/). Stations latitudes range from N 32.76° to N 53.38° and their altitude varies from 2.74 m to 1342.6 m.

The available data comprise mean temperature, relative humidity, sunshine duration and wind velocity. At all CIMIS stations the data covers the period from October 1992 to September 2012 while the European stations cover the period from January 1948 to December 2013. The choice of the time-periods was based on the simultaneous availability of the four required hydrometeorological variables (temperature, sunshine duration, humidity, wind speed). Additionally, the selection of each station and especially those from the CIMIS network was based on the existence of adequate length time series for the processes involved, i.e. 20 years.

Table 11. Meteorological stations used for the evaluation of the potential evapotranspiration methods

No.	Station name, Location	No.	Station name, Location	No.	Station name, Location
1	Five Points, U.S.A.	19	Buntigville, U.S.A.	37	De Laveaga, U.S.A.
2	Davis, U.S.A.	20	Temecula, U.S.A.	38	Westlands, U.S.A.
3	Firebaugh Teles, U.S.A.	21	Santa Ynez, U.S.A.	39	Sanel Valley, U.S.A.
4	Gerber, U.S.A.	22	Seeley, U.S.A.	40	Aachen, Germany
5	Durham, U.S.A.	23	Manteca, U.S.A.	41	Angermunde, Germany
6	Carmino, U.S.A.	24	Modesto, U.S.A.	42	Bremen-Seefahrtshule, Germany
7	Stratford, U.S.A.	25	Irvine, U.S.A.	43	Dresden-Klotzsche, Germany
8	Castorville, U.S.A.	26	Oakville, U.S.A.	44	Dusseldorf, Germany
9	Kettleman, U.S.A.	27	Pomona, U.S.A.	45	Frankfurt, Germany
10	Bishop, U.S.A.	28	Frenso State, U.S.A.	46	Hamburg Fuhlsbuettel, Germany
11	Parlier, U.S.A.	29	Santa Rosa, U.S.A.	47	Karlsrhue, Germany
12	Calipatria, U.S.A.	30	Browns Valley, U.S.A.	48	Muenchen-Flughafen, Germany
13	Mc Arthur, U.S.A.	31	Lindcove, U.S.A.	49	Stuggart-Schnarreberg, Germany
14	UC Riverside, U.S.A.	32	Meloland, U.S.A.	50	Alicante, Spain
15	Brentwood, U.S.A.	33	Alturas, U.S.A.	51	Badajoz Televera, Spain
16	San Luis Obispo, U.S.A.	34	Cuyama, U.S.A.	52	Valencia, Spain
17	Blackwells Corner, U.S.A.	35	Tulelake, U.S.A.	53	Zaragoza Aeropuerto, Spain
18	Los Banos, U.S.A.	36	Windsor, U.S.A.		

The time series processing along for the implementation of the different approaches for potential evapotranspiration estimation, i.e. Penman-Monteith, parametric and Hargreaves, was carried out using the free software application Hydrognomon (Kozanis et al. 2010, http://hydrognomon.org/), while the remaining expressions (Jensen, McGuiness and Oudin) were evaluated through spreadsheets.

4.5   Statistical criteria

The main statistical criterion used for the evaluation of the methodologies performance against the values computed by the Penman Monteith method (PM) was the coefficient of efficiency (CE), introduced by Nash & Sutcliffe (1970):

$$CE = 1 - \frac{\sum_{i=1}^{n}(PE_i - PM_i)^2}{\sum_{i=1}^{n}(\overline{PM} - PM_i)^2} \tag{21}$$

where PMi and PEi are the potential evapotranspiration values of month i, computed by the Penman-Monteith method and the other model respectively, $\overline{\text{PM}}$ is the monthly average over the common data period estimated by the Penman-Monteith formula while n is the sample size.

Additionally, we applied several statistical measures, such as the mean bias error:

$$\text{MBE} = \frac{1}{n} \sum_{i=1}^{n} (\text{PE}_i - \text{PM}_i) \tag{22}$$

the mean average error: $\text{MAE} = \frac{1}{n} \sum_{i=1}^{n} |\text{PE}_i - \text{PM}_i| \tag{23}$

and the root mean square error: $\text{RMSE} = \left[\frac{1}{n} \sum_{i=1}^{n} (\text{PE}_i - \text{PM}_i)^2 \right]^{1/2} \tag{24}$

CE ranges between $-\infty$ and 1 (1 inclusive), with CE = 1 being the optimal value. Values between 0 and 1 are generally regarded as acceptable levels of performance, whereas values less than 0 indicate that the mean observed value is a better predictor than the simulated value, which indicates unacceptable performance. MBE, MAE and RMSE values of 0 indicate a perfect fit (Moriasi et al. 2007).

4.6   Results

The implementation of the parametric model was accomplished by calculating the three parameters involved at each station, as mentioned above. This procedure is automated via a least square optimization technique, embedded in the Hydrognomon software (Kozanis et al. 2010, http://hydrognomon.org/), providing means for acquiring optimized values of a, b and c parameters for the parametric method application.

The calculated monthly Penman-Monteith potential evapotranspiration time series acted as the reference data sets against which the comparisons between the different methodologies took place. Table 12 summarizes the values of the parameters for each of the 53 stations, acquired by the procedure described above.

Table 12: Meteorological stations numbers and corresponding parameter values for the parametric method

Station No.	a (kg kJ^{-1})	b (kg m^{-2})	c (°C^{-1})	Station No.	a (kg kJ^{-1})	b (kg m^{-2})	c (°C^{-1})
1	$1.47\ 10^{-4}$	1.49	$1.58\ 10^{-2}$	28	$1.29\ 10^{-4}$	1.3	$1.73\ 10^{-2}$
2	$1.04\ 10^{-4}$	$6.51\ 10^{-1}$	$2.15\ 10^{-2}$	29	$8.88\ 10^{-5}$	$6.09\ 10^{-1}$	$2.63\ 10^{-2}$
3	$1.46\ 10^{-4}$	1.48	$1.47\ 10^{-2}$	30	$8.95\ 10^{-5}$	$4.07\ 10^{-1}$	$2.11\ 10^{-2}$
4	$1.02\ 10^{-4}$	$4.97\ 10^{-1}$	$1.93\ 10^{-2}$	31	$1.12\ 10^{-4}$	1.04	$1.74\ 10^{-2}$
5	$1.97\ 10^{-4}$	2.07	$-2.70\ 10^{-4}$	32	$2.12\ 10^{-4}$	2	$4.94\ 10^{-3}$
6	$8.82\ 10^{-5}$	$2.49\ 10^{-1}$	$2.34\ 10^{-2}$	33	$7.92\ 10^{-5}$	$-2.20\ 10^{-1}$	$2.44\ 10^{-2}$
7	$1.12\ 10^{-4}$	$-2.50\ 10^{-1}$	$1.44\ 10^{-2}$	34	$1.08\ 10^{-4}$	$4.03\ 10^{-1}$	$1.97\ 10^{-2}$
8	$1.68\ 10^{-4}$	1.06	$-3.60\ 10^{-2}$	35	$9.28\ 10^{-5}$	$5.20\ 10^{-2}$	$2.12\ 10^{-2}$
9	$1.34\ 10^{-4}$	1.23	$1.62\ 10^{-2}$	36	$8.65\ 10^{-5}$	$5.66\ 10^{-1}$	$2.60\ 10^{-2}$
10	$1.43\ 10^{-4}$	$7.39\ 10^{-1}$	$1.05\ 10^{-2}$	37	$1.02\ 10^{-4}$	$5.82\ 10^{-1}$	$1.24\ 10^{-2}$
11	$1.29\ 10^{-4}$	1.32	$1.61\ 10^{-2}$	38	$1.40\ 10^{-4}$	1.33	$1.67\ 10^{-2}$
12	$1.69\ 10^{-4}$	1.32	$8.86\ 10^{-3}$	39	$9.88\ 10^{-5}$	$6.54\ 10^{-1}$	$2.37\ 10^{-2}$
13	$9.75\ 10^{-5}$	$4.26\ 10^{-1}$	$2.36\ 10^{-2}$	40	$3.96\ 10^{-5}$	$-2.46\ 10^{-1}$	$2.62\ 10^{-2}$
14	$8.68\ 10^{-5}$	$5.10\ 10^{-2}$	$1.78\ 10^{-2}$	41	$3.96\ 10^{-5}$	$-2.58\ 10^{-1}$	$2.73\ 10^{-2}$
15	$1.11\ 10^{-4}$	$9.00\ 10^{-1}$	$2.09\ 10^{-2}$	42	$4.28\ 10^{-5}$	$-1.64\ 10^{-1}$	$2.68\ 10^{-2}$
16	$8.10\ 10^{-5}$	$1.60\ 10^{-1}$	$2.28\ 10^{-2}$	43	$3.67\ 10^{-5}$	$-3.45\ 10^{-1}$	$2.81\ 10^{-2}$
17	$1.21\ 10^{-4}$	1.02	$1.89\ 10^{-2}$	44	$4.12\ 10^{-5}$	$-3.02\ 10^{-1}$	$2.64\ 10^{-2}$
18	$1.31\ 10^{-4}$	1.31	$1.81\ 10^{-2}$	45	$4.75\ 10^{-5}$	$-8.8\ 10^{-2}$	$2.62\ 10^{-2}$
19	$9.29\ 10^{-5}$	$-1.10\ 10^{-1}$	$2.11\ 10^{-2}$	46	$4.18\ 10^{-5}$	$-1.66\ 10^{-1}$	$2.66\ 10^{-2}$
20	$6.66\ 10^{-5}$	$-2.80\ 10^{-1}$	$2.10\ 10^{-2}$	47	$4.64\ 10^{-5}$	$-6.6\ 10^{-2}$	$2.58\ 10^{-2}$
21	$9.44\ 10^{-5}$	$4.91\ 10^{-1}$	$2.06\ 10^{-2}$	48	$4.69\ 10^{-5}$	$-8.8\ 10^{-2}$	$2.51\ 10^{-2}$
22	$2.50\ 10^{-4}$	2.58	$7.52\ 10^{-4}$	49	$4.53\ 10^{-5}$	$-1.64\ 10^{-1}$	$2.52\ 10^{-2}$
23	$1.13\ 10^{-4}$	1.02	$2.03\ 10^{-2}$	50	$5.89\ 10^{-5}$	$-4.67\ 10^{-1}$	$1.84\ 10^{-2}$
24	$1.17\ 10^{-4}$	1.08	$2.00\ 10^{-2}$	51	$6.24\ 10^{-5}$	$1.72\ 10^{-1}$	$2.35\ 10^{-2}$
25	$6.64\ 10^{-5}$	$-4.40\ 10^{-2}$	$2.28\ 10^{-2}$	52	$5.34\ 10^{-5}$	$-1.93\ 10^{-1}$	$1.96\ 10^{-2}$
26	$8.42\ 10^{-5}$	$4.29\ 10^{-1}$	$2.54\ 10^{-2}$	53	$7.00\ 10^{-5}$	$-2.2\ 10^{-2}$	$2.39\ 10^{-2}$
27	$1.13\ 10^{-4}$	1.25	$2.00\ 10^{-2}$				

4.7 Comparison with radiation-based methods

Figure 17 presents the mean annual potential evapotranspiration calculated by the Penman-Monteith method for each one of the 39 CIMIS stations against the parametric and the other four methods. It is clear that the parametric, Hargreaves and McGuiness models respect the variation of

the over-annual potential evapotranspiration, while the other two models, i.e. Oudin and Jensen-Haise underestimate and overestimate respectively, the potential evapotranspiration values.
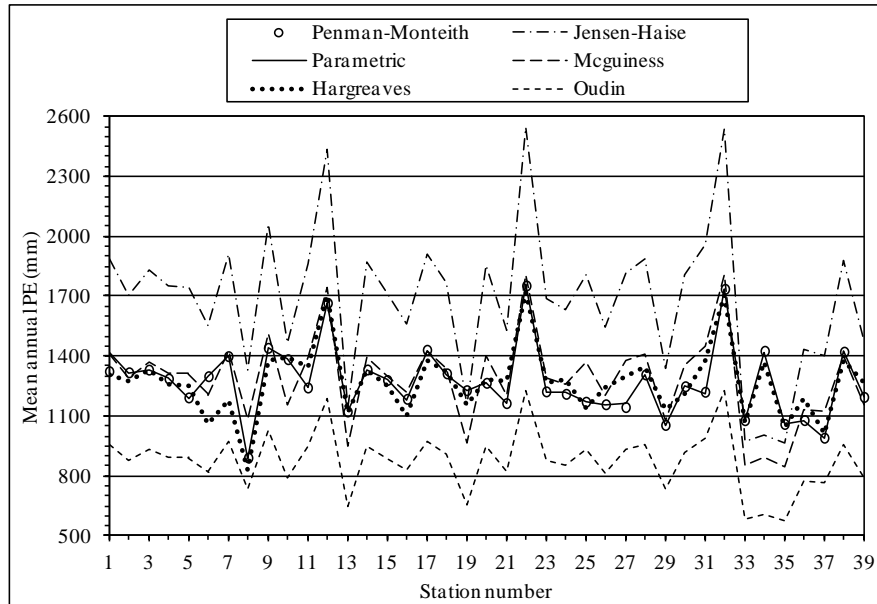
Figure 17. Mean annual Penman-Monteith potential evapotranspiration (symbols) for the 39 CIMIS stations against the parametric model and the other four methods

The performance indices presented in Table 13 confirm the good performance of the parametric method, which has the highest CE and excellent results in the other statistical indices. The Hargreaves model follows with CE 78.9%, similar MBE and worst MAE and RMSE than the parametric model. The McGuiness method gave moderate results, while the Jensen-Haise and Oudin models totally fail to represent the physical flux.

Table 13 Values of performance indices used to evaluate the parametric method, in the estimation of mean annual potential evapotranspiration for the 39 CIMIS stations, against the other four models

Method	CE (%)	MBE (mm)	MAE (mm)	RMSE (mm)
Parametric	99.1	4	6	17
Hargreaves	78.9	2	60	82
Jensen-Haise	< 0	417	452	493
McGuiness	30.1	19	111	149
Oudin	< 0	-393	393	411

For further comparison of the parametric method against the four radiation-based methods, in terms of the achieved CE distribution from estimating monthly PE, each time series was split into two parts. The first 13 years were used as the calibration data set for the parametric model, while the remaining 7 years were used for validation. Table 14 presents the CE distribution, for the

calibration (Cal) and the validation (Val) data set for 39 CIMIS stations, while that of the European stations is presented in Table 15.

Table 14 Distribution of CE values of radiation-based approaches in CIMIS network

CE (%)	Parametric		Hargreaves		Jensen-Haise		McGuiness		Oudin	
	Cal	Val	Cal	Val	Cal	Val	Cal	Val	Cal	Val
95-100	26	26	26	23	0	7	16	15	0	0
90-95	11	5	10	7	0	2	6	7	0	0
80-90	2	8	3	9	1	2	10	10	1	0
70-80	0	0	0	0	6	3	3	3	3	5
60-70	0	0	0	0	1	6	2	3	7	4
50-60	0	0	0	0	3	4	1	1	12	6
0-50	0	0	0	0	16	9	1	0	16	24
<0	0	0	0	0	12	6	0	0	0	0

The results for both periods and in different climatic regimes are satisfactory for the parametric model, with the average CE values for the calibration period being 94.80% for CIMIS stations and 96.52% for European stations, while for the validation period the corresponding values are 94.34% for CIMIS stations and 90.06% for the European stations. Altogether, the application of the parametric model in 26 stations from the 39 stations achieved CE values between 90 and 95%.

Table 15 Distribution of CE values of radiation-based approaches in European stations

CE	Parametric		Hargreaves		Jensen-Haise		Mcguiness		Oudin	
	Cal	Val	Cal	Val	Cal	Val	Cal	Val	Cal	Val
95-100	10	9	6	0	0	0	0	0	9	1
90-95	4	4	4	6	0	0	0	0	2	8
80-90	0	0	3	7	0	0	0	0	0	2
70-80	0	0	1	1	0	0	7	1	1	1
60-70	0	0	0	0	0	0	3	1	1	1
50-60	0	0	0	0	0	0	3	1	1	0
0-50	0	1	0	0	5	1	2	9	0	1
<0	0	0	0	0	9	13	1	2	0	0

The Hargreaves model achieved satisfactory results especially in the case of CIMIS network, where the model has been developed; while in European stations the acquired CE values are lower.

The McGuiness model acquired lower CE values in the CIMIS network than Parametric and Hargreaves with 87.14% in calibration period and 87.76% in the validation period. The Oudin model presented moderate results in the CIMIS network (52.18% in the calibration and 46.82% in the validation period) but considerably better results in European stations (89.37 % calibration and 82.82% validation period). By taking into account the similar results presented by Tegos *et al.* (2013), the Oudin model seems to perform better in humid than in arid climatic conditions.

Finally, the Jensen-Haise model totally failed to produce physically meaningful results, since the achieved CE values were very low (Table 13Table 14Table 15).

4.8   Comparison with temperature-based methods

The performance of the parametric model with two well-known empirical formulas of Thornthwaite and Blaney-Criddle (Table 16Table 17) was compared. Both approaches have wide application in data-scarce regions. In the CIMIS network the average CE for the Thornthwaite model was 20.53% for the calibration period and less than zero in the validation period, while in European stations the CE is 84.58% (calibration) and 78.27% (validation). The Blaney-Criddle method achieved average CE 69.99% (calibration), 69.82% (validation) in the CIMIS network and 15.69% (calibration) and <0 (validation) in European stations. Finally, the Thornthwaite model seems to be suitable for use in cold and humid climates (94.84% CE in German stations for the calibration period) and improper in arid regimes, while for the Blaney-Criddle model the opposite occurs.

Table 16 Distribution of CE values of temperature-based approaches in CIMIS network

CE	Thornthwaite		Blaney-Criddle	
	Cal	Val	Cal	Val
95-100	0	0	0	0
90-95	0	0	0	0
80-90	0	0	10	16
70-80	0	0	18	12
60-70	1	0	5	5
50-60	4	3	2	1
0-50	24	21	3	4
<0	10	15	1	1

Table 17 Distribution of CE values of temperature-based approaches in European stations

CE	Thornthwaite		Blaney-Criddle	
	Cal	Val	Cal	Val
95-100	5	0	0	0
90-95	5	1	0	0
80-90	0	9	0	0
70-80	2	1	1	1
60-70	0	1	0	0
50-60	1	1	0	1
0-50	1	1	12	1
<0	0	0	1	11

4.9   Spatial analysis of the parameters

The knowledge of the spatial variability of the PET is crucial in geosciences and the use of the appropriate interpolation technique significant (Mancosu *et al*. 2014) The key idea of the parametric model is the replacement of some of the variables and constants that are used in standardized Penman-Monteith formula by three parameters, which are regionally varying and estimated through calibration using a reference evapotranspiration data set.

In this context, two applications are implemented. The first is the analysis of the parameters' correlation to latitude and elevation, while the second is their estimation, through spatial interpolation techniques, along an extensive study area such as California, which provides sufficient data to perform the necessary calibration procedures.

4.10   Correlation to latitude and elevation

Through regression analysis, the correlation of every parameter (a, b, c) with latitude φ and elevation was investigated. Six scatter plots of Figure 18 show that parameters a, b are negatively correlated to latitude and elevation, in contrast to parameter c. This is similar to the findings of the previous study over the Greek territory (Tegos *et al.* 2013) for parameter a. It also appears a noticeable correlation of parameter b with elevation (R = –0.50) and insignificant correlation of parameter c with elevation and latitude. Furthermore, Figure 18 shows that the relation of the three parameters to latitude and elevation is far from linear.
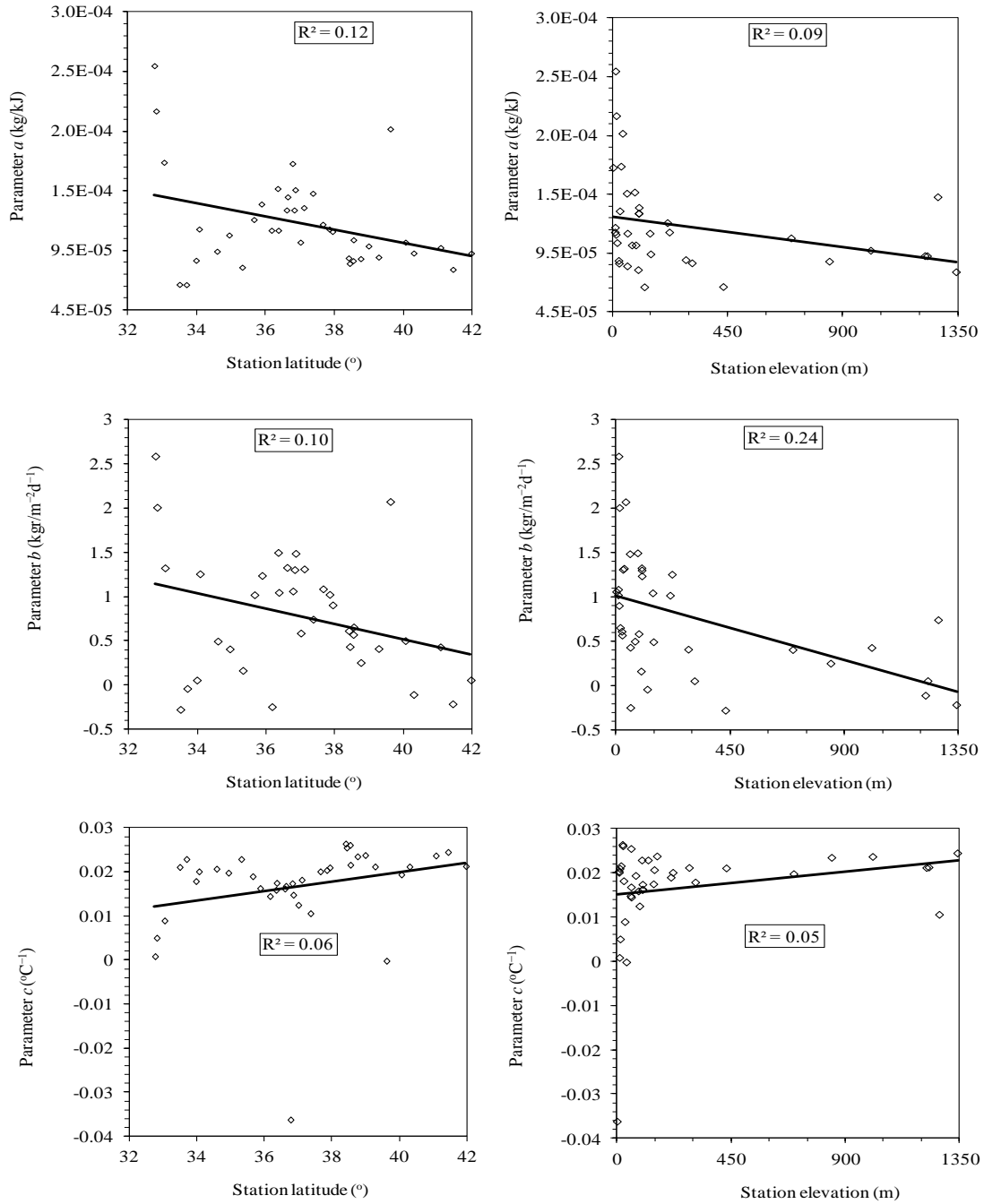
Figure 18. Scatter plots of parameters against latitude and elevation

4.11 Spatial interpolation over California

Currently, a lot of methods exist which can accomplish spatial interpolation using available computer codes. In the present study, the three parameters' spatial variability was investigated by

four different methodologies: (1) Inverse Distance Weighting (IDW); (2) Natural Neighbours (NaN); (3) Ordinary Kriging (OK); and (4) Bilinear Surface Smoothing (BSS)

The first three are well established and commonly used in spatial interpolation of environmental variables (Li and Heap, 2008). The Bilinear Surface Smoothing methodology is a new approach that approximates a surface that may be drawn for the data points with consecutive bilinear surfaces which can be numerically estimated by means of a least squares fitting procedure into a surface regression model with known break points and adjustable weights defined by means of angles formed by those bilinear surfaces. The BSS theory and basic features are presented in Malamos and Koutsoyiannis (2015) while applications and field validation are presented in Malamos and Koutsoyiannis (2015) . BSS is implemented by means of a dynamic link library in Object Pascal (Delphi) programming language linked to MS-Excel. The parameter estimation is based on the generalized cross-validation methodology as described in Malamos and Koutsoyiannis (2015-a). The obtained optimal values of the four adjustable parameters: the number of intervals according to x and y directions, i.e. mx, my and the corresponding smoothing parameters $\tau\lambda x$ and $\tau\lambda y$, are presented in Table 18:

Table 18 BSS parameters optimal values for the CIMIS network (California area)

Parameter	mx	my	$\tau_{\lambda x}$	$\tau_{\lambda y}$
a (kg kJ^{-1})	3	8	0.082	0.001
b (kg m^{-2})	3	28	0.001	0.01
c (°C^{-1})	3	8	0.001	0.001

IDW and NaN were implemented in ESRI's ArcGIS environment using the default settings, while for OK all semivariogram models available in that software were investigated, i.e. circular, exponential, spherical, linear and Gaussian,. In every case, the embedded fitting procedure ensured the minimization of the weighted sum of squares between experimental and model semivariogram values.

Table 19 presents the values of the statistical criteria for each one of the implemented semivariogram models, sorted according to the CE criterion for each of the three parameters. It is obvious that the circular semivariogram achieved the best overall performance.

Table 19 Values of the statistical criteria used to assess the performance of the different kriging semivariogram models

Parameter	kriging semivariogram	CE (%)	MBE	MAE	RMSE
a $(kg\ kJ^{-1})$	circular	99.9	$1.03\ 10^{-8}$	$5.18\ 10^{-7}$	$8.93\ 10^{-7}$
	exponential	99.9	$1.03\ 10^{-8}$	$5.18\ 10^{-7}$	$8.93\ 10^{-7}$
	linear	99.9	$1.03\ 10^{-8}$	$5.18\ 10^{-7}$	$8.93\ 10^{-7}$
	spherical	99.9	$1.03\ 10^{-8}$	$5.18\ 10^{-7}$	$8.93\ 10^{-7}$
	gaussian	44.6	$1.24\ 10^{-6}$	$1.86\ 10^{-5}$	$2.88\ 10^{-5}$
b $(kg\ m^{-2})$	exponential	72.8	$3.12\ 10^{-3}$	$2.50\ 10^{-1}$	$3.43\ 10^{-1}$
	circular	68.6	$4.24\ 10^{-3}$	$2.71\ 10^{-1}$	$3.68\ 10^{-1}$
	spherical	67.4	$5.46\ 10^{-3}$	$2.77\ 10^{-1}$	$3.76\ 10^{-1}$
	linear	66.6	$6.00\ 10^{-3}$	$2.81\ 10^{-1}$	$3.80\ 10^{-1}$
	gaussian	29.7	$4.09\ 10^{-2}$	$4.07\ 10^{-1}$	$5.51\ 10^{-1}$
c $(°C^{-1})$	circular	39.3	$3.56\ 10^{-4}$	$4.62\ 10^{-3}$	$8.19\ 10^{-3}$
	spherical	11.7	$4.64\ 10^{-4}$	$5.60\ 10^{-3}$	$9.88\ 10^{-3}$
	exponential	11.0	$4.67\ 10^{-4}$	$5.62\ 10^{-3}$	$9.92\ 10^{-3}$
	linear	11.0	$4.67\ 10^{-4}$	$5.62\ 10^{-3}$	$9.92\ 10^{-3}$
	gaussian	11.0	$4.67\ 10^{-4}$	$5.62\ 10^{-3}$	$9.92\ 10^{-3}$

All three parameters of the parametric model were estimated over California by applying the four spatial interpolation methods. The input data set consists of the calculated parameters values at the 39 CIMIS stations (Figure 19, Table 3).
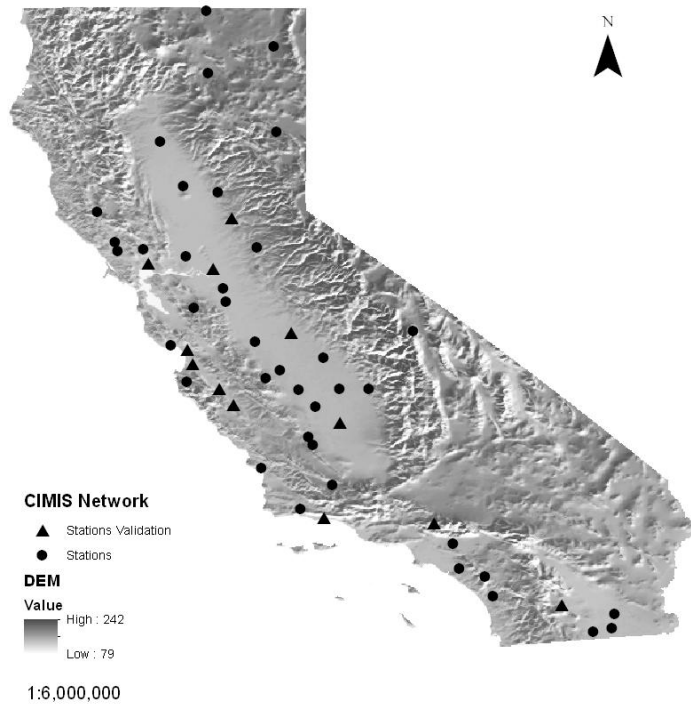
Figure 19 Study area and the CIMIS Stations used for spatial analysis

Table 20 presents the values of the statistical criteria used to assess the performance of the spatial interpolation methods with respect to the input data set. It is apparent that both non-geostatistical methods, according to the statistical criteria used, outperform ordinary kriging and bilinear surface smoothing, which performed similarly. This is not a surprise because both IDW and NaN, from construction, use as best local predictor the available data points (Li and Heap, 2008).

Table 20 Values of the statistical criteria used to assess the performance of the spatial interpolation methods with respect to the input data set

Parameter	Interpolation Method	CE (%)	MBE	MAE	RMSE
a (kg kJ^{-1})	IDW	100	$3.59\ 10^{-8}$	$1.08\ 10^{-7}$	$1.97\ 10^{-7}$
	NaN	100	$-1.03\ 10^{-7}$	$4.77\ 10^{-7}$	$8.95\ 10^{-7}$
	OK	99.9	$1.03\ 10^{-8}$	$5.18\ 10^{-7}$	$8.93\ 10^{-7}$
	BSS	73.2	$4.36\ 10^{-8}$	$1.35\ 10^{-5}$	$2.01\ 10^{-5}$
b (kg m^{-2})	IDW	100	$2.95\ 10^{-4}$	$1.72\ 10^{-3}$	$3.06\ 10^{-3}$
	NaN	99.9	$-9.48\ 10^{-4}$	$1.16\ 10^{-2}$	$2.12\ 10^{-2}$
	OK	68.6	$4.24\ 10^{-3}$	$2.71\ 10^{-1}$	$3.68\ 10^{-1}$
	BSS	65.2	$1.97\ 10^{-4}$	$2.68\ 10^{-1}$	$3.88\ 10^{-1}$
c $(°\text{C}^{-1})$	IDW	100	$2.56\ 10^{-7}$	$8.82\ 10^{-6}$	$1.52\ 10^{-5}$
	NaN	99.9	$1.54\ 10^{-6}$	$1.50\ 10^{-4}$	$3.10\ 10^{-4}$
	OK	39.3	$3.56\ 10^{-4}$	$4.62\ 10^{-3}$	$8.19\ 10^{-3}$
	BSS	68.9	$-2.57\ 10^{-7}$	$3.25\ 10^{-3}$	$5.87\ 10^{-3}$

However, the above statistical indices may not be representative with respect to the validity of the interpolation results in other locations, except for those incorporated in the interpolation procedure. In this context, a validation procedure was implemented by means of comparing the reference potential evapotranspiration estimates acquired from the implementation of the parametric method, using the parameter estimates of the four interpolation methods, against those of the eleven additional CIMIS stations with adequate time series length, shown in Table 21 along with the estimated parameter values, in the case of IDW.

Table 21 CIMIS Stations used for validation purposes and estimated parameters values in the case of IDW

Station	a (kg kJ^{-1})	b (kg m^{-2})	c (°C^{-1})
Arroyo Seco	$1.38\ 10^{-4}$	1.06	$1.20\ 10^{-3}$
Carneros	$9.10\ 10^{-5}$	$5.48\ 10^{-1}$	$2.42\ 10^{-2}$
Green Valley Road	$1.16\ 10^{-4}$	$7.75\ 10^{-1}$	$7.26\ 10^{-3}$
King City Oasis	$1.34\ 10^{-4}$	1.09	$9.53\ 10^{-3}$
Santa Barbara	$1.03\ 10^{-4}$	$5.56\ 10^{-1}$	$1.98\ 10^{-2}$
Alpaugh	$1.23\ 10^{-4}$	$8.27\ 10^{-1}$	$1.67\ 10^{-2}$
Auburn	$1.04\ 10^{-4}$	$6.20\ 10^{-1}$	$1.99\ 10^{-2}$
Borrego Springs	$1.73\ 10^{-4}$	1.44	$9.33\ 10^{-3}$
Lodi West	$1.10\ 10^{-4}$	$8.54\ 10^{-1}$	$2.05\ 10^{-2}$
Merced	$1.30\ 10^{-4}$	1.20	$1.73\ 10^{-2}$
Palmdale	$1.01\ 10^{-4}$	$7.86\ 10^{-1}$	$2.00\ 10^{-2}$

The performance of each method is presented in Table 22, which summarizes the CE values acquired from the validation procedure. It is apparent that IDW outperforms the other three methods in the majority of the cases. This is an interesting fact, since the IDW method is the effortless of the four methodologies. On the other hand, the BSS performance is analogous or better to that of the input data setdata set. NaN and OK performed similarly, with the first achieving slightly superior outcome, since OK in the case of Borrego Springs resulted in negative CE value.

Table 22 CE values for every interpolation method in validation procedure stations

Station	IDW	NaN	OK	BSS
Arroyo Seco	77.7	78.9*	76.8	66.8
Carneros	96.1	96.2*	83.6	95.9
Green Valey Road	71.6*	69.5	70.2	65.7
King City Oasis	85.1	60.3	93.6*	64.3
Santa Barbara	47.9	72.4	78.2*	23.4
Alpaugh	95.7	95.5	96.0*	95.9
Auburn	94.4*	93.6	94.3	85.8
Borrego Springs	85.3*	81.3	<0	70.1
Lodi West	94.0*	93.7	92.9	92.3
Merced	96.9	97.1*	96.9	89.5
Palmdale	69.6	70.3	91.1*	56.0

The variation of the three parameters over California produced by the IDW technique is illustrated in Figure 20. It is apparent that both a and c present an increasing North to South gradient, while

the opposite occurs for parameter b. This remark coincides with the previous findings concerning the relation of the three parameters to latitude.
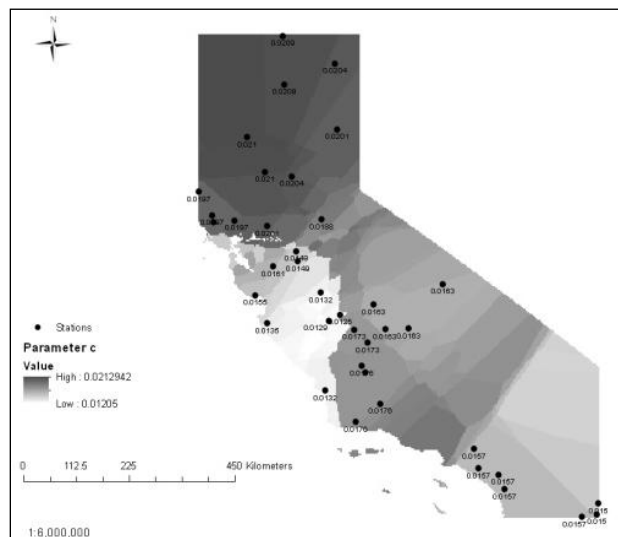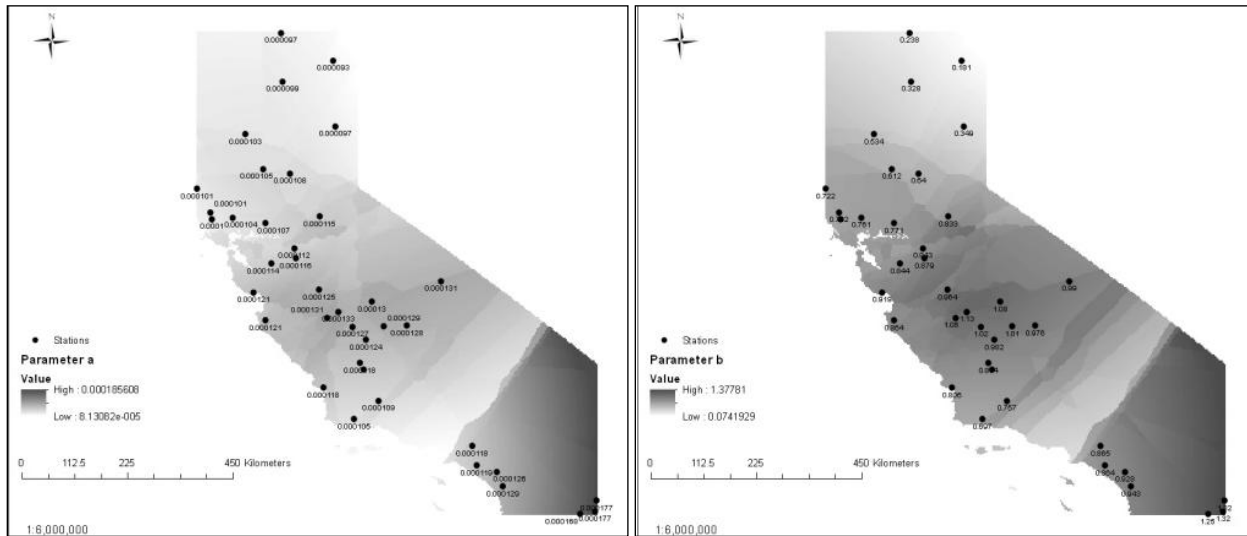
Figure 20 Parameters maps produced by the IDW method, for the California region

4.12 Discussions and Conclusions

The parametric model is a parsimonious radiation-based and physically consistent approach derived from a simplification of the Penman-Monteith equation, which requires three parameters to be calibrated prior to its application. By systematic application of the method the parameters can be eventually provided by maps.

The comparison, on the basis of monthly and annual evapotranspiration data, with commonly used radiation-based models (Hargreaves, McGuiness, Jensen-Haise and Oudin models) and

temperature-based models (Thorthwaite and Blaney-Criddle), verified the parametric model's high efficiency in different climatic regimes.

A parameters analysis, through regression techniques, was conducted in order to investigate their correlation to latitude and elevation variation. Moreover, the parameters' spatial estimation was accomplished by implementing interpolation techniques such as: Inverse Distance Weighting (IDW), Natural Neighbours (NaN), Ordinary Kriging (OK) and Bilinear Surface Smoothing (BSS), along an extensive study area such as California. The validation procedure was implemented by comparing the reference potential evapotranspiration estimates acquired from the implementation of the parametric method, using the parameter estimates of the four interpolation methods, against those of the eleven additional CIMIS stations. This combined evaluation of the four different interpolation approaches, indicated that the simple and effortless IDW method performs better than the other three methodologies. Regarding the application of the new methodology, BSS's efficiency to perform interpolation between data points that are interrelated in a complicated manner was confirmed, acquiring high CE values analogous to those of the other three methods.

Overall, the key idea of the parametric model methodology, which is the simplification of the Penman-Monteith formula by introducing three parameters, which are regionally varying and estimated through calibration using a reference evapotranspiration data set, was very successful.

5 Global PET maps based on monthly remote temperatures

5.1 Introduction

Evapotranspiration (ET) is a crucial element of the hydrological cycle affecting a wide range of geosciences, since it is referred as the combined water losses from soil surface and vegetation influence by several meteorological variables such as the air temperature, the solar radiation, the wind speed and the relative humidity. The literature proposes several approaches to quantify the process in terms of actual evapotranspiration, potential evapotranspiration (PET) or reference evapotranspiration. By definition the PET refers to "the rate at which evapotranspiration would occur from a large area completely and uniformly covered with growing vegetation, which has access to an unlimited supply of soil water, and without advection or heating effects" (Dingman, 1994), and differs to Actual Evatranspiration based on the soil water supply mainly driven by the precipitation regime.In the last decades advanced methods were introduced for the ET and PET estimation with the most recent being the remote sensing techniques incorporating aerial and satellite imagery. Generally, the classification of the remote sensing for ET assessment includes four groups referred to as empirical, direct, residual, inference and deterministic models (Nouri et al., 2013). The most well-known approach for the actual evapotranspiration estimation for daily and monthly time step is the modified surface energy balance algorithm for land (SEBAL) model [Bhattarai, *et al*, 2012]. A limited number of studies have focused on the global PET assessment utilizing remote sensing tools. Specifically, the global distribution of potential evaporation has been calculated from the Penman-Monteith equation using satellite and assimilated data for a 24-month period, i.e. January 1987 to December 1988 (Choudhury., 1997).

The Parametric model is a radiation-based model that requires only temperature data and utilizes a parsimonious expression for the potential evapotranspiration (PET) estimation. It replaces some of the variables and constants that are used in the standard Penman-Monteith model by regionally varying parameters, which are estimated through calibration (Tegos et al., 2015). The large scale Parametric model application was satisfactory and the models outperform the efficiency of a number of simplifies models such as Hargeaves, Thorthwaite, Oudin, Jensen-Haise.

In this study a new global PET monthly dataset is introduced, by applying the Parametric model using the remote sensing data (LANDSAT) of mean air temperature provided by the Goddard Space Flight Center NASA, Global Land Data Assimilation System, NOAA. As the majority of global applications refer to the actual evapotranspiration assessment (Mu et al, 2011, Ghilain and Gellens-Meulenberghs 2014, Vinukollu *et al*. 2011, Yuan *et al.* 2010) this dataset will contribute to hydrological balance modelling and agrometeorological applications.

5.2 Materials and Methods

The Parametric model employs physically consistent parameters distributed over the globe, overcoming the main weakness of the Penman-Monteith model which is the necessity of

simultaneous observations of four meteorological variables (Tegos *et al.* 2007, Tegos *et al.* 2013, Tegos *et al.* 2015, Tegos *et al* 2015, Tegos *et al.* 2017).

The modified Parametric model implements two instead of three parameters (parameter a' in the numerator and parameter c' in the denominator) by the formula (9).

The model was applied globally using calibrated values of parameters a' and c' at the locations of the 4088 stations of the FAO-CLIMWAT database (Figure 21), which provides monthly data of the required variables for PET estimation. These values were interpolated over the globe using the inverse distance weighting (IDW) technique into a geographical information system (GIS). The extraterrestrial radiation (Ra) monthly raster datasets were derived by using an analytical mathematical expression (Tegos *et al.* 2017), while the mean air temperature values, covering a period from 1973 to 2016, were acquired as raster datasets from the Goddard Space Flight Center NASA, Global Land Data Assimilation System. All three layers of information were embedded in GIS and constituted a framework that permitted quality control screening by application of logical thresholds in order to minimize the extreme (outliers) PET values.
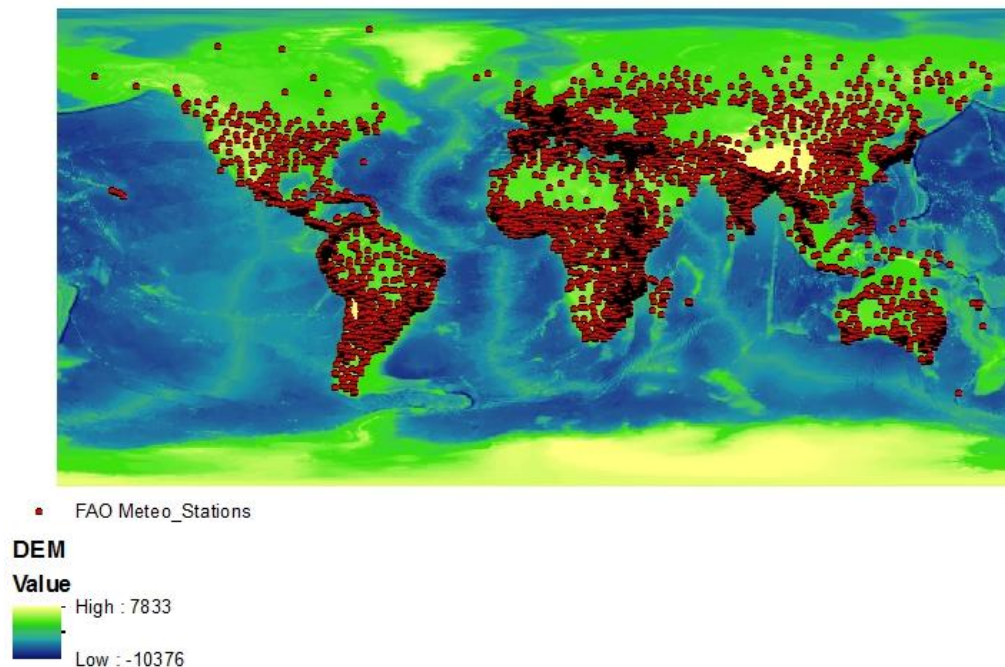
Figure 21 CLIMWAT meteorological stations network.

The maps obtained using the parametric method (PET/PAR) were produced in a GIS environment by applying equation (1) with the required raster datasets, i.e. parameters a' and c', extra-terrestrial radiation Ra, and monthly mean air temperature T.

5.3   Results

PET Global mapping

Following the above presented procedures, a monthly PET global dataset was produced covering a significant time period. Figure 22Figure 23Figure 24 visualize the PET distribution for representative months across the continents.

Specifically, Figure 22 presents the PET map of Eurasia for August, where PET values range from 0 to 15 mm day^{-1}, increasing from north to south. The latter is well explained from the similar variation of temperature and extraterrestrial radiation. The highest values were observed at the Middle East where extremely arid climatic conditions occur.
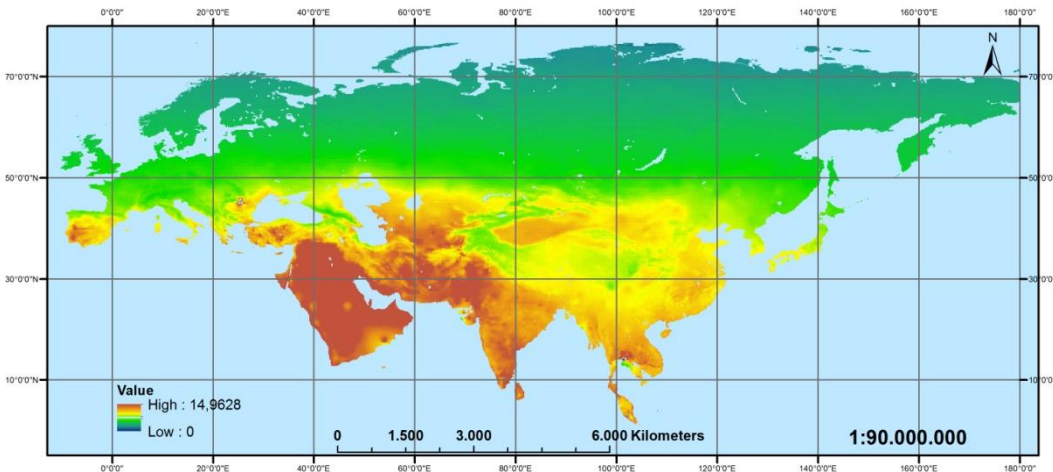
Figure 22 Eurasia PET map for August (PET: mm/day)

Figure 23 portays the PET pattern in North America for May. A pattern similar to Eurasia is obvious with highest values at regions near the equator (e.g. Mexico) ,and lowest in Canada and Alaska and Greenland. PET variability in South America in January with values decreasing from north to south. Some inconsistencies in the area of Amazon and some peculiarly low values in the area of equator can be explained from the limitations of the Parametric model to represent the combined effect on PET estimation of relative humidity and wind speed, which are key drivers of the evapotranspiration processes across these areas, influencing the net incoming solar radiation and the evaporation demand, as detailed in Tegos *et al.* (2017).
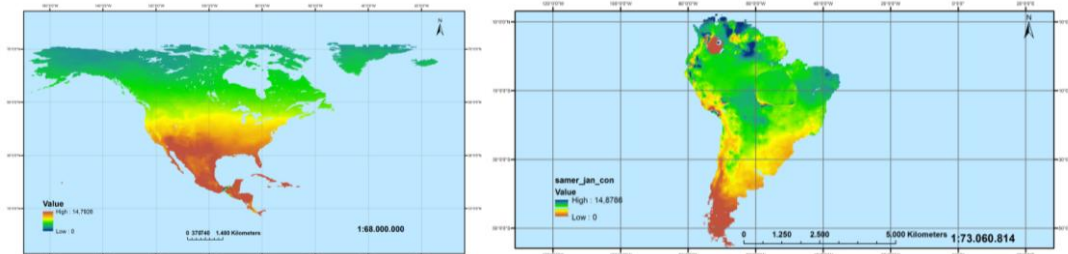
Figure 23 North America PET map for May- South America PET map for January (PET: mm/day)

PET variability over Africa in January is shown in Figure 24. High monthly PET values were acquired in the equatorial zone, mainly in the lower Congo, where the hydro-meteorological

observations were limited during the parametric model calibration. The decreasing trend from south to north in Oceania follows the pattern of radiation and air temperature variation.
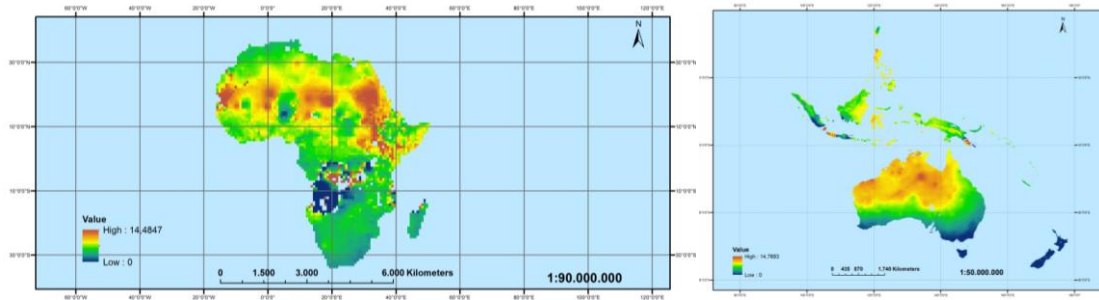
Figure 24 Africa/Oceania PET map for January-Oceania PET for December (PET: mm/day)

5.4 Validation

For identifying the efficiency of the PET remote sensing dataset we compared PET/PAR monthly sample the against a Penman Monteith timeseries, estimated at the Davis station of the well-known PET data of CIMIS network. The validation was carried out for 3-years periods from 1/2010 to 12/2012 and the coefficient of efficient (CE) was satisfactory equal to 87.6%.

5.5 Further PET improvements

Having reviewed new remote monthly temperature dataset which are recently freely available, we reassessed the monthly PET with a recently published monthly dataset which provides high global temperature accuracy (Hooker *et al*. 2018).

Following the above mentioned framework the monthly PET maps were produced and a first validation with site meteorological estimate for the Davis station is shown in Figure 25. The preliminary results are very satisfactory since the coefficient of efficiency is 93.2%. The new monthly PET dataset based on remote monthly temperature is named RASPOTION and is object for further validation across the globe.
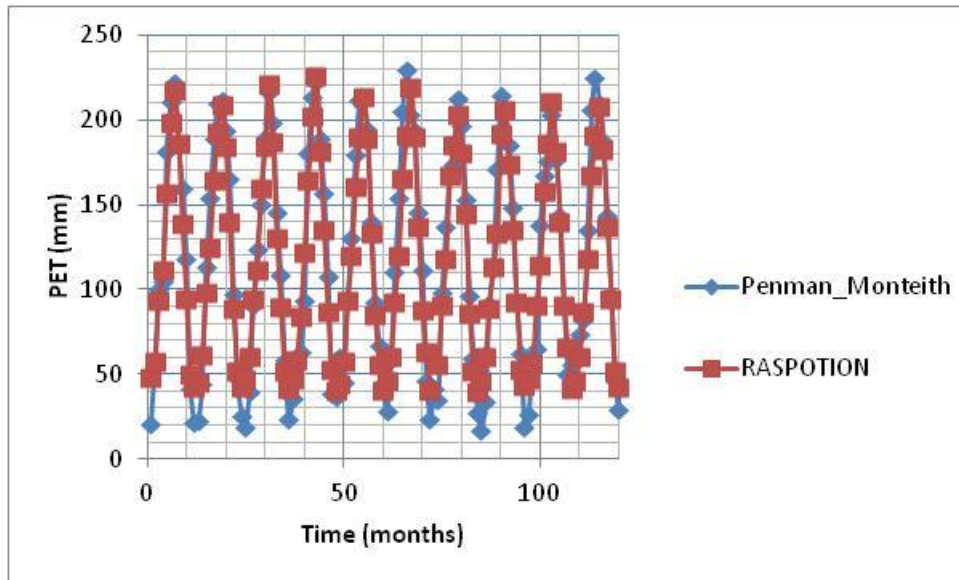
Figure 25 Monthly PM point vs RASPOTION estimate (Davis Station)

5.6   Discussion

In some areas with high values of relative humidity and wind speed, the existing PET parametric approach fails to reproduce efficiently the PET regime and further improvements of the parametric approach are recommended locally.

In some areas the FAO-CLIMWAT data were scarce and poor (i.e Brazil and Rebublic of Congo). In these areas the calibrated parameter a' and c' are indicative and further calibration should take place.

In every case, hydrologists, agronomists and other scientists of potential interest for this dataset could make efficient use of it, in about 80% of the earth's territory based on our previous studies (Tegos *et al.* 2015, Tegos *et al.* 2017). The new datasets could provide positive benefits in the scientific disciplines by taking in to account the global PET datasets are non available, thus is of interest:

In the applications of physical –based hydrological model which use as PET as an input descriptor of the sub-catchment, since we are moving forward in global scale hydrological models.

In the crop demand assessment since the integration of the monthly PET and the cropping pattern quantify the monthly water needs at each type of plant.

5.7   Conclusions

As part of the PET Parametric model, a new global PET monthly dataset based on remote sensing temperature data was introduced covering the period 1973-2016. This global dataset was extracted

using the Parametric formula which uses as input variables the extraterrestrial radiation and the mean air temperature. The latter have been taken from a freely available dataset provided by NASA. Further analysis was made with new temperature dataset resulting a new promising PET dataset namely RASPOTION. Previous analyses with this approach showed satisfying performance, through validation under several climatic regimes and different validation procedures. In regions where the available hydro-meteorological information was scarce or insufficient, the modelling results were weak in terms of PET's physical interpretation. In these areas the PET/PAR should be used with caution. Overall, for the majority of the Earth's globe surface a reliable monthly PET dataset is compiled and is freely available to scientists across different research disciplines in order to assist decisions for both short- and long-term hydro-climatic policy actions.

6 Investigation of long-term persistence in PET

6.1 A summary on the long-term persistence behaviour

The high complexity and uncertainty of climate dynamics has been long identified through plain observations as well as extended analyses of hydrometeorological processes such as temperature, humidity, surface wind, precipitation, atmospheric pressure, river discharges etc. Particularly, all these processes from global and local scale analyses seem to exhibit the so-called clustering behaviour (Dimitriadis, 2017). Interestingly, this HK behaviour has been first identified in Nature by Hurst (1951) while analyzing water levels from the Nile for optimum dam design. However, the mathematical description and analysis of this behaviour through a power-law autocorrelation function (vs. lag) is attributed to Kolmogorov (1940) who developed it earlier while studying turbulence. To give credits to both scientists Koutsoyiannis (2010) named this behaviour as Hurst-Kolmogorov (HK) behaviour (Dimitriadis, 2017).

6.2 Introduction

Trend estimation in hydro-climatic time series has focused the attention of the scientific community (Sen, 2013). Many studies have examined the trend of precipitation, streamflow, groundwater regime, temperature, potential evapotranspiration both in annual and seasonal basis (Markonis *et al.* 2016, Stevens *et al.* 2016, Panda *et al.* 2012, Arora *et al.* 2005, Kumar *et al.* 2010). Specifically, trend estimation in the potential or actual evapotranspiration pay the attention of the researchers (Gocic and Trajkovic, 2014, Mo *et al.* 2015, Tabari *et al.*, 2011). Generally, the trend results are mixed across different climatic regions, as Tabari *et al* (2011) found a positive trend for 70% of 20 Iranian meteorological stations during the period 1996-2005, Gocic and Trajkovic (2014) calculated a significant increasing downward trend in 70% of 12 Serbian meteorological stations (study period 1980-2010). Finally, Mo *et al.* 2015, by investigating the areal evapotranspiration in China for the period 1981-2010 with remote sense data, observed an increasing trend from the 1980s to the mid-1990s, followed by a decreasing trend. For the examination of the physical variability, the Mann-Kendall under the independence assumption has been proposed as a standard statistical measure for the evaluation and the quantification of the trends (Ahn and Palmer, 2015).

Furthermore, different statistical methodologies have developed and proposed, namely the Mann–Kendall under the Markovian behavior assumption after trend-free pre-whitening, the Mann–Kendall with complete autocorrelation structure and the Mann–Kendall under the long-term persistence assumption (Kumar *et al.* 2009). The latter test, proposed by Hamed (2008) offers a consistent framework to consider the Hurst phenomenon, which is observed in many climatological and hydrological processes, resulting in the increase of physical variability (Koutsoyiannis 2003; Koutsoyiannis and Montanari 2007). Hurst coefficient was first introduced by engineer Harold Hurst during the design of the Aswan reservoir (Sutcliffe *et al.* 2016) and plays a significant role in

the hydrological variability (O'Connell *et al*, 2016). Its presence in large measured hydrometeorological samples is ubiquitous (Iliopoulou *et al.* 2016) Comparative analysis of different trend model shows significant differences in the totally results (Hamed 2008, Kumar *et al.* 2009) and thus a physical consistent framework is needed.

The following chapters present an R function embedded in an automatic and user-friendly environment following modern views of water resources modeling tools (Guo *et al.* 2016, Turner and Ganelli 2016). The package implements the modified Hamed's (2008) framework and the procedure is tested in annual parametric PET time series from 10 sites in Greece, which cover the period 1950-2000.

6.3 Materials and methods

6.3.1 Mann-Kendall test under the scaling hypothesis

The Mann-Kendall test under the scaling hypothesis consists of three consecutive hypothesis tests, namely O (Original MK test), H (Hurst Parameter test) and M. The mathematic background and framework are presented from Hamed (2008). Let H0i denote the null hypothesis of each test and let H1i denote the alternative hypothesis, where i = O, H, M denotes the step of the Mann-Kendall test under the scaling hypothesis. We define:

H0O: No trend under the independence assumption

H1O: Significant trend under the independence assumption.

H0H: No significant LTP.

H1H: Significant LTP.

H0M: No trend under LTP assumption.

H1M: Significant trend exists under LTP assumption.

Then the three steps of the test are summarized by the following sequences

{H0O}: No trend.

{H1O}: Possible significant trend. Proceed to step H.

{H1O, H0H}: Significant trend exists.

{H1O, H1H}: Possible LTP effect. Proceed to step M.

{H1O, H1H, H0M}: No trend.

{H1O, H1H, H1M}: Significant trend exists.

Hurst coefficient can be defined by a simple power-law relationship of its standard deviation:

$$\sigma^\kappa = \kappa^{H-1}\sigma$$

(25)

where $\sigma \equiv \sigma(1)$ and H is the entropy production in logarithmic time (Koutsoyiannis 2011), and the parameter ranges between 0 and 1. For values H > 0.5, the process exhibits long-term persistence, while for H < 0.5 the process is anti-persistent.

For the test implementation, the R function MannKendallLTP from the HKprocess R package (Tyralis, 2015) was used. The R function computes the p-value in each step of the test. If the p-value is higher than a predefined significance level α (e.g. α = 0.05), then we cannot reject H0. A p-value less than or equal to α gives evidence that H1 is true.

6.3.2   Study area and procedures

Ten meteorological stations (National Meteorological Services of Greece) well- distributed over Greece were used. Table 23 presents the list of the meteorological stations used in our study.

Table 23. Meteorological stations with their latitude (φ^o) and elevation (z).

Stations	$\varphi(^o)$	z (m)
Heraklion	35.20	39
Ioannina	39.42	484
Kavala	40.54	63
Kerkyra	39.37	2
Kozani	40.18	626
Larissa	39.39	74
Lemnos	39.54	17
Methoni	36.50	34
Skyros	38.54	5
Tripoli	37.32	663

Based on our previous study (Tegos *et al*. 2013) the parametric model was calibrated and tested in monthly time step for the period 1968-1989. For the purposes of this study, monthly air temperature data for the period 1950-2000 were collected and the parametric model was applied to the total length. Finally, every monthly time series was aggregated in annual step with the use of HYDROGNOMON software (Kozanis *et a*l. 2010).

6.3.3   Results

Table 24 presents the results of our analysis. In seven out of the ten stations tested, no trends were found under the independence assumption. The estimate of the Hurst parameter for annual PET time series varies in the range 0.43 to 0.76. Out of the three stations that had significant trends under the independence assumption, only two stations (Ioannina, Lemnos) showed a significant downward trend.

Table 24. Summary results of the application of the Mann-Kendall modified test to the PET data. The Hurst parameter was estimated using the maximum likelihood estimator (Tyralis and Koutsoyiannis 2011). The trend identification is performed for a predefined level α = 0.05 in each step.

Stations	Hurst parameter estimate	Mann-Kendall 2-sided p-value (Step O)	Significance of H, 2-sided p-value (Step H)	Mann-Kendall LTP 2-sided p-value (Step M)	Trend identification
Heraklion	0.67	0.31			{H0O}, no trend
Ioannina	0.58	0.05	0.27		{H1O,H0H}, trend exists
Kavala	0.76	0.63			{H0O}, no trend
Kerkyra	0.71	0.90			{H0O}, no trend
Kozani	0.63	0.31			{H0O}, no trend
Larissa	0.76	0.04	0.00	0.42	{H1O,H1H,HOM} no trend
Lemnos	0.74	0.00	0.26		{H1O,H0H}, trend exists
Methoni	0.69	0.06			{H0O}, no trend
Skyros	0.46	0.40			{H0O}, no trend
Tripoli	0.43	0.46			{H0O}, no trend

In Figure 26 PET in Ioannina is presented . In Table 23 we observe a significant trend under the independence assumption is observed. This assumption is valid. At Kerkyra (see Figure 27) there is no any significant trend. At Larissa (Figure 28), a significant trend under the independence assumption is detected; however, this trend is not significant under the long-term dependence assumption. Finally, we observe a significant trend under a valid independence assumption at Lemnos is observed (Figure 29).
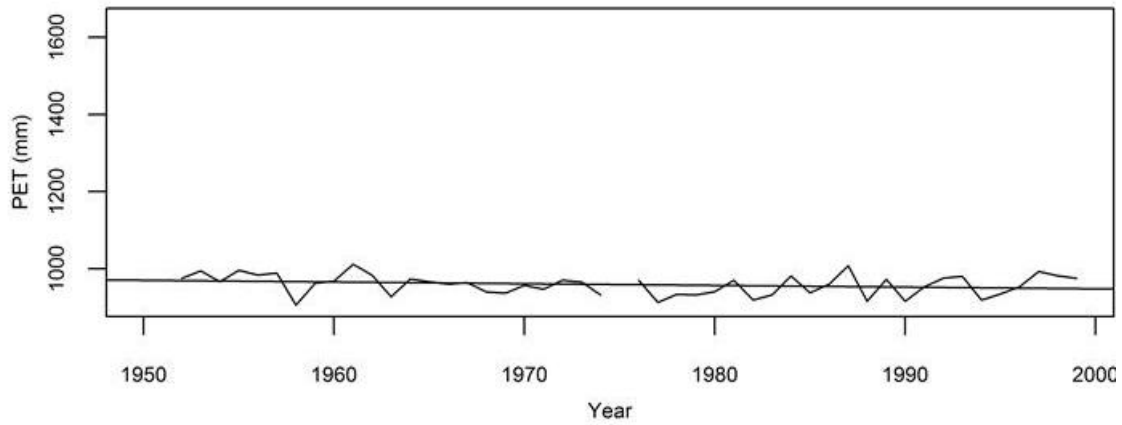
Figure 26. Annual PET at Ioannina
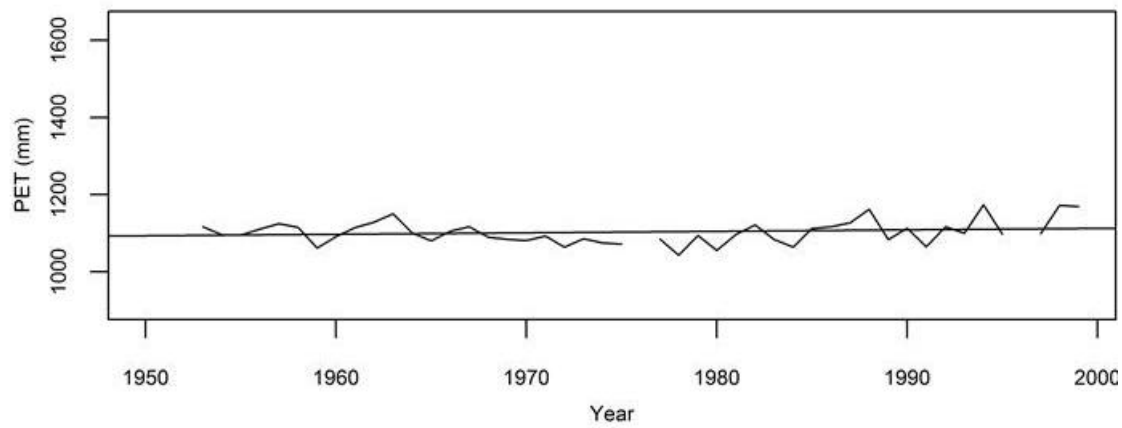
Figure 27. Annual PET at Kerkyra
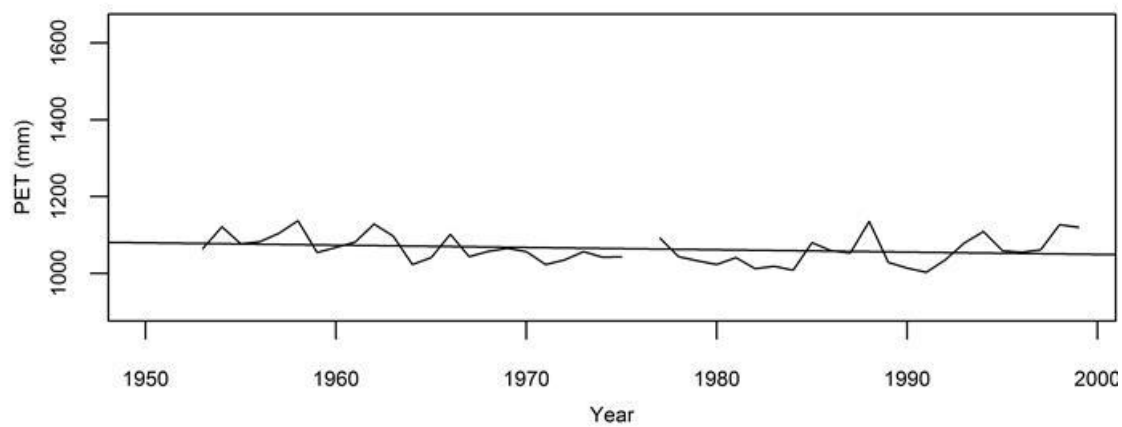
Figure 28. Annual PET at Larissa
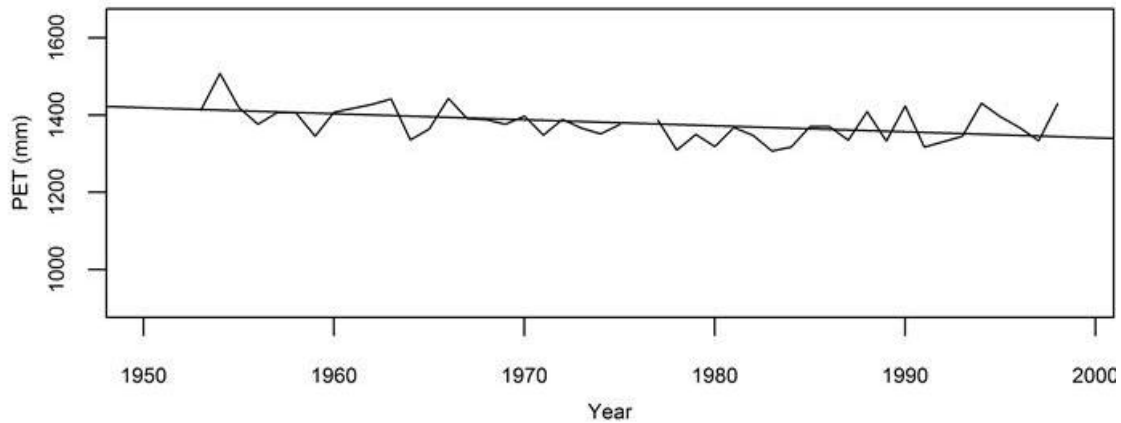
Figure 29. Annual PET at Lemnos

6.3.4 Discussion and conclusions

An R function that implements the Mann- Kendall test under the long-term persistence hypothesis was presented. The test applied and tested in annual time series of PET estimated from a recent parametric approach. The parametric model estimation allows the consistent estimation of the PET with minimal data requirements and it's useful for climatic studies when crucial hydrometerological data are missing (wind velocity, relative humidity, extraterrestrial radiation). The results of our preliminary case study analysis show that in seven cases, no significant trend was detected under the independence assumption. In one case, no significant trend was detected under the long-term persistence assumption, while the trend was significant under the independence assumption. In the remaining two cases, we found a significant downward trend under both the independence and the long-term persistence assumptions. In total, an R function is ready and user-friendly for extensive use in other field of water resources and technological- related studies.

6.4 Temperature variability over Greece : Links between space and time

The long-term alteration of the meteorological paid the attention of the scientific community the last decades by linking it with the well-known "climate-change" interest. It is therefore necessary to examine long term instrumental observations or reliable estimate to quantify the fluxes trends. In this respect, meteorological data from 35 stations of HNMS were collected and used (monthly timeseries 1950-2000), with a rather uniform spatial distribution as it can be seen Figure 30.

For studying the climatic behaviors the stations was classified in three categories: continental, coastal and inland stations.

67
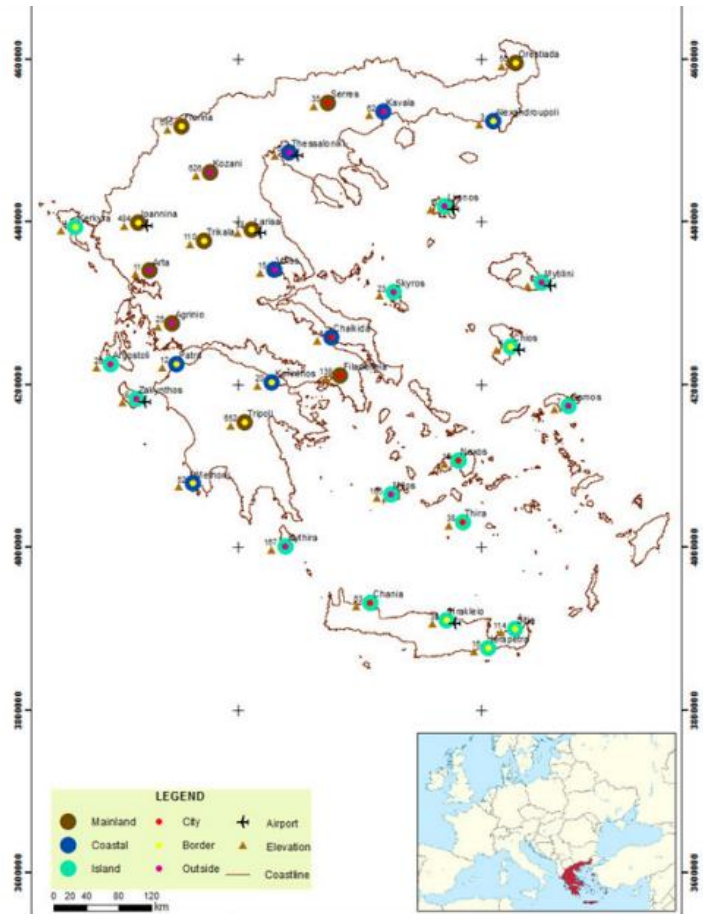
Figure 30. Study Area- meteorological stations locations

Attention was paid to the temperature monthly dataset and as visualizes the Figure 31 the inter-annual variation (i.e. the mean standard deviation of the monthly temperatures of each year) shows that the variability of temperature parameters is higher to continental stations than to coastal or island regions.
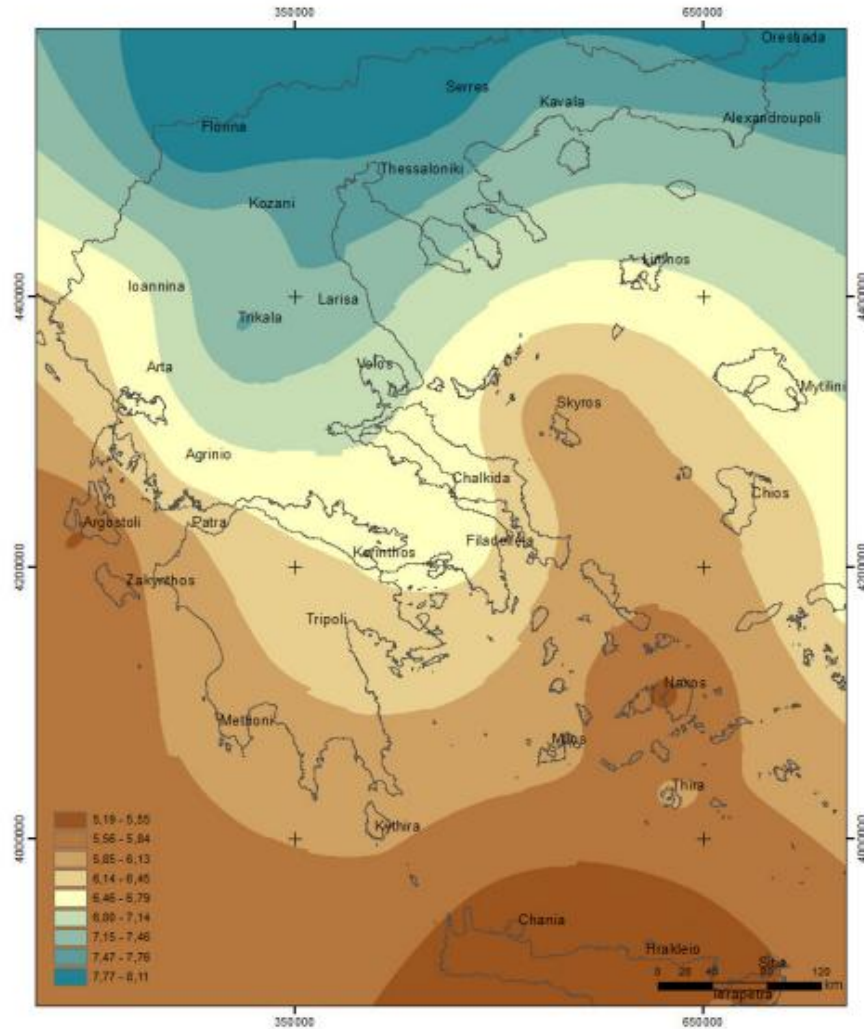
Figure 31. Inter-annual temperature variability

Overall, temperature in Greece has been relatively stable for the last 50 years as shown in the Figure 32.
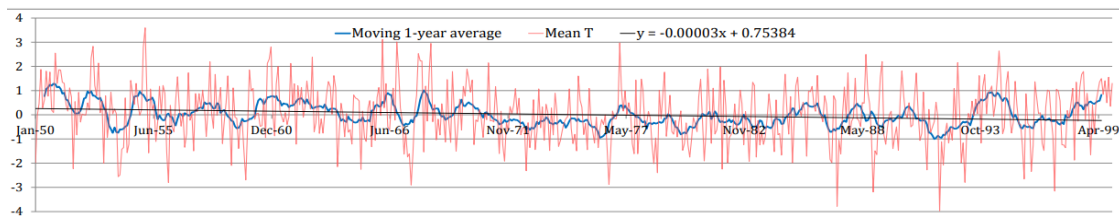
Figure 32. Study Area- locations of meteorological stations

Monthly potential evapotranspiration for each station was estimated by the parametric model (Tegos *et al*. 2013, Tegos *et al*. 2015): dependent only to temperature Tα and incoming solar

radiation Rα and two coefficients, a (kg/kJ) and c (C $^{-1}$). The proposed parameters was extracted by the study Tegos *et al.* 2013 and Tegos (2017).

The results portray in Figure 33, which include both annual PET (background coloring) and monthly change over the examined period (bars).

It can be concluded that PET has been declining during the last 50 years, which is expected as it follows the temperature decrease. It must be noted though that some station in Eastern Greece show increase during the summer.

Conclusively, the potential evapotranspiration has decreased in winter all over Greece, and has increased only in a few Aegean islands during summer (N. Bountas *et al.* 2013).
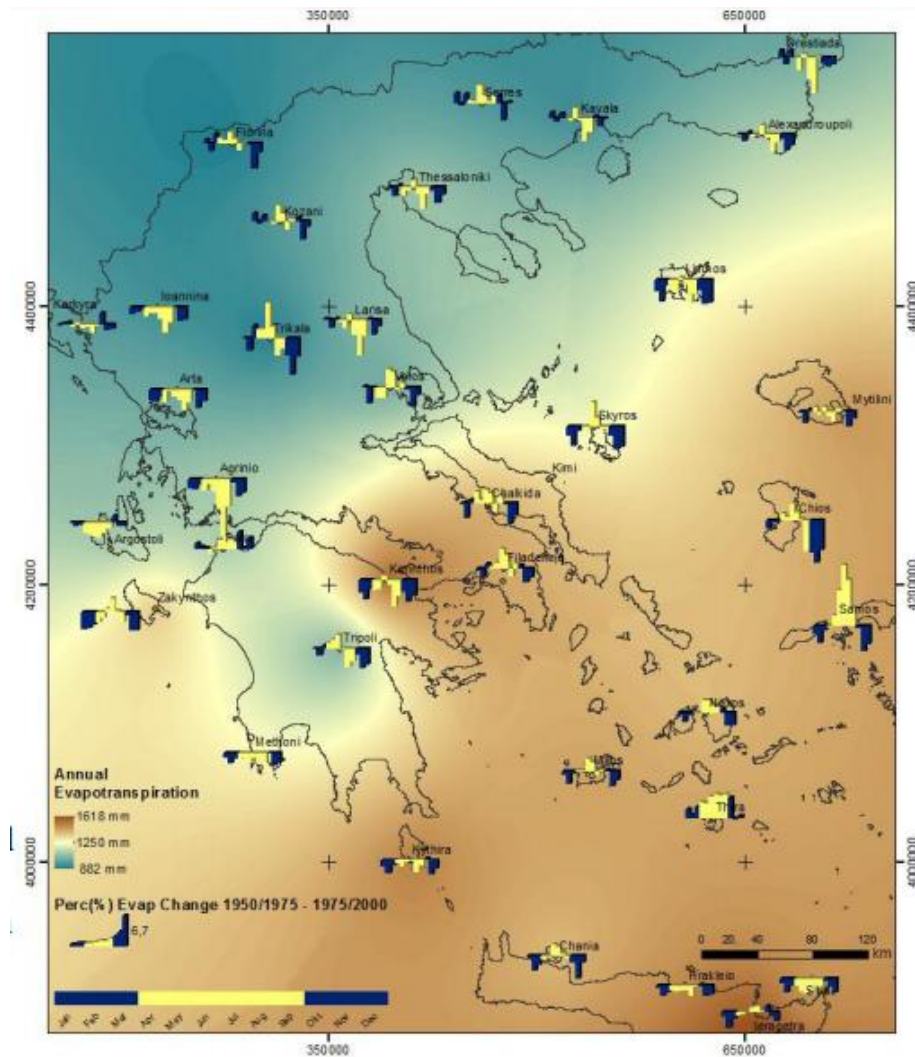
Figure 33. Annual PET variation

7 Applications in agricultural design

7.1 Spatial interpolation methods in PET estimate

7.1.1 Introduction

Potential evapotranspiration (PET) is a crucial parameter of several applications in hydrological modelling, irrigation and environmental studies. Especially, precision irrigation requires daily or even hourly PET estimates in order to increase the efficiency of water use through optimization procedures that include the use of sensors along with extensive soil, water and crop data. A significant concept for precision irrigation design is the spatial variability of the PET since the well-established FAO Penman-Monteith model (Allen *et al.* 1998), but also alternative frameworks (Tegos *et al.* 2015) provide point estimates.

Precision irrigation constitutes a breakthrough for agricultural water management since it provides means to optimal water use. In recent years several applications of precision irrigation are implemented based on spatial data from different origins, i.e. meteorological stations networks, remote sensing data and in situ measurements. One of the factors affecting optimal irrigation system design and management is the daily potential evapotranspiration (PET). A commonly used approach is to estimate the daily PET for the representative day of each month during the irrigation period. The implementation of the recently introduced non-parametric bilinear surface smoothing (BSS) methodology for spatial interpolation of daily PET is presented. The study area was the plain of Arta which is located at the Region of Epirus at the North West Greece. Daily PET was estimated according to the FAO Penman-Monteith methodology with data collected from a network of six agrometeorological stations, installed in early 2015 in selected locations throughout the study area. For exploration purposes, PET maps for the Julian dates: 105, 135, 162, 199, 229 and 259 were produced, thus covering the entire irrigation period of 2015. Also, comparison and cross validation against the calculated FAO Penman-Monteith PET for each station, were performed between BSS and a commonly used interpolation method, i.e. inverse distance weighted (IDW). During the leave-one-out cross validation procedure, BSS yielded very good results, outperforming IDW. Given the simplicity of the BSS, its overall performance is satisfactory, providing maps that represent the spatial and temporal variation of daily PET.

7.1.2 Study area and meteorological stations network

The study area was located at the plain of Arta (453.29 km², the biggest of the region), at the Region of Epirus at the north west coast of Greece (Figure 34). It is part of the Arachthos and Louros hydrological basins and borders with Amvrakikos Wetlands National Park. The local climate is of Mediterranean type, characterized by dry and hot summers and rainy and moderately cool winters.
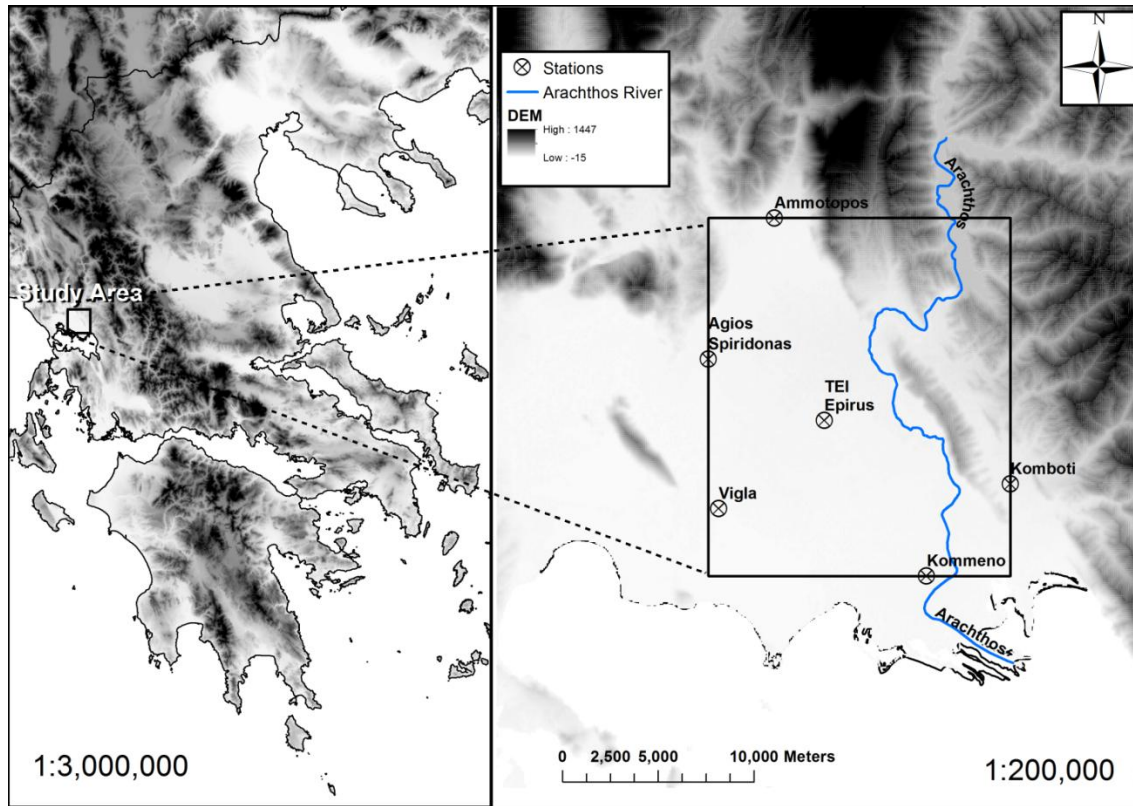
Figure 34. The Arta plain along with the study area and the agrometeorological stations network

Irrigation in the area is performed by means of surface irrigation, sprinkler irrigation and drip systems in proportions of about 40%, 40% and 20% respectively (Tsirogiannis and Triantos, 2009), with a continuous diminution of surface irrigation. The vast majority of farmers irrigate based on experience and inherited practical advices. As water is plentiful and cheap, most farmers over irrigate using water by the old open canal scheme that covers part of the plain and from numerous boreholes.

An agrometeorological stations network of six fully equipped weather stations was installed in early 2015 for the implementation of IRMA_SYS project (Malamos *et al.* 2016 - http://arta.irrigation-management.eu/) in order to monitor evapotranspiration related parameters. The data from the six meteorological stations are available at http://openmeteo.org/ under Database Contents License v.1.0 for individual measurements and Open Database License v.1.0 for the data series as they are published at Open Data Commons (http://opendatacommons.org/).

The analysis extend (mask) boundaries were defined by the coordinates of the outermost stations according to each one of the four cardinal directions. This was mandatory in order to ensure that the PET estimates adjacent to the boundaries of the study area are obtained from interpolation rather than extrapolation. The maps were produced using a 500 × 500 m grid for practical and computational reasons, covering an area of approximately 294.8 km^2 inside the plain of Arta.

7.1.3 Spatial interpolation methods

The mathematical framework of Bilinear Surface Smoothing (Malamos and Koutsoyiannis 2016a), suggests that fit is meant in terms of minimizing the total square error among the set of original points $z_i(x_i, y_i)$ for $i = 1,..., n$ and the fitted bilinear surface, that in matrix form, can be written as:

$$p = \|\mathbf{z} - \hat{\mathbf{z}}\|^2 \tag{26}$$

where $\mathbf{z} = [z_1,..., z_n]^T$ is the vector of known applicates of the given data points with size n (the superscript T denotes the transpose of a matrix or vector) and $\hat{\mathbf{z}} = [\hat{z}_1,..., \hat{z}_n]^T$ is the vector of estimates with size n.

The details of the method including the algorithms and derivations of the equations are available at (Malamos and Koutsoyiannis 2016a).

The parameters required to implement the methodology, are the segments of the bilinear surface, i.e. mx, my and the smoothing parameter λ. These parameters can be estimated by transforming the smoothing parameter λ in terms of tension: τ_λ whose values are restricted in the interval [0, 1], for both directions i.e. $\tau_{\lambda x}$ and $\tau_{\lambda y}$ (Malamos and Koutsoyiannis 2016a). This transformation provides a convenient search in terms of computational time and is based on the generalized cross-validation (GCV - Craven and Wahba 1978) methodology. Thus, for a given combination of segments mx, my, the minimization of GCV results in the optimal values of $\tau_{\lambda x}$, $\tau_{\lambda y}$. This can be repeated for several trial combinations of mx, my values, until the global minimum of GCV is reached.

On the other hand, the Inverse Distance Weighting (IDW) method was implemented as a quick interpolator capable to address the characteristics of the study area regarding the limited number of meteorological stations. IDW is a straightforward and non-computationally intensive method (Burrough and McDonnell 1998). The IDW implementation for producing the PET maps of the study area was performed by means of ESRI's ArcGIS environment.

7.1.4 Results and discussion

In order to evaluate the performance of the BSS methodology for spatial interpolation of daily PET, we interpolated the Penman-Monteith PET values acquired at the stations locations (Table 25) using both BSS and IDW for the characteristic day of each month for the 2015 irrigation period as presented in Figure 35 Figure 36.

Table 25. Penman-Monteith PET values at the locations of each of the six stations

Julian dates	PM PET (mm)					
	Agios Spiridonas	Vigla	Ammotopos	TEI of Epirus	Kommeno	Kompoti
105	3.4	3.2	3.4	3.2	3.2	3.1
135	4.1	4.4	4.5	4.4	4.5	4.1
162	4.8	4.4	5.2	4.9	5.5	5.4
199	6.2	5.2	6.7	6.4	6.1	6.3
229	4.6	4.7	5.0	4.7	4.9	4.8
259	3.8	3.4	3.8	3.7	3.6	3.6
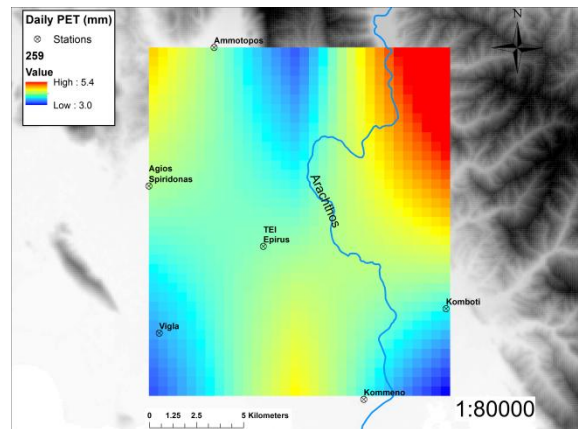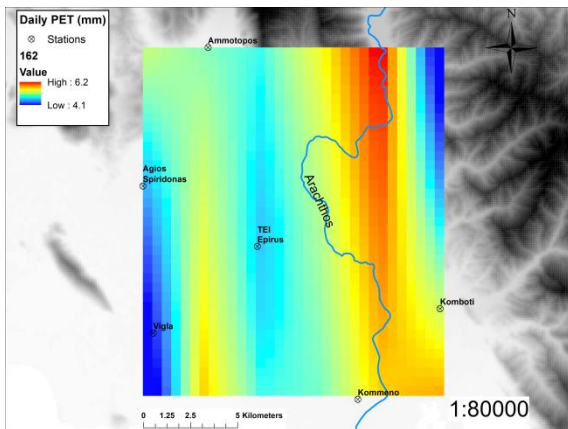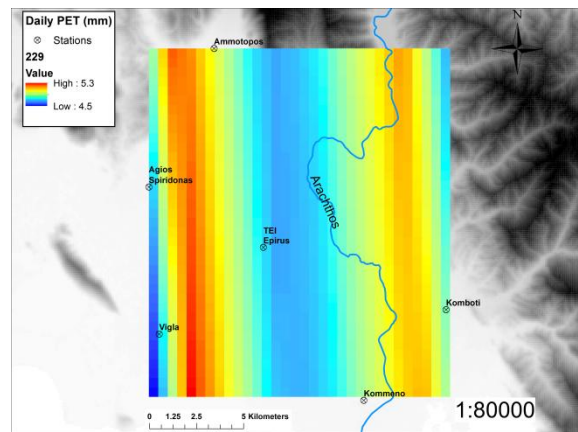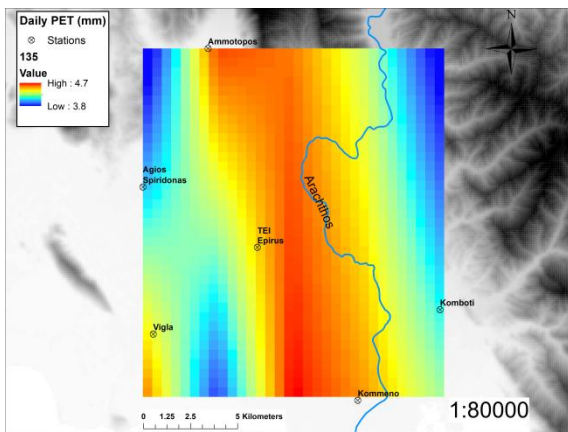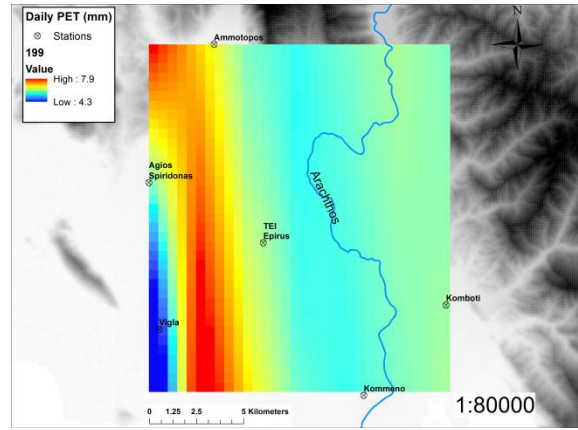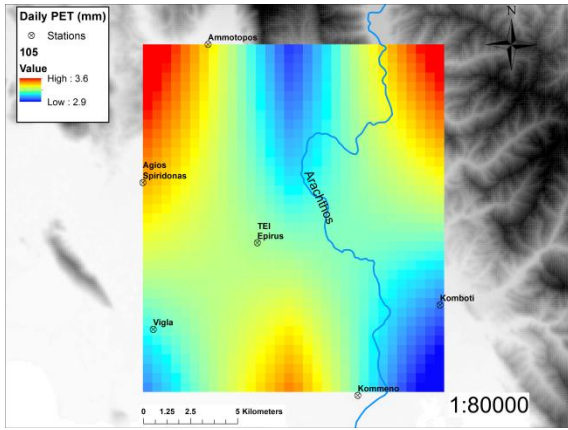
Figure 35. BSS PET maps for Julian dates 105, 135, 162, 199, 229, 259 of year 2015
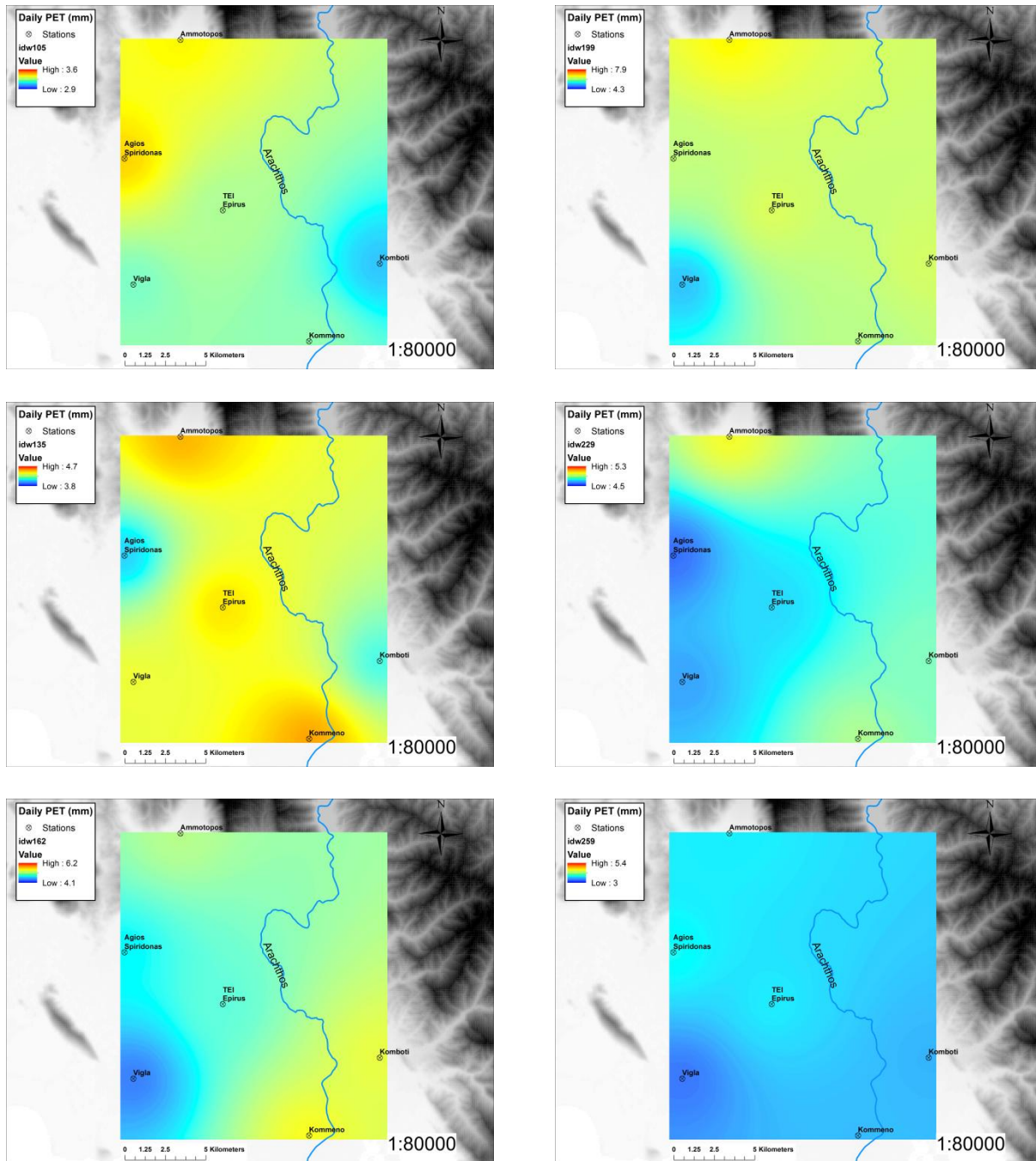
Figure 36. IDW PET maps for Julian dates 105, 135, 162, 199, 229, 259 of year 2015

From the comparison of the produced maps it is obvious that the BSS modelled PET values, have wider range than those of IDW, thus producing very plausible interpolation surfaces that respect the variation due to terrain, avoiding the characteristic IDW's bull's eye shaped artefacts.

Considering BSS's implementation, the global minimum of GCV for each day was reached by implementing it for different numbers of segments mx and my ($1 \leq mx \leq 15$ and $1 \leq my \leq 15$, while $m + 1 \geq 6$) and minimizing GCV for each one, by altering the adjustable parameters.

The results of the above procedure are presented in Table 26, along with the corresponding mean square error values. It is obvious that the BSS implementation resulted in very small mean square error values, respecting the estimated PM PET values at the stations locations. It can be assumed that there is no need to present the corresponding mean square error values for the IDW at the given data points i.e. the stations locations, since it is an exact method of interpolation so its results respect the data points exactly.

Table 26. BSS optimal parameter values and performance indices

Julian dates	mx	my	$\tau_{\lambda x}$	$\tau_{\lambda y}$	Mean square error	Global minimum GCV
105	2	3	0.902	0.154	1.75×10^{-5}	2.93×10^{-3}
135	4	5	0.003	0.765	1.42×10^{-5}	3.76×10^{-3}
162	5	4	0.99	0.001	1.13×10^{-5}	4.95×10^{-3}
199	6	12	0.76	0.019	7.42×10^{-5}	3.15×10^{-2}
229	14	6	0.201	0.001	3.77×10^{-6}	6.35×10^{-4}
259	2	6	0.784	0.067	2.47×10^{-5}	5.11×10^{-3}

Also, the above criteria of performance may not be representative with respect to the validity of the interpolation results in other locations, except for those incorporated in the interpolation procedure. So, an alternative technique was implemented for the evaluation of the bilinear surface smoothing method efficiency, in terms of performing a leave-one-out cross validation procedure of the two methods. The procedure was implemented in MS-Excel© and included a loop in which the PET values at the location of each station were estimated using the remaining five as the input dataset to each one of the two interpolation methods. In this way, we acquired a total of six, one for every day, PET estimates at the stations locations which were compared against the already acquired daily PM PET values. We should note that BSS was implemented using the previously obtained parameter values as presented in Table 26.

The performance of each method was evaluated by using statistical criteria such as: mean bias error (MBE), mean absolute error (MAE), root mean square error (RMSE), mean square error (MSE) and modelling efficiency (EF) which is calculated on the basis of the relationship between the observed and predicted mean deviations (Malamos and Koutsoyiannis 2016b). As Table 27 states, BSS clearly outperformed IDW in all circumstances, apart from the EF and RMSE criteria at the Kompoti station. In this case, both methods failed to provide satisfactory estimates of PET values. An explanation to this behaviour is the fact that the Kompoti station is placed on the east side of the study area close to the mountains so when it is missing, the available information is inadequate to describe the orography effects, thus resulting in insufficient estimates.

Table 27. Performance of BSS and IDW against PM PET values in the leave-one-out cross validation procedure

	Agios Spiridonas		Vigla		Ammotopos		TEI of Epirus		Kommeno		Kompoti	
	BSS	IDW	BSS	IDW	BSS	IDW	BSS	IDW	BSS	IDW	BSS	IDW
MBE (mm)	0.0	0.8	0.0	0.4	0.0	0.4	0.0	0.1	-0.5	1.6	-1.7	1.7
MAE (mm)	0.1	0.8	0.1	0.4	0.0	0.4	0.1	0.1	0.5	1.6	1.7	1.7
RMSE (mm)	0.1	0.8	0.2	0.5	0.1	0.4	0.1	0.1	0.8	1.6	1.9	1.7
EF	0.99	0.18	0.95	0.47	1.00	0.85	0.99	0.98	0.44	-1.55	-2.02	-1.44

7.1.5 Conclusions

Two different approaches for spatial interpolation of daily potential evapotranspiration were implemented using data from six meteorological stations located in the plain of Arta, at the Region of Epirus. Both approaches were implemented for the characteristic day of each month for the 2015 irrigation period, i.e. Julian dates: 105, 135, 162, 199, 229 and 259. The objective was to evaluate the performance of bilinear surface smoothing (BSS) method against the inverse distance weighting (IDW) method. The comparison against the estimated values of the FAO Penman-Monteith (PM) PET for each station showed that BSS yielded very good results with very small mean square error values, respecting the given PM PET values.

Also, a leave-one-out cross-validation procedure per station was used for validating the performance of both spatial interpolators. Thus we acquired a total of six, one for every day, PET estimates at the stations locations which were compared against the already acquired daily PM PET values. During this cross validation procedure BSS clearly outperformed IDW in almost every case, respecting the variation of the terrain and also avoiding the characteristic IDW's bull's eye shaped artefacts. Given the simplicity of the BSS methodology, its overall performance is satisfactory, providing maps that represent the spatial and temporal variation of daily PET, thus granting the necessary tools for implementing precision irrigation on daily or finer time scale.

7.2 Regional daily/monthly parametric model in Arta valey

7.2.1 Introduction

The parametric model was applied in the Arta a strong irrigated value in western East of Greece (Figure 37).
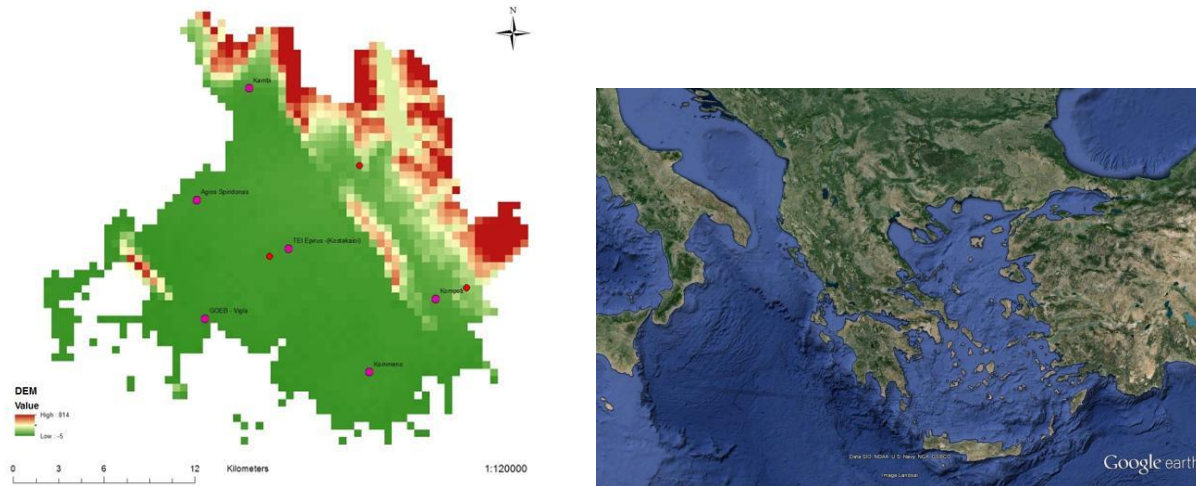
Figure 37. Study Area

Meteorological data was collected from 3 meteorological stations and the following computational procedures was made:

- Calibration of the using historical data from 3 stations and regionalization of the parameters throughout Arta plain. Fit of the parametric formula at daily and monthly in the samples of the three stations and extraction of the parameters a,b,c. High CE was observed for the parametric model using PM as base sample.

- Regionalization of daily and monthly temperatures from 6 stations located in Arta plain using I.D.W method as providing by a newer meteorological network.

- Production of 10 raster maps (5 for mean monthly temperature and 5 for mean daily day of the 15th day of each month)

- Appropriate coding of extraterrestrial radiation and production of the corresponding raster files

7.2.2   Daily PET Spatial variability

Figure 38 illustrates the spatial variation of PET at each month. The main outcomes are as follows:

- PET high values are observed in North for every month and low values in the South adjacent to the shore.

- Mean daily ranges from 2 mm (April) to 4.9 mm (July).

- Significant PET spatial variation in daily scale and for all months.

- Non standard spatial direction for every month in the study period.

79
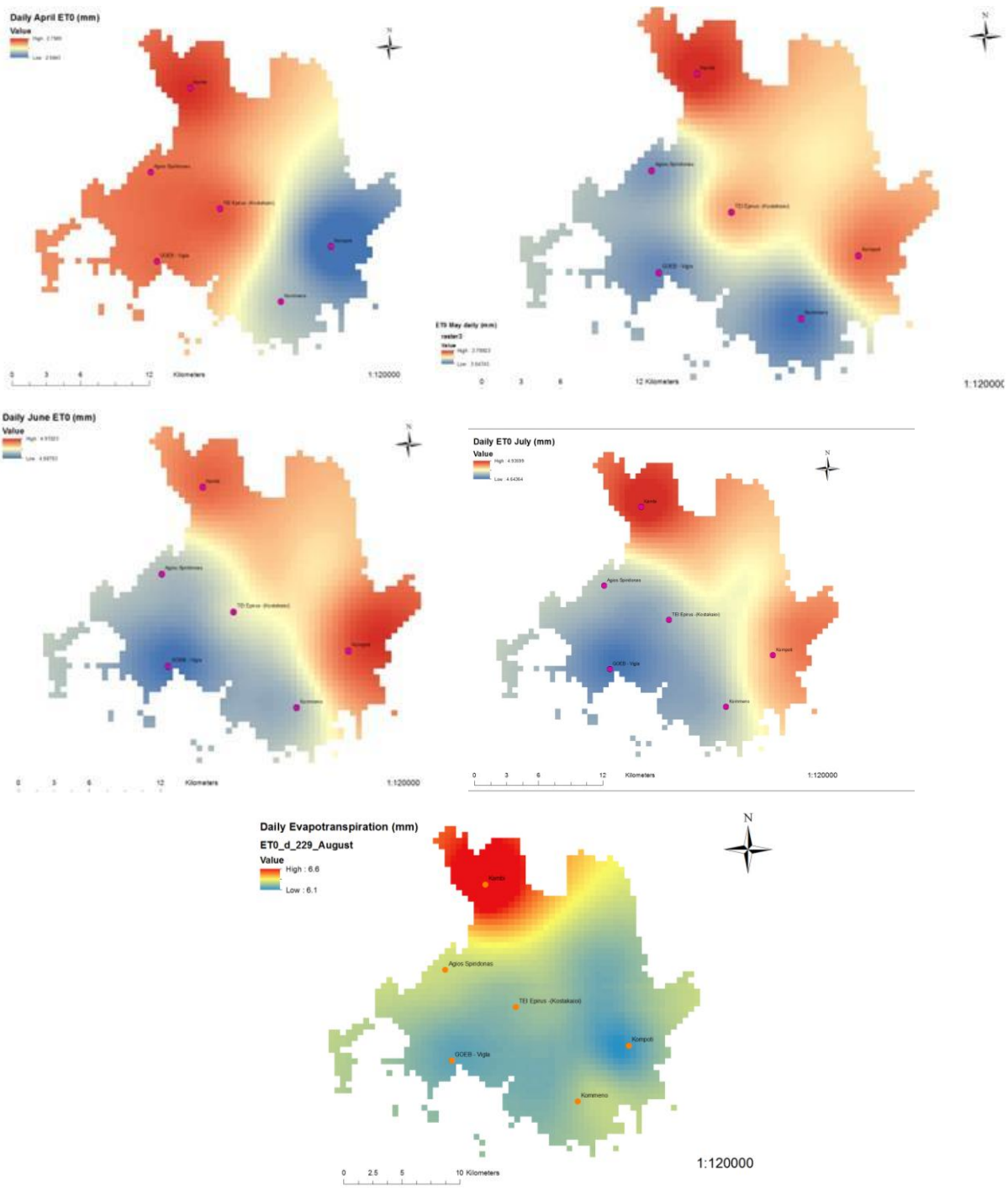
Figure 38. PET daily spatial variability

7.2.3 Monthly PET Spatial variability

Figure 39 visualizes PET monthly variability for each month. In respect the results it can be concluded the following:

- Gradient of the monthly PET from North to South direction (limited in April)

- Mean monthly PET ranges between 80.6 mm (April) to 174 mm (July)

- Insignificant spatial variation for spring months (April, May) and significant in summer months (June, July, August)
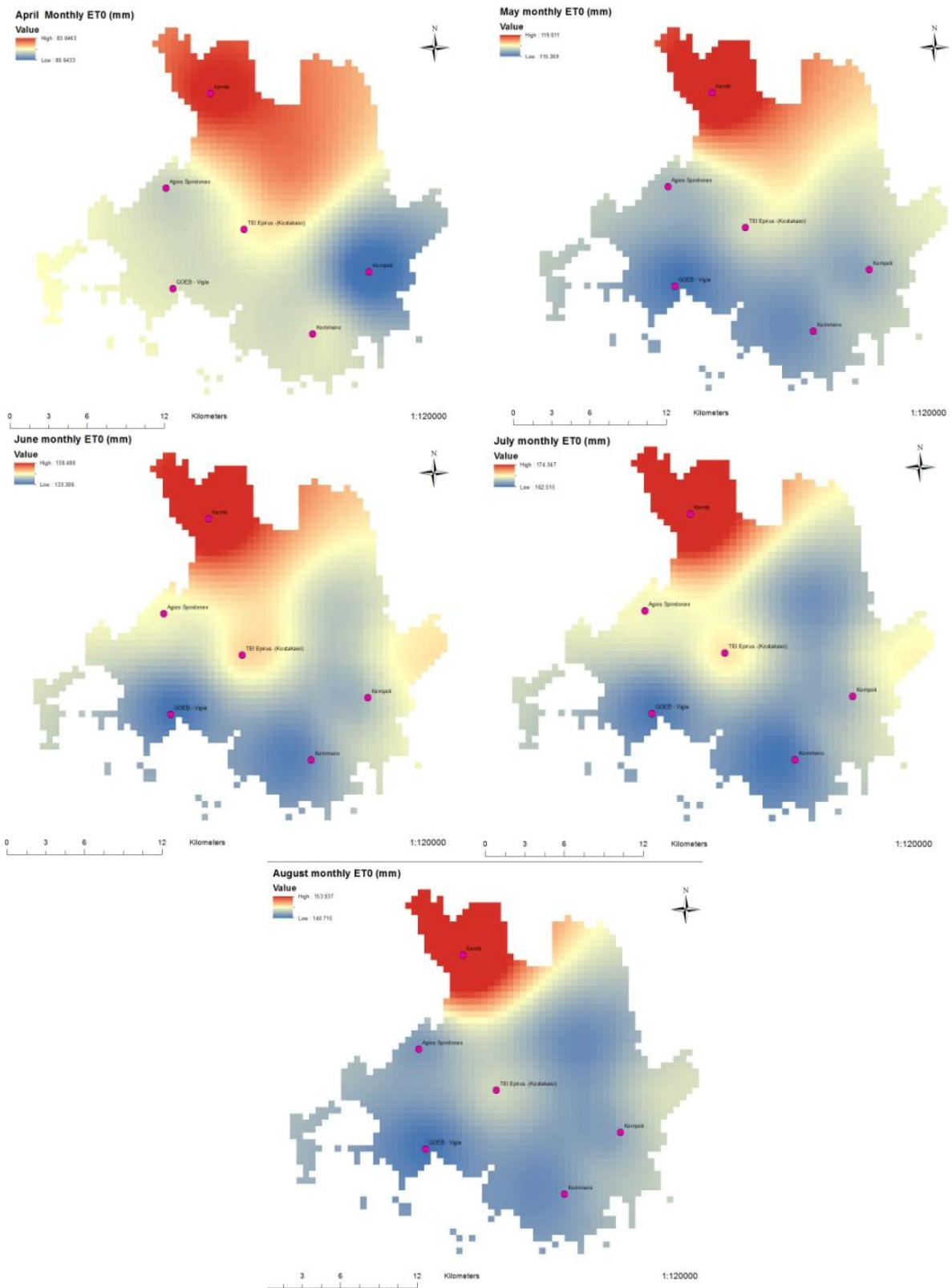
Figure 39. PET monthly variability

8 Conclusions and Discussion

The major innovations of the thesis is the development of a new parametric radiation-based PET model which can be considered as simplification of the Penman-Monteith formula, in an attempt to combine parsimony, in terms of model structure and data requirements, and physical consistency. The parametric model is a parsimonious radiation-based and physically consistent approach derived from a simplification of the Penman-Monteith equation. It requires in its first exhibition three parameters to be calibrated prior to its application and two parameters in its second global format. Specifically, two model versions were presented in this respect, the first one was applied in the well-known CIMIS network and the second a slightly modifications of the first expression in the Global Dataset of CLIMWAT.

The model ensures excellent predictive capacity (in terms of reproducing monthly PET estimations through the Penman-Monteith) in the majority of the examined in both applications. In the first application (CIMIS), the model outperforms all the radiation-based and empirical formulas and in the global application provided better performance in comparison with the Hargreaves model. It's worth mentioning that a main hint point of this thesis is that the local calibration of the simplified models is reqired, in assessing consistent PET since the comparisons across different climates reveal the great advantage of parametric approaches against radiation-based ones, since calibration allows the coefficients that are involved in the mathematical formulas to be fitted to local climatic conditions. The parameters of the new model have some physical background, since they substitute, to some extent, the three missing meteorological variables namely the humidity, the wind velocity and the radiation. Taking into account the limited availability of data capable to acquire the set of parameters of the Parametric method into timescales finer than monthly e.g. daily or even hourly, an interesting study could be the investigation of downscaling them against time.

This investigation might be performed by applying a regression analysis that involves establishing a mathematical relationship between the large scale acquired parameters against those of finer scale.

Another point of interest of this thesis was the investigation of the optimal spatial technique in converting the point scale estimate into regional, by implementing interpolation techniques such as: Inverse Distance Weighting (IDW), Natural Neighbours (NaN), Ordinary Kriging (OK) and Bilinear Surface Smoothing (BSS), along an extensive study area such as California. The validation procedure was implemented by comparing the reference potential evapotranspiration estimates acquired from the implementation of the parametric method, using the parameter estimates of the four interpolation methods, against those of the eleven additional CIMIS stations. This combined evaluation of the four different interpolation approaches, indicated that the simple and effortless IDW method performs better than the other three methodologies. Regarding the application of the new methodology, BSS's efficiency to perform interpolation between data points that are interrelated in a complicated manner was confirmed, acquiring high CE values analogous to those of the other three methods. In this light, global parameters map was provided using IDW for direct application of the parametric expression across the globe.

Numerous applications were presented including the development of a R software script for estimating the annual trend under Hurst-Kolmogorov behavior and a global remote sensing PET monthly dataset.

Incidental contributions, moderate innovations and future research required are summarized below:

Future research attempt requires a detailed investigation of the factors affecting the model poor performance in specific areas over the globe, in order to recognize whether these can be handled through a slightly different model structure or they do require the use of additional explanatory variables or parameters. Apparently, this will require the use of full meteorological time series instead of climatic data, which is a very challenging task at global scale. Another challenging task is a survey of the calibration results against different climatic zones that will further highlight the model advantages, as well as potential shortcomings.

Since the need of the large-scale hydrological modeling is under high development at least last decade, the Global PET maps at multiple time scale extracted by in-situ measurements or by combining remote sensing measurements can be support the hydrological community by providing reliable PET estimates which are required input-data in numerous well known model such as SWAT. To achieve that, future research shall focus in the production of reliable PET estimate integrating site temperature and remote sensing samples. A first which was presented in this Thesis is very promising since the new PET monthly dataset (RASPOTION) provided very satisfactory results.

Reliable global PET estimate could be useful and in another hydrological science field referring to the low-flow assessment in ungauged catchments. Typically, the most recent scientific attempts in this regard use the PET as explanatory variable of regression models and therefore PET accuracy is noteworthy for estimating the flow duration curves in ungauged catchments.

Another interesting for further research survey is the use of the parametric framework within the field of agronomical studies and especially in the forecasting of the crop water requirements for scheduling the irrigation program in timely manner. The key idea of the Parametric model owing to minimal input data requirements can be decrease the overall uncertainty of the PET projection at short-term forecast (up to 3-days) and therefore the short term weather prediction can be incorporated to an efficiency Decision Support System for the crop assessment in local and large scale precision agriculture.

Conclusively, the Parametric Model is a robust model with numerous potential applications in different disciplines related to hydrology and geosciences as well, since PET is a critical input variable of hydrological modeling, in assessing the crop water demands of several agronomist studies, in physical based estimation of the low flow in ungauged catchments, in assessing the long-term trends of hydrometerological variables.

References

Ahn, K. H., & Palmer, R. N. (2015). Trend and Variability in Observed Hydrological Extremes in the United States. Journal of Hydrologic Engineering, 21(2), 04015061.

Alexandris, S., Kerkides, P., 2003. New empirical formula for hourly estimations of reference evapotranspiration. Agric. Water Manag. 60, 157–180.

Allen, R.G., Jensen, M.E., Wright, J.L., Burman, R.D., 1989. Operational Estimates of Reference Evapotranspiration. Agron. J. 81, 650.

Allen, R.G., L.S. Pereira, D. Raes, & M. Smith, Crop evapotranspiration: Guidelines for computing crop water requirements, FAO Irrigation and Drainage Paper 56, Rome, 1998.

Allen, R.G.; Pruitt, W.O. Rational use of the FAO Blaney-Criddle formula. J. Irrig. Drain. Eng. 1986, 112, 139–155.

Amatya, D.M.; Skaggs, R.W.; Gregory, J.D. Comparison of methods for estimating REF-ET. J. Irrig. Drain. Eng. 1995, 121, 427–435.

Arora, Manohar, N. K. Goel, and Pratap Singh. "Evaluation of temperature trends over India."Hydrological sciences journal 50.1 (2005).

Azhar, A.H., Perera, B.J.C., 2011. Evaluation of Reference Evapotranspiration Estimation Methods under Southeast Australian Conditions. J. Irrig. Drain. Eng. 137, 268–279.

Blaney, H.F., Criddle, W.D., 1962. Determining consumptive use and irrigation water requirements (No. 1275). US Department of Agriculture.

Bhattarai, N., Dougherty, M., Marzen, L.J. and Kalin, L., 2012. Validation of evaporation estimates from a modified surface energy balance algorithm for land (SEBAL) model in the south-eastern United States. Remote sensing letters, 3(6), pp.511-519.

Birhanu, D., Kim, H., Jang, C., & Park, S. (2018). Does the Complexity of Evapotranspiration and Hydrological Models Enhance Robustness?. Sustainability, 10(8), 2837.

Burrough, P.A. and McDonnell, R.A., 1998. Principles of Geographical Information Systems. New York: Oxford University Press.

Choudhury, B.J., 1997. Global pattern of potential evaporation calculated from the Penman-Monteith equation using satellite and assimilated data. Remote Sensing of Environment, 61(1), pp.64-81.

Craven, P. and Wahba, G., 1978. Smoothing noisy data with spline functions - Estimating the correct degree of smoothing by the method of generalized cross-validation. Numerische Mathematik, 31 (4), 377–403.

Dalezios, N.R.; Loukas, A.; Bampzelis, D. Spatial variability of reference evapotranspiration in Greece. Phys. Chem. Earth Parts A/B/C 2002, 27, 1031–1038.

Dimitriadis, P., Hurst-Kolmogorov dynamics in hydroclimatic processes and in the microscale of turbulence, Ph.D thesis, Department of Water Resources and Environmental Engineering – National Technical University of Athens, 2017.

Dingman, S.L. Physical Hydrology; MacMillan Publishing Company: New York, NY, USA, 1994.

Doorenbos, J.; Pruitt, W.O. Guidelines for predicting crop water requirements: Rome, Italy, food and agricultural organization of the United Nations. FAO Irrigation and Drainage Paper 24, 1977)

Droogers, P., & Allen, R. G. (2002). Estimating reference evapotranspiration under inaccurate data conditions. Irrigation and drainage systems, 16(1), 33-45.

Efstratiadis, A.; Koutsoyiannis, D. One decade of multiobjective calibration approaches in hydrological modelling: A review. Hydrol. Sci. J. 2010, 55, 58–78.

Efstratiadis, A.; Koutsoyiannis, D. An evolutionary annealing-simplex algorithm for global optimisation of water resource systems. Hydroinformatics 2002: Proceedings of the Fifth International Conference on Hydroinformatics, International Water Association: London, UK, 2002; pp.1423–1428.

FAO. CLIMWAT for CROPWAT, A climatic database for irrigation planning and management, FAO Irrigation & Drainage Paper No. 49, Rome, 1993. Available online: http://www.fao.org/nr/water/infores_databases_climwat. html

Farquhar, G.D., Roderick M.L., 2007. Worldwide changes in evaporative demand, Proceedings of the Pontifical Academy of Sciences, 2005.

Fooladmand, H.R.; Haghighat, M. Spatial and temporal calibration of Hargreaves equation for calculating monthly ET0 based on Penman-Monteith method. Irrig. Drain. 2007, 56, 439–449.

Foyster, A.M. Application of the grid square technique to mapping of evapotranspiration. J. Hydrol. 1973, 19, 205–226.

Gavilán, P.; Lorite, I.J.; Tornero, S.; Berengena, J. Regional calibration of Hargreaves equation for estimating reference ET in a semiarid environment. Agric. Water Manag. 2006, 81, 257–281.

Ghilain, N. and Gellens-Meulenberghs, F., 2014. Assessing the impact of land cover map resolution and geolocation accuracy on evapotranspiration simulations by a land surface model. Remote sensing letters, 5(5), pp.491-499.

Gocic, Milan, and Slavisa Trajkovic. "Analysis of trends in reference evapotranspiration data in a humid climate."Hydrological Sciences Journal 59.1 (2014): 165-180.

Guo, D., Westra, S., & Maier, H. R. (2016). An R package for modelling actual, potential and reference evapotranspiration. Environmental Modelling & Software, 78, 216-224

Guo, D.; Westra, S.; Maier, H.R. Sensitivity of potential evapotranspiration to changes in climate variables for different climatic zones. Hydrol. Earth Syst. Sci. 2016, 1–43.

Hamed KH (2008) Trend detection in hydrologic data: The Mann-Kendall trend test under the scaling hypothesis. Journal of Hydrology 349(3-4):350-363.

Hargreaves G.H, and Z.A. Samani Z.A, Estimating potential evapotranspiration, Technical note, J. Irrig. Drain.e Eng., 108(3), 225-300, 1982.

Hansen S. Estimation of potential and actual evapotranspiration.Nordic Hydrol 1984, 15:205–212

Hargreaves G. H.; Samani, Z. A. Reference crop evaporation from temperature. Appl. Eng. Agric. 1985, 1, 96–99.

Hart, Q.J., Brugnach, M., Temesgen, B., Rueda, C., Ustin, S.L., Frame, K., 2009. Daily reference evapotranspiration for California using satellite imagery and weather station measurement interpolation. Civ. Eng. Environ. Syst. 26, 19–33.

Haslinger, K.; Bartsch, A. Creating long-term gridded fields of reference evapotranspiration in Alpine terrain based on a recalibrated Hargreaves method. Hydrol. Earth Sys. Sci. 2016, 20, 1211–1223.

Hooker, J., Duveiller, G., & Cescatti, A. (2018). A global dataset of air temperature derived from satellite remote sensing and weather stations. Scientific data, 5(1), 1-11.

Hu, Q.F.; Yang, D.W.; Wang, Y.T.; Yang, H.B. Global calibration of Hargreaves equation and its applicability in China. Adv. Water Sci. 2011, 22, 160–167.

Iliopoulou, T., Papalexiou, S. M., Markonis, Y., & Koutsoyiannis, D. (2016). Revisiting long-range dependence in annual precipitation. Journal of Hydrology.

Irmak, S., Allen, R.G., Whitty, E.B., 2003. Daily Grass and Alfalfa-Reference Evapotranspiration Estimates and Alfalfa-to-Grass Evapotranspiration Ratios in Florida. J. Irrig. Drain. Eng. 129, 360–370.

Jensen, M.E., Haise, H.R., 1963. Estimating evapotranspiration from solar radiation. Proc. Am. Soc. Civ. Eng. J. Irrig. Drain. Div. 89, 15–41.

Jensen M., and H. Haise, Estimating evapotranspiration from solar radiation, J. Irrig. Drain. Div., 89(1R4), 15–41, 1989.

Kitanidis, P.K. Introduction to Geostatistics: Applications in Hydrogeology; Cambridge University Press: New York, NY, USA, 1997.

Klok, E.J., Klein Tank, A.M.G., 2009. Updated and extended European dataset of daily climate observations. Kozanis, S., Christofides, A., Mamassis, N., Efstratiadis, A., Koutsoyiannis D., 2010. Hydrognomon – open source software for the analysis of hydrological data, EGU General Assembly 2010, Geophysical Research Abstracts, Vol. 12, Vienna, 12419.

Kozanis, S., Christofides, A., Mamassis, N., Efstratiadis, A. and Koutsoyiannis, D., 2010, May. Hydrognomon–open source software for the analysis of hydrological data. In EGU General Assembly Conference Abstracts (Vol. 12, p. 12419).

Koutsoyiannis, D.; Mamassis, N.; Tegos, A. Logical and illogical exegeses of hydrometeorological phenomena in ancient Greece. Water Sci. Technol.: Water Supply 2007, 7, 13–22.

Koutsoyiannis, D., 2003. Climate change, the Hurst phenomenon, and hydrological statistics. Hydrological Sciences-Journal-des Sciences Hydrologiques 48 (1).

Koutsoyiannis, D., 2009. Seeking parsimony in hydrology and water resources technology (solicited), European Geosciences Union General Assembly 2009, Geophysical Research Abstracts, Vol. 11, Vienna, 11469. (http://www.itia.ntua.gr/en/docinfo/906/)

Koutsoyiannis, D., 2014. Reconciling hydrology with engineering. Hydrol. Res. 45 (1), 2-24.

Li, J., Heap, A.D., 2008. A Review of Spatial Interpolation Methods for Environmental Scientists, Geoscience Australia. Geoscience Australia, GPO Box 378, Canberra, ACT 2601, Australia.

Koutsoyiannis D. 2011. Hurst–Kolmogorov dynamics as a result of extremal entropy production. Physica A: Statistical Mechanics and its Applications, 390(8): 1424-1432

Koutsoyiannis, D., and Th. Xanthopoulos, Engineering Hydrology, National Technical University of Athens, 1999.

Koutsoyiannis, D., Hydrology and Change. Hydrol. Sci. J. 2013, 58, 1177–1197.

Koutsoyiannis, D., Montanari, A., 2007. Statistical analysis of hydroclimatic time series: uncertainty and insights. Water Resources Research 43, W05429.

Kumar, S., Merwade, V., Kam, J., & Thurner, K. (2009). Streamflow trends in Indiana: effects of long term persistence, precipitation and subsurface drains. Journal of Hydrology, 374(1), 171-183.

Li, Z.; Chen, Y.; Shen, Y.; Liu, Y.; Zhang, S. Analysis of changing pan evaporation in the arid region of Northwest China. Water Resour. Res. 2013, 49, 2205–2212.

Lofgren, B.M.; Hunter, T.S.; Wilbarger, J. Effects of using air temperature as a proxy for evapotranspiration in climate change scenarios of Great Lakes basin hydrology. J. Gt. Lakes Res. 2011, 37, 744–752.

Longley, P.A., Goodchild, M.F., Maguire, D.J., Rhind, D.W., 2005. Geographic information system and Science, second ed, England: John Wiley & Sons, Ltd, West Sussex PO19 8SQ, England, pp. 333–335.

Lu, J., Sun, G., McNulty, S.G., Amatya, D.M., 2005. A comparison of six potential comparison evapotranspiration methods for regional use in the Southeastern United States. J. Am. Water Resour. Assoc. 41, 621–633.

Makkink, G.F. (1957). Testing the Penman formula by means of lysimeters. J. Inst. Water Engng. 11 (3): 277-288

Malamos, N. and Koutsoyiannis, D., 2016a. Bilinear surface smoothing for spatial interpolation with optional incorporation of an explanatory variable. Part 1: Theory. Hydrological Sciences Journal, 61 (3), 519–526.

Malamos, N. and Koutsoyiannis, D., 2016b. Bilinear surface smoothing for spatial interpolation with optional incorporation of an explanatory variable. Part 2: Application to synthesized and rainfall data. Hydrological Sciences Journal, 61 (3), 527–540.

Malamos, N., Tsirogiannis, I.L., and Christofides, A., 2016. Modelling irrigation management services: the IRMA_SYS case. International Journal of Sustainable Agricultural Management and Informatics, 2 (1), 1–18.

Malamos, N.; Tegos, A.; Tsirogiannis, I.L.; Christofides, A.; Koutsoyiannis, D. Implementation of a regional parametric model for potential evapotranspiration assessment. In Proceedings of IrriMed 2015—Modern Technologies, Strategies and Tools for Sustainable Irrigation Management and Governance in Mediterranean Agriculture, Bari, Italy, 23–25 September 2015.

Malamos, N.; Tsirogiannis, I.L.; Tegos, A.; Efstratiadis, A.; Koutsoyiannis, D. Spatial interpolation of potential evapotranspiration for precision irrigation purposes. In Proceedings of 10th World Congress on Water Resources and Environment, Athens, Greece, 5–9 July 2017.

Mamassis, N., Panagoulia, D., Novcovic, A., 2014. Sensitivity analysis of Penman evaporation method, Global NEST Journal, Vol.16, No 4, pp. 628-639.

Mancosu, N., Snyder, R.L., Spano, D., 2014. Procedures to Develop a Standardized Reference Evapotranspiration Zone Map. J. Irrig. Drain. Eng. 140, A4014004.

Mardikis, M.G.; Kalivas, D.P.; Kollias, V.J. Comparison of interpolation methods for the prediction of reference evapotranspiration—An application in Greece. Water Resour. Manag. 2005, 19, 251–278.

Markonis, Y., Batelis, S. C., Dimakos, Y., Moschou, E., & Koutsoyiannis, D. (2016). Temporal and spatial variability of rainfall over Greece. Theoretical and Applied Climatology, 1-16.

McGuiness J.L., and E.F. Bordne, A comparison of lysimeter-derived potential evapotranspiration with computed values, Technical Bulletin 1452, Agricultural Research Service, US Department of Agriculture, Washington, DC, 1972.

McMahon, T.A., M.C. Peel, L. Lowe, R. Srikanthan, and T.R. McVicar, Estimating actual, potential, reference crop and pan evaporation using standard meteorological data: a pragmatic synthesis, Hydrol. Earth Sys. Sci., 17, 1331-1363, 2013.

McMahon, T.A.; Finlayson, B.L.; Peel, M.C. Historical developments of models for estimating evaporation using standard meteorological data. Wiley Interdiscip. Rev. Water 2016, 3, 788–818.

McVicar, T.R.; Roderick, M.L.; Donohue, R.J.; Li, L.T.; Van Niel, T.G.; Thomas, A.; Grieser, J.; Jhajharia, D.; Himri, Y.; Mahowald, N.M.; Mescherskaya, A.V.; Kruger, A.C.; Rehman, S.; Dinpashoh, Y. Global review and synthesis of trends in observed terrestrial near-surface wind speeds: Implications for evaporation. J. Hydrol. 2012, 416–417, 182–205.

Merz R.; Blöschl, G. Regionalisation of catchment model parameters. J. Hydrol. 2004, 287, 95–123.

X., Liu, S., Lin, Z., Wang, S., & Hu, S. (2015). Trends in land surface evapotranspiration across China with remotely sensed NDVI and climatological data for 1981–2010.Hydrological Sciences Journal, 60(12), 2163-2177.

Mohawesh, O.E. Spatio-temporal calibration of Blaney–Criddle equation in arid and semiarid environment. Water Resour. Manag. 2010, 24, 2187–2201.

Monteith, J.L., Evaporation and the environment: The state and movement of water in living organism, XIXth Symposium, Cambridge University Press, Swansea, 1965.

Monteith, J.L., 1981. Evaporation and environment. Symp. Soc. Exp. Biol. Vol. 19. No. 205-23.

Monteith, J.L., 1981. Evaporation and surface temperature. Q. J. R. Meteorol. Soc. 107, 1–27.

Moriasi, D.N., Arnold, J.G., Van Liew, M.W., Bingner, R.L., Harmel, R.D., Veith, T.L., 2007. Model Evaluation Guidelines for Systematic Quantification of Accuracy in Watershed Simulations. Trans. ASABE 50, 885–900.

Mu, Q., Heinsch, F.A., Zhao, M. and Running, S.W., 2007. Development of a global evapotranspiration algorithm based on MODIS and global meteorology data. Remote sensing of Environment, 111(4), pp.519-536.

Mu, Q., Zhao, M. and Running, S.W., 2011. Improvements to a MODIS global terrestrial evapotranspiration algorithm. Remote Sensing of Environment, 115(8), pp.1781-1800.

N. Bountas, N. Boboti, E. Feloni, L. Zeikos, Y. Markonis, A. Tegos, N. Mamassis, and D. Koutsoyiannis, Temperature variability over Greece: Links between space and time, Facets of

Uncertainty: 5th EGU Leonardo Conference – Hydrofractals 2013 – STAHY 2013, Kos Island, Greece, doi:10.13140/RG.2.2.17739.80164, European Geosciences Union, International Association of Hydrological Sciences, International Union of Geodesy and Geophysics, 2013

Nash, J.E., Sutcliffe, J.V., 1970. River flow forecasting through conceptual models part I - A discussion of principles. J. Hydrol. 10, 282–290.

Nouri, H., Beecham, S., Kazemi, F., Hassanli, A. M., & Anderson, S. (2013). Remote sensing techniques for predicting evapotranspiration from mixed vegetated surfaces. Hydrology and Earth System Sciences Discussions, 10(3), 3897-3925.

O'Connell, P. E., Koutsoyiannis, D., Lins, H. F., Markonis, Y., Montanari, A., & Cohn, T. (2016). The scientific legacy of Harold Edwin Hurst (1880–1978). Hydrological Sciences Journal, 1-20.

Oudin L., F. Hervieu, C. Michel, and C. Perrin, Which potential evapotranspiration input for a lumped rainfall–runoff model? Part 2—Towards a simple and efficient potential evapotranspiration model for rainfall–runoff modelling, J. Hydrol, 303(1-4), 290–306, 2005.

Panda, D. K., A. Mishra, and A. Kumar. "Quantification of trends in groundwater levels of Gujarat in western India."Hydrological Sciences Journal57.7 (2012): 1325-1336.

Penman, H.L., Natural evaporation from open water, bare soil and grass, Proc. Royal Society of London, 193, 120–145, 1948.

Pereira, A.R., Pruitt, W.O., 2004. Adaptation of the Thornthwaite scheme for estimating daily reference evapotranspiration. Agric. Water Manag. 66, 251–257.

Pereira, L.S.; Allen, R.G.; Smith, M.; Raes, D. Crop evapotranspiration estimation with FAO56: Past and future. Agric. Water Manag. 2015, 147, 4–20.

Priestley C.H.B.; Taylor, R.J. On the assessment of surface heat fluxes and evaporation using large-scale parameters. Mon. Weather Rev. 1972, 100, 81–92.

Rayner, D.P.; Wind run changes: The dominant factor affecting pan evaporation trends in Australia. J. Clim. 2017, 20, 3379–3394.

Roderick, M.L.; Rotstayn, L.D.; Farquhar, G.D.; Hobbins, M.T. On the attribution of changing pan evaporation. Geophys. Res. Lett. 2007, 34, 251–270

Roderick, M.L.; Hobbins, M.T.; Farquhar, G. D. Pan evaporation trends and the terrestrial water balance. II. Energy balance and interpretation. Geogr. Compass 2009, 3, 761–780.

Samani, Z. "Estimating solar radiation and evapotranspiration using minimum climatological data." Journal of Irrigation and Drainage Engineering 126.4 (2000): 265-267.

Samaras, D.A., Reif, A., Theodoropoulos, K., 2013. Evaluation of Radiation-Based Reference Evapotranspiration Models Under Different Mediterranean Climates in Central Greece. Water Resour. Manag. 28, 207–225.

Samaras, Dimitrios A., Albert Reif, and Konstantinos Theodoropoulos. "Evaluation of Radiation-Based Reference Evapotranspiration Models Under Different Mediterranean Climates in Central Greece." Water Resources Management 28.1 (2014): 207-225.

Seiller, G., & Anctil, F. (2016). How do potential evapotranspiration formulas influence hydrological projections?. Hydrological Sciences Journal, 61(12), 2249-2266.

Sentelhas, P.C.; Gillespie, T.J.; Santos, E.A. Evaluation of FAO Penman-Monteith and alternative methods for estimating reference evapotranspiration with missing data in Southern Ontario, Canada. Agric. Water Manag. 2010, 97, 635–644.

Shahidian, S., Serralheiro, R.P., Serrano, J., Teixeira, J.L., 2013. Parametric calibration of the Hargreaves-Samani equation for use at new locations. Hydrol. Process. 27, 605–616.

Smith, M., 1993. CLIMWAT for CROPWAT: A climatic database for irrigation planning and management. FAO Irrigation and Drainage Paper No. 49, Rome. (CLIMWAT 2.0), http://www.fao.org/nr/water/infores_databases_climwat.html.

Stephens JC, Stewart EH. A comparison of procedures for computing evaporation and evapotranspiration. In: IASH, Proceedings of General Assembly, Berkeley, California, USA, 1963, 62, 123–133

Stevens, Andrew J., Derek Clarke, and Robert J. Nicholls. "Trends in reported flooding in the UK: 1884–2013."Hydrological Sciences Journal 61.1 (2016): 50-63.

Sutcliffe, J., Hurst, S., Awadallah, A. G., Brown, E., & Hamed, K. (2016). Harold Edwin Hurst: the Nile and Egypt, past and future. Hydrological Sciences Journal, 1-14.

Tabari, H., 2009. Evaluation of Reference Crop Evapotranspiration Equations in Various Climates. Water Resour. Manag. 24, 2311–2337.

Tabari H.. "Evaluation of reference crop evapotranspiration equations in various climates." Water resources management 24.10 (2010): 2311-2337

Tabari, H., Talaee, P.H., 2011. Local Calibration of the Hargreaves and Priestley-Taylor Equations for Estimating Reference Evapotranspiration in Arid and Cold Climates of Iran Based on the Penman-Monteith Model. J. Hydrol. Eng. 16, 837–845.

Tabari, H., Marofi, S., Aeini, A., Talaee, P. H., & Mohammadi, K. (2011). Trend analysis of reference evapotranspiration in the western half of Iran. Agricultural and Forest Meteorology, 151(2), 128-136.

Tegos A. (2007). Estimation of Potential Evapotranspiration in Greece (Msc Thesis, National Technical University of Athens)

Tegos, A., Mamassis, N., Koutsoyiannis, D., 2009. Estimation of potential evapotranspiration with minimal data dependence. EGU General Assembly Conference Abstracts. Vol. 11. (http://www.itia.ntua.gr/en/docinfo/905/)

Tegos, A., A. Efstratiadis, and D. Koutsoyiannis, A parametric model for potential evapotranspiration estimation based on a simplified formulation of the Penman-Monteith equation, Evapotranspiration - An Overview, edited by S. Alexandris, 143–165, InTech, 2013.

Tegos, A., Malamos, N., and Koutsoyiannis, D., 2015. A parsimonious regional parametric evapotranspiration model based on a simplification of the Penman–Monteith formula. Journal of Hydrology, 524, 708–717.

Tegos, A., Efstratiadis, A., Malamos, N., Mamassis, N., & Koutsoyiannis, D. (2015). Evaluation of a parametric approach for estimating potential evapotranspiration across different climates. Agriculture and Agricultural Science Procedia, 4, 2-9.

Tegos, A.; Malamos, N.; Efstratiadis, A.; Tsoukalas, I.; Karanasios, A.; Koutsoyiannis, D. Parametric Modelling of Potential Evapotranspiration: A Global Survey. Water 2017, 9, 795

Tegos, A.; Tyralis, H.; Koutsoyiannis, D.; Hamed, K. An R function for the estimation of trend significance under the scaling hypothesis-application in PET parametric annual time series. Open Water J. 2017, 4, 6.

Temesgen, B. et al. "Comparison of some reference evapotranspiration equations for California." Journal of irrigation and drainage engineering 131.1 (2005): 73-84.

Thepadia, M., Martinez, C.J., 2012. Regional Calibration of Solar Radiation and Reference Evapotranspiration Estimates with Minimal Data in Florida. J. Irrig. Drain. Eng. 138, 111–119.

Thornthwaite, C.W., 1948. An approach toward a rational classification of climate. Geographical Review, 55-94.

Tsoukalas, I.; Kossieris, P.; Efstratiadis, A.; Makropoulos, C. Surrogate-enhanced evolutionary annealing simplex algorithm for effective and efficient optimization of water resources problems on a budget. Environ. Modell. Software 2016, 77, 122–142.

Tsirogiannis I., Triantos S., 2009. Survey of irrigation practice in Arta and development of web tools for irrigation management. National Conference of the Greek Society of Agricultural Engineers, Thessaloniki, 8-10/10/2009, 51-58 (in Greek).

Turc, L., (1961). Evaluation des besoins en eau d'irrigation, evapotranspiration potentielle, formule climatique simplifice et mise a jour. (in French). Ann. Agron. 12:13-49. 9

Turner, S. W. D., & Galelli, S. (2016). Water supply sensitivity to climate change: An R package for implementing reservoir storage analysis in global and regional impact studies. Environmental Modelling & Software, 76, 13-19.

Tyralis H, Koutsoyiannis D (2011) Simultaneous estimation of the parameters of the Hurst-Kolmogorov stochastic process. Stochastic Environmental Research and Risk Assessment 25(1):21-33.

Tyralis H. (2016). HKprocess: Hurst-Kolmogorov process. R package version 0.0-2. https://CRAN.R-project.org/package=HKprocess

Valiantzas J "Simplified versions for the Penman evaporation equation using routine weather data." Journal of Hydrology 331.3 (2006): 690-702.

Valiantzas J. "Simplified forms for the standardized FAO-56 Penman–Monteith reference evapotranspiration using limited weather data." Journal of Hydrology 505 (2013): 13-23.

Vicente-Serrano, S.M.; Lanjeri, S.; López-Moreno, J.I. Comparison of different procedures to map reference evapotranspiration using geographical information systems and regression-based techniques. Int. J. Climatol. 2007, 27, 1103–1118.

Vinukollu, R.K., Wood, E.F., Ferguson, C.R. and Fisher, J.B., 2011. Global estimates of evapotranspiration for climate studies using multi-sensor remote sensing data: Evaluation of three process-based approaches. Remote Sensing of Environment, 115(3), pp.801-823.

Wang, Jianzhong, and Konstantine P. Georgakakos. "Estimation of potential evapotranspiration in the mountainous Panama Canal watershed." Hydrological processes 21.14 (2007): 1901-1917.

Wang, W.; Shao, Q.; Peng, S.; Xing, W.; Yang, T.; Luo, Y.; Xu, J. Reference evapotranspiration change and the causes across the Yellow River Basin during 1957–2008 and their spatial and seasonal differences. Water Resour. Res. 2012, 48, 113–122

Xu, C.Y., Singh, V.P., 2001. Evaluation and generalization of temperature-based methods for calculating evaporation. Hydrol. Process. 15, 305–319.

Ward, W.C.; Robinson, M. Principles of Hydrology; McGraw-Hill: New York, NY, USA, 1990.

Xu, C. Y., and Singh, V. P. (2002). "Cross comparison of empirical equations for calculating potential evapotranspiration with data fromSwitzerland." Water Resources Management, 16(3), 197–219.

Yuan, W., Liu, S., Yu, G., Bonnefond, J.M., Chen, J., Davis, K., Desai, A.R., Goldstein, A.H., Gianelle, D., Rossi, F. and Suyker, A.E., 2010. Global estimates of evapotranspiration and gross primary production based on MODIS and global meteorology data. Remote Sensing of Environment, 114(7), pp.1416-1431.Author 1, A.B.; Author 2, C.D. Title of the article. Abbreviated Journal Name Year, Volume, page range, DOI.

List of peer-review publications

Publication in scientific journals

1. Ph.D related

Tegos A., N. Malamos, A. Efstratiadis, I. Tsoukalas, A. Karanasios, and D. Koutsoyiannis, *Parametric modelling of potential evapotranspiration: a global survey*, Water, 9 (10), 795, doi:10.3390/w9100795, 2017

<u>Cited by:</u>

1. Elferchichi, A., G. A. Giorgio, N. Lamaddalena, M. Ragosta, and V. Telesca, Variability of temperature and its impact on reference evapotranspiration: the test case of the Apulia region (Southern Italy), Sustainability, 9(12), 2337, doi:10.3390/su9122337, 2017.
2. Li, M., R. Chu, S. Shen, and A. R. T. Islam, Quantifying climatic impact on reference evapotranspiration trends in the Huai River Basin of Eastern China, Water, 10(2), 144, doi:10.3390/w10020144, 2018.
3. Yan, N., F. Tian, B. Wu, W. Zhu, and M. Yu, Spatiotemporal analysis of actual evapotranspiration and its causes in the Hai basin, Remote Sensing, 10(2), 332; doi:10.3390/rs10020332, 2018.
4. Li, M., R. Chu, A.R.M.T. Islam, and S. Shen, Reference evapotranspiration variation analysis and its approaches evaluation of 13 empirical models in sub-humid and humid regions: A case study of the Huai River Basin, Eastern China, Water, 10(4), 493, doi:10.3390/w10040493, 2018.
5. Hao, X., S. Zhang, W. Li, W. Duan, G. Fang, Y. Zhang , and B. Guo, The uncertainty of Penman-Monteith method and the energy balance closure problem, Journal of Geophysical Research – Atmospheres, 123(14), 7433-7443, doi:10.1029/2018JD028371, 2018.
6. Dalezios, N. R., Dercas, N., Blanta, A., & Faraslis, I. N. (2018). Remote sensing in water balance modelling for evapotranspiration at a rural watershed in Central Greece. International Journal of Sustainable Agricultural Management and Informatics, 4(3-4), 306-337.
7. Giménez, P. O., and S. G. García-Galiano, Assessing Regional Climate Models (RCMs) ensemble-driven reference evapotranspiration over Spain, Water, 10(9), 1181, doi:10.3390/w10091181, 2018.
8. Storm, M. E., R. Gouws, and L. J. Grobler, Novel measurement and verification of irrigation pumping energy conservation under incentive-based programmes, Journal of Energy in Southern Africa, 29(3), 10–21, doi:10.17159/2413-3051/2018/v29i3a3058, 2018.
9. Tam, B. Y., K. Szeto, B. Bonsal, G. Flato, A. J. Cannon, and R. Rong, CMIP5 drought projections in Canada based on the Standardized Precipitation Evapotranspiration Index, Canadian Water Resources Journal, doi:10.1080/07011784.2018.1537812, 2018.
10. Gan, G.; Liu, Y.; Pan, X.; Zhao, X.; Li, M.; Wang, S. Testing the Symmetric Assumption of Complementary Relationship: A Comparison between the Linear and Nonlinear Advection-Aridity Models in a Large Ephemeral Lake. Water 2019, 11, 1574
11. Zhang, T., Y. Chen, and K. Tha Paw U, Quantifying the impact of climate variables on reference evapotranspiration in Pearl River Basin, China, Hydrological Sciences Journal, doi:10.1080/02626667.2019.1662021, 2019

A. Tegos, H. Tyralis, D. Koutsoyiannis, and K. H. Hamed, *An R function for the estimation of trend signifcance under the scaling hypothesis- application in PET parametric annual time series*, Open Water Journal, 4 (1), 66–71, 6, 2017

<u>Cited by:</u>

1. H. Tyralis, P. Dimitriadis, D. Koutsoyiannis, P.E. O'Connell, K. Tzouka, and T. Iliopoulou, On the long-range dependence properties of annual precipitation using a global network of instrumental measurements, Advances in Water Resources, 111, 301–318, doi:10.1016/j.advwatres.2017.11.010, 2018
2. Yuke, Z. (2019). Characterizing the Spatio-Temporal Dynamics and Variability in Climate Extremes Over the Tibetan Plateau during 1960–2012. Journal of Resources and Ecology, 10(4), 397-414.
3. Iliopoulou, T., & Koutsoyiannis, D. (2019). Revealing hidden persistence in maximum rainfall records. Hydrological Sciences Journal.

N. Malamos, I. L. Tsirogiannis, **A. Tegos**, A. Efstratiadis, and D. Koutsoyiannis, *Spatial interpolation of potential evapotranspiration for precision irrigation purposes*, European Water, 59, 303–309, 2017

Cited by:

1. N. Malamos, and D. Koutsoyiannis, Field survey and modelling of irrigation water quality indices in a Mediterranean island catchment: A comparison between spatial interpolation methods, Hydrological Sciences Journal, 63 (10), 1447–1467, doi:10.1080/02626667.2018.1508874, 2018
2. da Silva Júnior, J. C., Medeiros, V., Garrozi, C., Montenegro, A., & Gonçalves, G. E. (2019). Random forest techniques for spatial interpolation of evapotranspiration data from Brazilian's Northeast. Computers and Electronics in Agriculture, 166, 105017.

A. Tegos, A. Efstratiadis, N. Malamos, N. Mamassis, and D. Koutsoyiannis, *Evaluation of a parametric approach for estimating potential evapotranspiration across different climates*, Agriculture and Agricultural Science Procedia, 4, 2–9, doi:10.1016/j.aaspro.2015.03.002, 2015

Cited by:

1. Stan, F.I., G. Neculau, L. Zaharia, G. Ioana-Toroimac, and S. Mihalache, Study on the evaporation and evapotranspiration measured on the Căldăruşani Lake (Romania), Procedia Environmental Sciences, 32, 281–289, doi:10.1016/j.proenv.2016.03.033, 2016.
2. Esquivel-Hernández, G., R. Sánchez-Murillo, C. Birkel, S. P. Good, and J. Boll, Hydro-climatic and ecohydrological resistance/resilience conditions across tropical biomes of Costa Rica, Ecohydrology, 10(6), e1860, doi:10.1002/eco.1860, 2017.
3. Hodam, S., S. Sarkar, A.G.R. Marak, A. Bandyopadhyay, and A. Bhadra, Spatial interpolation of reference evapotranspiration in India: Comparison of IDW and Kriging methods, Journal of The Institution of Engineers (India): Series A, 98(4), 551-524, doi:10.1007/s40030-017-0241-z, 2017.
4. Deng, H., and J. Shao, Evapotranspiration and humidity variations in response to land cover conversions in the Three Gorges Reservoir Region, Journal of Mountain Science, 15(3), 590-605, doi:10.1007/s11629-016-4272-0, 2018.
5. Nadyozhina, E. D., I. M. Shkolnik, A. V. Sternzat, B. N. Egorov, and A. A. Pikaleva, Evaporation from irrigated lands in arid regions as inferred from the regional climate model and atmospheric boundary layer model simulations, Russian Meteorology and Hydrology, 43(6), 404-411, doi:10.3103/S1068373918060080, 2018

A. Tegos, N. Malamos, and D. Koutsoyiannis, *A parsimonious regional parametric evapotranspiration model based on a simplification of the Penman-Monteith formula, Journal of Hydrology*, 524, 708–717, doi:10.1016/j.jhydrol.2015.03.024, 2015.

Cited by:

1. Mwangi, H. M., Julich, S., Patil, S. D., McDonald, M. A., & Feger, K. H. (2016). Relative contribution of land use change and climate variability on discharge of upper Mara River, Kenya. Journal of Hydrology: Regional Studies, 5, 244-260.
2. Djaman, K., Rudnick, D., Mel, V. C., Mutiibwa, D., Diop, L., Sall, M., ... & Irmak, S. (2017). Evaluation of Valiantzas' Simplified Forms of the FAO-56 Penman-Monteith Reference Evapotranspiration Model in a Humid Climate. Journal of Irrigation and Drainage Engineering, 143(8), 06017005.
3. McMahon, T. A., Finlayson, B. L., & Peel, M. C. (2016). Historical developments of models for estimating evaporation using standard meteorological data. Wiley Interdisciplinary Reviews: Water, 3(6), 788-818.
4. Izady, A., Sanikhani, H., Abdalla, O., Chen, M., & Kisi, O. (2017). Impurity effect on clear water evaporation: toward modelling wastewater evaporation using ANN, ANFIS-SC and GEP techniques. Hydrological Sciences Journal, 62(11), 1856-1866.
5. Malamos, N., & Koutsoyiannis, D. (2018). Field survey and modelling of irrigation water quality indices in a Mediterranean island catchment: a comparison between spatial interpolation methods. Hydrological sciences journal, 63(10), 1447-1467.
6. Li, M., Chu, R., Shen, S., & Islam, A. (2018). quantifying climatic impact on reference evapotranspiration trends in the huai river basin of Eastern China. Water, 10(2), 144.
7. Wang, G., Gong, T., Lu, J., Lou, D., Hagan, D. F. T., & Chen, T. (2018). On the long-term changes of drought over China (1948–2012) from different methods of potential evapotranspiration estimations. International Journal of Climatology, 38(7), 2954-2966.

8. Lang, D., Zheng, J., Shi, J., Liao, F., Ma, X., Wang, W., ... & Zhang, M. (2017). A comparative study of potential evapotranspiration estimation by eight methods with FAO Penman–Monteith method in southwestern China. Water, 9(10), 734.

9. Mentzafou, A., Wagner, S., & Dimitriou, E. (2018). Historical trends and the long-term changes of the hydrological cycle components in a Mediterranean river basin. Science of The Total Environment, 636, 558-568.

10. Amatya, D. M., Muwamba, A., Panda, S., Callahan, T., Harder, S., & Pellett, C. A. (2018). Assessment of Spatial and Temporal Variation of Potential Evapotranspiration Estimated by Four Methods for South Carolina. Journal of South Carolina Water Resources, 5(1), 5.

11. Haslinger, K., & Bartsch, A. (2016). Creating long-term gridded fields of reference evapotranspiration in Alpine terrain based on a recalibrated Hargreaves method. Hydrology & Earth System Sciences, 20(3).

12. Yang, D., Bian, Z., Zhang, K., Xiong, J., & Lei, S. (2017). Modeling Root Growth, Crop Growth and N Uptake of Winter Wheat Based on SWMS_2D: Model and Validation. Revista Brasileira de Ciência do Solo, 41.

13. Li, M., Chu, R., Islam, A., & Shen, S. (2018). Reference Evapotranspiration Variation Analysis and Its Approaches Evaluation of 13 Empirical Models in Sub-Humid and Humid Regions: A Case Study of the Huai River Basin, Eastern China. Water, 10(4), 493.

14. Wang, P., Qiu, J., Huo, Z., Anderson, M., Zhou, Y., Bai, Y., ... & Chen, P. (2017). Temporal Downscaling of Crop Coefficients for Winter Wheat in the North China Plain: A Case Study at the Gucheng Agro-Meteorological Experimental Station. Water, 9(3), 155.

15. Elferchichi, A., Giorgio, G., Lamaddalena, N., Ragosta, M., & Telesca, V. (2017). Variability of temperature and its impact on reference evapotranspiration: The test case of the Apulia Region (Southern Italy). Sustainability, 9(12), 2337.

16. Giménez, P., & García-Galiano, S. (2018). Assessing regional climate models (RCMs) ensemble-driven reference evapotranspiration over Spain. Water, 10(9), 1181.

17. Wang, W., Dong, X., Lu, Y., Liu, X., Zhang, R., Li, M., ... & Pu, X. (2018). Soil Water Balance and Water Use Efficiency of Rain-fed Maize under a Cool Temperate Climate as Modeled by the AquaCrop. In MATEC Web of Conferences (Vol. 246, p. 01059). EDP Sciences.

18. Xu, S., Qin, M., Ding, S., Zhao, Q., Liu, H., Li, C., ... & Ji, X. (2019). The Impacts of Climate Variation and Land Use Changes on Streamflow in the Yihe River, China. Water, 11(5), 887.

19. Amatya, D. M., & Harrison, C. A. (2016). Grass and forest potential evapotranspiration comparison using five methods in the Atlantic coastal plain. Journal of Hydrologic Engineering, 21(5), 05016007.

20. Zhang, T., & Chen, Y. (2017). Analysis of Dynamic Spatiotemporal Changes in Actual Evapotranspiration and Its Associated Factors in the Pearl River Basin Based on MOD16. Water, 9(11), 832.

21. Yang, Q., Ma, Z., Zheng, Z., & Duan, Y. (2017). Sensitivity of potential evapotranspiration estimation to the Thornthwaite and Penman–Monteith methods in the study of global drylands. Advances in Atmospheric Sciences, 34(12), 1381-1394.

22. Deng, H., & Shao, J. A. (2018). Evapotranspiration and humidity variations in response to land cover conversions in the Three Gorges Reservoir Region. Journal of Mountain Science, 15(3), 590-605.

23. Hodam, S., Sarkar, S., Marak, A. G., Bandyopadhyay, A., & Bhadra, A. (2017). Spatial interpolation of reference evapotranspiration in india: Comparison of idw and kriging methods. Journal of The Institution of Engineers (India): Series A, 98(4), 511-524.

24. Sagar, A., & Singh, P. K. (2019). Evapotranspiration Based Micro Irrigation Scheduling of Tomato Crop under Naturally Ventilated Polyhouse. Current Journal of Applied Science and Technology, 1-7.

25. Zhang, T., Y. Chen, and K. Tha Paw U, Quantifying the impact of climate variables on reference evapotranspiration in Pearl River Basin, China, Hydrological Sciences Journal, doi:10.1080/02626667.2019.1662021, 2019

3. Other publications

Koskinas, **A. Tegos**, P. Tsira, P. Dimitriadis, T. Iliopoulou, P. Papanicolaou, D. Koutsoyiannis, and T. Williamson, *Insights into the Oroville Dam 2017 spillway incident*, Geosciences, 9 (37), doi:10.3390/geosciences9010037, 2019.

Cited by:

1. Langat, P. K., Kumar, L., & Koech, R. (2019). Identification of the Most Suitable Probability Distribution Models for Maximum, Minimum, and Mean Streamflow. Water, 11(4), 734.

2. Kacimov, A. R., Yakimov, N. D., & Šimůnek, J. (2019). Phreatic seepage flow through an earth dam with an impeding strip. Computational Geosciences, 1-19.

3. Tapete, D. Key Topics and Future Perspectives in Natural Hazards Research. Geosciences 2020, 10, 22.

Tegos, W. Schlüter, N. Gibbons, Y. Katselis, and A. Efstratiadis, *Assessment of environmental flows from complexity to parsimony - Lessons from Lesotho*, Water, 10 (10), 1293, doi:10.3390/w10101293, 2018.

Cited by:

1. Yang, Z., Yang, K., Su, L., & Hu, H. (2019). The multi-objective operation for cascade reservoirs using MMOSFLA with emphasis on power generation and ecological benefit. Journal of Hydroinformatics, 21(2), 257-278.
2. Langat, P. K., Kumar, L., & Koech, R. (2019). Identification of the Most Suitable Probability Distribution Models for Maximum, Minimum, and Mean Streamflow. Water, 11(4), 734.
3. Sahoo, B. B., R. Jha, A. Singh, A. and D. Kumar, Long short-term memory (LSTM) recurrent neural network for low-flow hydrological time series forecasting, Acta Geophysica, doi:10.1007/s11600-019-00330-1, 2019.
4. Ding, L., Q. Li, J. Tang, J. Wang, and X. Chen, Linking land use metrics measured in aquatic-terrestrial interfaces to water quality of reservoir-based water sources in Eastern China, Sustainability, 11(18), 4860, doi:10.3390/su11184860, 2019.

H. Tyralis, **A. Tegos**, A. Delichatsiou, N. Mamassis, and D. Koutsoyiannis, *A perpetually interrupted interbasin water transfer as a modern Greek drama: Assessing the Acheloos to Pinios interbasin water transfer in the context of integrated water resources management*, Open Water Journal, 4 (1), 113–128, 12, 2017

Cited by:

1. Shumilova, O., Tockner, K., Thieme, M., Koska, A., & Zarfl, C. (2018). Global Water Transfer Megaprojects: A Potential Solution for the Water-Food-Energy Nexus?. Frontiers in Environmental Science, 6, 150.
2. Jin, S., Liu, H., Ding, W., Shang, H., & Wang, G. (2018). Sensitivity Analysis for the Inverted Siphon in a Long Distance Water Transfer Project: An Integrated System Modeling Perspective. Water, 10(3), 292.
3. Zhang, X., Li, L., Jin, S., Tan, Y., & Wu, Y. (2019). Impact Analysis of Slope on the Head Loss of Gas-Liquid Two-Phase Flow in Siphon Pipe. Water, 11(5), 1095.

Tegos, M., Nalbantis, I., & **Tegos, A**. (2017). *Environmental flow assessment through integrated approaches*. Eur. Water, 60, 167-173.

Cited by:

1. Książek, L., Woś, A., Florek, J., Wyrębek, M., Młyński, D., & Wałęga, A. (2019). Combined use of the hydraulic and hydrological methods to calculate the environmental flow: Wisloka river, Poland: case study. Environmental Monitoring and Assessment, 191(4), 254.

P. Dimitriadis, **A. Tegos**, A. Petsiou, V. Pagana, I. Apostolopoulos, E. Vassilopoulos, M. Gini, A. D. Koussis, N. Mamassis, D. Koutsoyiannis, and P. Papanicolaou, *Flood Directive implementation in Greece: Experiences and future improvements,* European Water 57: 35-41, 2017.

Cited by:

1. Dimitriadis, P., Gournary, N., Petsiou, A., & Koutsoyiannis, D. (2018). How to adjust the fGn stochastic model for statistical bias when handling a single time series; application to annual flood inundation. EPiC Series in Engineering, 3, 607-614.

P. Dimitriadis, **A. Tegos**, A. Oikonomou, V. Pagana, A. Koukouvinos, N. Mamassis, D. Koutsoyiannis, and A. Efstratiadis, *Comparative evaluation of 1D and quasi-2D hydraulic models based on benchmark and real-world applications for uncertainty assessment in flood mapping*, Journal of Hydrology, 534, 478–492, doi:10.1016/j.jhydrol.2016.01.020, 2016

Cited by:

1. Apel, H., O. Martínez Trepat, N. N. Hung, D. T. Chinh, B. Merz, and N. V. Dung, Combined fluvial and pluvial urban flood hazard analysis: concept development and application to Can Tho city, Mekong Delta, Vietnam, Natural Hazards and Earth System Sciences, 16, 941-961, doi:10.5194/nhess-16-941-2016, 2016.

2. Papaioannou , G., A. Loukas, L. Vasiliades, and G. T. Aronica, Flood inundation mapping sensitivity to riverine spatial resolution and modelling approach, Natural Hazards, 83, 117-132, doi:10.1007/s11069-016-2382-1, 2016.

3. #Santillan, J. R., A. M. Amora, M. Makinano-Santillan, J. T. Marqueso, L. C. Cutamora, J. L. Serviano, and R. M. Makinano, Assessing the impacts of flooding caused by extreme rainfall events through a combined geospatial and numerical modeling approach, The International Archives of the Photogrammetry, Remote Sensing and Spatial Information Sciences, Vol. XLI-B8, 2016, XXIII ISPRS Congress, Prague, doi:10.5194/isprs-archives-XLI-B8-1271-2016, 2016.

4. Cheviron, B. and R. Moussa, Determinants of modelling choices for 1-D free-surface flow and morphodynamics in hydrology and hydraulics: a review, Hydrology and Earth System Sciences, 20, 3799-3830, doi:10.5194/hess-20-3799-2016, 2016.

5. Anees, M.T., K. Abdullah, M.N.M. Nawawi, N. N. N. Ab Rahman, A. R. Mt. Piah, N. A. Zakaria, M.I. Syakir, and A.K. Mohd. Omar, Numerical modeling techniques for flood analysis, Journal of African Earth Sciences, 124, 478–486, doi:10.1016/j.jafrearsci.2016.10.001, 2016.

6. Skublics, D., G. Blöschl, and P. Rutschmann, Effect of river training on flood retention of the Bavarian Danube, Journal of Hydrology and Hydromechanics, 64(4), 349-356, doi:10.1515/johh-2016-0035, 2016.

7. Doong, D.-J., W. Lo, Z. Vojinovic, W.-L. Lee, and S.-P. Lee, Development of a new generation of flood inundation maps—A case study of the coastal City of Tainan, Taiwan, Water, 8(11), 521, doi:10.3390/w8110521, 2016.

8. #Cartaya, S., and R. Mantuano-Eduarte, Identificación de zonas en riesgo de inundación mediante la simulación hidráulica en un segmento del Río Pescadillo, Manabí, Ecuador, Revista de Investigación, 40(89), 158-170, 2016.

9. Javadnejad, F., B. Waldron, and A. Hill, LITE Flood: Simple GIS-based mapping approach for real-time redelineation of multifrequency floods, Natural Hazards Review, 18(3), doi:10.1061/(ASCE)NH.1527-6996.0000238, 2017.

10. Shrestha, A., M. S. Babel, S. Weesakul, and Z. Vojinovic, Developing intensity–duration–frequency (IDF) curves under climate change uncertainty: The case of Bangkok, Thailand, Water, 9(2), 145, doi:10.3390/w9020145, 2017.

11. Roushangar, K., M. T. Alami, V. Nourani, and A. Nouri, A cost model with several hydraulic constraints for optimizing in practice a trapezoidal cross section, Journal of Hydroinformatics, 19(3), 456-468, doi:10.2166/hydro.2017.081, 2017.

12. Papaioannou, G., L. Vasiliades, A. Loukas, and G. T. Aronica, Probabilistic flood inundation mapping at ungauged streams due to roughness coefficient uncertainty in hydraulic modelling, Advances in Geosciences, 44, 23-34, doi:10.5194/adgeo-44-23-2017, 2017.

13. Anees, M. T., K. Abdullah, M. N. M. Nawawi, N. N. N. Ab Rahman, A. R. Mt. Piah, M. I. Syakir, A. K. M. Omar, and K. Hossain, Applications of remote sensing, hydrology and geophysics for flood analysis, Indian Journal of Science and Technology, 10(17), doi:10.17485/ijst/2017/v10i17/111541, 2017.

14. Fuentes-Andino, D., K. Beven, S. Halldin, C.-Y. Xu, J. E. Reynolds, and G. Di Baldassarre, Reproducing an extreme flood with uncertain post-event information, Hydrology and Earth System Sciences, 21, 3597-3618, doi:10.5194/hess-21-3597-2017, 2017.

15. #Anees, M. T., K. Abdullah, M. N. M. Nordin, N. N. N. Ab Rahman, M. I. Syakir, and M. O. A. Kadir, One- and two-dimensional hydrological modelling and their uncertainties, Flood Risk Management, T. Hromadka and P. Rao (editors), Chapter 11, doi:10.5772/intechopen.68924, 2017.

16. #Papaioannou, G., A. Loukas, L. Vasiliades, and G. T. Aronica, Sensitivity analysis of a probabilistic flood inundation mapping framework for ungauged catchments, Proceedings of the 10th World Congress of EWRA "Panta Rhei", European Water Resources Association, Athens, 2017.

17. Bangira, T., S. M. Alfieri , M. Menenti, A. van Niekerk, and Z. Vekerdy, A spectral unmixing method with ensemble estimation of endmembers: Application to flood mapping in the Caprivi floodplain, Remote Sensing, 9, 1013, doi:10.3390/rs9101013, 2017.

18. Carisi, F., A. Domeneghetti, M. G. Gaeta, and A. Castellarin, Is anthropogenic land subsidence a possible driver of riverine flood-hazard dynamics? A case study in Ravenna, Italy, Hydrological Sciences Journal, 62(15), 2440-2455, doi:10.1080/02626667.2017.1390315, 2017.

19. Podhoranyi, M., P. Veteska, D. Szturcova, L. Vojacek, and A. Portero, A web-based modelling and monitoring system based on coupling environmental models and hydrological-related data, Journal of Communications, 12(6), 340-346, doi:10.12720/jcm.12.6.340-346, 2017.

20. Bhuyian, N. M., A. Kalyanapu, and F. Hossain, Evaluating conveyance-based DEM correction technique on NED and SRTM DEMs for flood impact assessment of the 2010 Cumberland river flood, Geosciences, 7(4), 132; doi:10.3390/geosciences7040132, 2017.

21. Zin, W., A. Kawasaki, W. Takeuchi, Z. M. L. T. San, K. Z. Htun, T. H. Aye, and S. Win, Flood hazard assessment of Bago river basin, Myanmar, Journal of Disaster Research, 13(1), 14-21, doi:10.20965/jdr.2018.p0014, 2018.

22. #Siregar, R. I., Hydraulic modeling of flow impact on bridge structures: a case study on Citarum bridge, IOP Conference Series: Materials Science and Engineering, 309, 012015, doi:10.1088/1757-899X/309/1/012015, 2018.

23. Lousada, S. A. N., D. Miranda, R. F. Camacho, and R. A. Castanho, Hydraulic studies and their influence for regional urban planning: a practical approach to Funchal's rivers, Revista Brasiliera de Planejamento e Desenvolvimento, 7(1), 145-164, doi:10.3895/rbpd.v7n1.7179, 2018.

24. Liu, W., and H. Liu, Integrating Monte Carlo and the hydrodynamic model for predicting extreme water levels in river systems, Preprints 2018, 2018030088, doi:10.20944/preprints201803.0088.v1, 2018.

25. #Indrawan, I., and R. I. Siregar, Analysis of flood vulnerability in urban area: a case study in Deli watershed, Journal of Physics Conference Series, 978(1), 012036, doi:10.1088/1742-6596/978/1/012036, 2018.

26. #Siregar, R. I., Land cover change impact on urban flood modeling (case study: Upper Citarum watershed), IOP Conference Series: Earth and Environmental Science, 126(1), 012027, doi:10.1088/1755-1315/126/1/012027, 2018.

27. #Ng, Z. F.., J. I. Gisen, and A. Akbari, Flood inundation modelling in the Kuantan river basin using 1D-2D flood modeller coupled with ASTER-GDEM, IOP Conference Series: Materials Science and Engineering, 318(1), 012024, doi:10.1088/1757-899X/318/1/012024, 2018.

28. Liu, Z., V. Merwade, and K. Jafarzadegan, Investigating the role of model structure and surface roughness in generating flood inundation extents using 1D and 2D hydraulic models, Journal of Flood Risk Management, doi:10.1111/jfr3.12347, 2018.

29. Kaya, C. M., G. Tayfur, and O. Gungor, Predicting flood plain inundation for natural channels having no upstream gauged stations, Journal of Water and Climate Change, doi:10.2166/wcc.2017.307, 2017.

30. Hdeib, R., C. Abdallah, F. Colin, L. Brocca, and R. Moussa, Constraining coupled hydrological-hydraulic flood model by past storm events and post-event measurements in data-sparse regions, Journal of Hydrology, 565, 160-175, doi:10.1016/j.jhydrol.2018.08.008, 2018.

31. Tan, F. J., E. J. R. Rarugal, and F. A. A. Uy, One-dimensional (1D) river analysis of a river basin in Southern Luzon Island in the Philippines using Lidar Digital Elevation Model, International Journal of Engineering & Technology, 7(3.7), 29-33, doi:10.14419/ijet.v7i3.7.16200, 2018.

32. Luo, P., D. Mu, H. Xue, T. Ngo-Duc, K. Dang-Dinh, K. Takara, D. Nover, and G. Schladow, Flood inundation assessment for the Hanoi Central Area, Vietnam under historical and extreme rainfall conditions, Scientific Reports, 8, 12623, doi:10.1038/s41598-018-30024-5, 2018.

33. Indrawan, I., and R. I. Siregar, Pemodelan Penerapan Terowongan Air (Tunnel) dalam Mengatasi Banjir Akibat Luapan Sungai Deli, Jurnal Teknik Sipil, 25(2), 113-120, doi:10.5614/jts.2018.25.2.4, 2018.

34. Petroselli, A., M. Vojtek, and J. Vojteková, Flood mapping in small ungauged basins: A comparison of different approaches for two case studies in Slovakia, Hydrology Research, doi:10.2166/nh.2018.040, 2018.

35. Agudelo-Otálora, L. M., W. D. Moscoso-Barrera, L. A. Paipa-Galeano, and C. Mesa-Sciarrotta, Comparison of physical models and artificial intelligence for prediction of flood levels, Water Technology and Sciences, 9(4), 209-236, doi:10.24850/j-tyca-2018-04-09, 2018.

36. Dysarz, T., Application of Python scripting techniques for control and automation of HEC-RAS simulations, Water, 10(10):1382, doi:10.3390/w10101382, 2018.

37. Chang, M.-J., H.-K. Chang, Y.-C. Chen, G.-F. Lin, P.-A. Chen, J.-S. Lai, and Y.-C. Tan, A support vector machine forecasting model for typhoon flood inundation mapping and early flood warning systems, Water, 10, 1734, doi:10.3390/w10121734, 2018.

38. Tscheikner-Gratl, F., V. Bellos, A. Schellart, A. Moreno-Rodenas, M. Muthusamy, J. Langeveld, F. Clemens, L. Benedetti, M.A. Rico-Ramirez, R. Fernandes de Carvalho, L. Breuer, J. Shucksmith, G.B.M. Heuvelink, and S. Tait, Recent insights on uncertainties present in integrated catchment water quality modelling, Water Research, 150, 368-379, doi:10.1016/j.watres.2018.11.079, 2019.

39. Zeleňáková, M., R. Fijko, S. Labant, E. Weiss, G. Markovič, and R. Weiss, Flood risk modelling of the Slatvinec stream in Kružlov village, Slovakia, Journal of Cleaner Production, 212, 109-118, doi:10.1016/j.jclepro.2018.12.008, 2019.

40. Wang, P., G. Zhang, and H. Leung, Improving super-resolution flood inundation mapping for multispectral remote sensing image by supplying more spectral information, IEEE Geoscience and Remote Sensing Letters, 16(5), 771-775, doi:10.1109/LGRS.2018.2882516, 2019.

41. Tehrany, M. S., S. Jones, and F. Shabani, Identifying the essential flood conditioning factors for flood prone area mapping using machine learning techniques, Catena, 175, 174-192, doi:10.1016/j.catena.2018.12.011, 2019.

42. Škarpich, V., T. Galia, S. Ruman, and Z. Máčka, Variations in bar material grain-size and hydraulic conditions of managed and re-naturalized reaches of the gravel-bed Bečva River (Czech Republic), Science of The Total Environment, 649, 672-685, doi:10.1016/j.scitotenv.2018.08.329, 2019.

43. Yang, Z., K. Yang, L. Su, and H. Hu, The multi-objective operation for cascade reservoirs using MMOSFLA with emphasis on power generation and ecological benefit, Journal of Hydroinformatics, 21(2), 257-278, doi:10.2166/hydro.2019.064, 2019.

44. Dysarz, T., J. Wicher-Dysarz, M. Sojka, and J. Jaskuła, Analysis of extreme flow uncertainty impact on size of flood hazard zones for the Wronki gauge station in the Warta river, Acta Geophysica, 67(2), 661-676, doi:10.1007/s11600-019-00264-8, 2019.

45. Fleischmann, A., R. Paiva, and W. Collischonn, Can regional to continental river hydrodynamic models be locally relevant? A cross-scale comparison, Journal of Hydrology X, 3, 100027, doi:10.1016/j.hydroa.2019.100027, 2019.

46. Gyasi-Agyei, Y., Propagation of uncertainties in interpolated rain fields to runoff errors, Hydrological Sciences Journal, 64(5), 587-606, doi:10.1080/02626667.2019.1593989. 2019.

47. Langat, P. K., L. Kumar, and R. Koech, Identification of the most suitable probability distribution models for maximum, minimum, and mean streamflow, Water, 11, 734, doi:10.3390/w11040734, 2019.

48. Papaioannou, G., A. Loukas, and L. Vasiliades, Flood risk management methodology for lakes and adjacent areas: The lake Pamvotida paradigm, Proceedings, 7, 21, doi:10.3390/ECWS-3-05825, 2019.

49. Hosseini, D., M. Torabi, and M. A. Moghadam, Preference assessment of energy and momentum equations over 2D-SKM method in compound channels, Journal of Water Resource Engineering and Management, 6(1), 24-34, 2019.

50. Oubennaceur, K., K. Chokmani, M. Nastev, Y. Gauthier, J. Poulin, M. Tanguy, S. Raymond, and R. Lhissou, New sensitivity indices of a 2D flood inundation model using Gauss quadrature sampling, Geosciences, 9(5), 220, doi:10.3390/geosciences9050220, 2019

51. Pinho, J. L. S., L. Vieira, J. M. P. Vieira, S. Venâncio, N. E. Simões, J. A. Sá Marques, and F. S. Santos, Assessing causes and associated water levels for an urban flood using hydroinformatic tools, Journal of Hydroinformatics, doi:10.2166/hydro.2019.019, 2019.

52. Saksena, S., V. Merwade, and P. J. Singhofen, Flood inundation modeling and mapping by integrating surface and subsurface hydrology with river hydrodynamics, Journal f Hydrology, 575, 1155-1177, doi:10.1016/j.jhydrol.2019.06.024, 2019

53. Fijko, R., and M., Zelenakova, Verification of the hydrodynamic model of the Slatvinec River in Kružlov, Air and Water Components of the Environment Conference Proceedings, 91-98, Cluj-Napoca, Romania, doi:10.24193/AWC2019_09, 2019

54. Luppichini, M., M. Favalli, I. Isola, L. Nannipieri, R. Giannecchini, and M. Bini, Influence of topographic resolution and accuracy on hydraulic channel flow simulations: Case study of the Versilia River (Italy), Remote Sensing, 11(13), 1630, doi:10.3390/rs11131630, 2019.

55. Liu, Z., and V. Merwade, Separation and prioritization of uncertainty sources in a raster based flood inundation model using hierarchical Bayesian model averaging, Journal of Hydrology, doi:10.1016/j.jhydrol.2019.124100, 2019

56. #Huţanu, E., A. Urzică, L. E. Paveluc, C. C. Stoleriu, and A. Grozavu, The role of hydro-technical works in diminishing flooded areas. Case study: the June 1985 flood on the Miletin River, 16th International Conference on Environmental Science and Technology, Rhodes, 2019.

57. Chen, Y.-M., C.-H. Liu, H.-J. Shih, C.-H. Chang, W.-B. Chen, Y.-C. Yu, W.-R. Su, and L.-Y. Lin, An operational forecasting system for flash floods in mountainous areas in Taiwan, Water, 11, 2100, doi:10.3390/w11102100, 2019.

58. Shustikova, I., A. Domeneghetti, J. C. Neal, P. Bates, and A. Castellarin, Comparing 2D capabilities of HEC-RAS and LISFLOOD-FP on complex topography, Hydrological Sciences Journal, doi:10.1080/02626667.2019.1671982, 2019.

59. Costabile, P., C. Costanzo, G. De Lorenzo, and F. Macchione, Is local flood hazard assessment in urban areas significantly influenced by the physical complexity of the hydrodynamic inundation model?, Journal of Hydrology, doi:10.1016/j.jhydrol.2019.124231, 2019.

60. Liu, W.-C., and H.-M. Liu, Integrating hydrodynamic model and Monte Carlo simulation for predicting extreme water levels in a river system, Terrestrial, Atmospheric & Oceanic Sciences, 30(4), 589-604, doi:10.3319/TAO.2019.01.18.01, 2019

61. Papaioannou, G., G. Varlas, G. Terti, A. Papadopoulos, A. Loukas, Y. Panagopoulos, and E. Dimitriou, Flood inundation mapping at ungauged basins using coupled hydrometeorological-hydraulic modelling: The catastrophic case of the 2006 flash flood in Volos City, Greece, Water, 11, 2328, doi:10.3390/w11112328, 2019

62. Stephens, T. A., and B. P. Bledsoe, Probabilistic mapping of flood hazards: depicting uncertainty in streamflow, land use, and geomorphic adjustment, Anthropocene, 29, 100231, doi:10.1016/j.ancene.2019.100231, 2020.

63. Papaioannou, G., C. Papadaki, and E. Dimitriou, Sensitivity of habitat hydraulic model outputs to DTM and computational mesh resolution, Ecohydrology, e2182, doi:10.1002/eco.2182, 2019.

64. Saksena, S., S. Dey, V. Merwade, and P. J. Singhofen, A computationally efficient and physically based approach for urban flood modeling using a flexible spatiotemporal structure, Water Resources Research, 56(1), e2019WR025769, doi:10.1029/2019WR025769, 2020.

65. Annis, A., F. Nardi, E. Volpi, and A. Fiori, Quantifying the relative impact of hydrological and hydraulic modelling parameterizations on uncertainty of inundation maps, Hydrological Sciences Journal, doi:10.1080/02626667.2019.1709640, 2020.

66. Syafri, R. R., M. P. Hadi, and S. Suprayogi, Hydrodynamic modelling of Juwana river flooding using HEC-RAS 2D, IOP Conference Series Earth and Environmental Science, 412, 012028, doi:10.1088/1755-1315/412/1/012028, 2020.

67. Gergeľová, M. B., Ž. Kuzevičová, S. Labant, J. Gašinec, J. Kuzevič, J. Unucka, and P. Liptai, Evaluation of selected sub-elements of spatial data quality on 3D flood event modeling: Case study of Prešov City, Slovakia, Applied Sciences, 10(3), 820, doi:10.3390/app10030820, 2020

A. Efstratiadis, **A. Tegos**, A. Varveris, and D. Koutsoyiannis, *Assessment of environmental flows under limited data availability – Case study of the Acheloos River, Greece*, Hydrological Sciences Journal, 59 (3-4), 731–750, doi:10.1080/02626667.2013.804625, 2014

Cited by:

1. Acreman, M. C., I. C. Overton, J. King, P. Wood, I. G. Cowx, M. J. Dunbar, E. Kendy, and W. Young, The changing role of ecohydrological science in guiding environmental flows, Hydrological Sciences Journal, 59(3–4), 1–18, 2014.

2. #Egüen, M., M. J. Polo, Z. Gulliver, E. Contreras, C. Aguilar, and M. A. Losada, Flood risk trends in coastal watersheds in South Spain: direct and indirect impact of river regulation, Changes in Flood Risk and Perception in Catchments and Cities, Proc. IAHS, 370, 51-56, doi:10.5194/piahs-370-51-2015, 2015.

3. Aguilar, C., and M. J. Polo, Assessing minimum environmental flows in nonpermanent rivers: The choice of thresholds, Environmental Modelling and Software, 79, 120-134, doi:10.1016/j.envsoft.2016.02.003, 2016.

4. Nerantzaki, S. D., G. V. Giannakis, N. P. Nikolaidis, I. Zacharias, G. P. Karatzas, and I. A. Sibetheros, Assessing the impact of climate change on sediment loads in a large Mediterranean watershed, Soil Science, 181(7), 306-314, 2016.

5. Poncelet, C., V. Andréassian, L. Oudin, and C. Perrin, The Quantile Solidarity approach for the parsimonious regionalization of flow duration curves, Hydrological Sciences Journal, 62(9), 1364-1380, doi:10.1080/02626667.2017.1335399, 2017.

6. Gemitzi, A., and V. Lakshmi, Evaluating renewable groundwater stress with GRACE data in Greece, Groundwater, 56(3), 501-514, doi:10.1111/gwat.12591, 2018.

7. Theodoropoulos, C., N. Skoulikidis, P. Rutschmann, and A. Stamou, Ecosystem-based environmental flow assessment in a Greek regulated river with the use of 2D hydrodynamic habitat modelling, River Research and Applications, 34(6), 538-547, doi:10.1002/rra.3284, 2018.

8. Zhao, C., S. Yang, J. Liu, C. Liu, F. Hao, Z. Wang, H. Zhang, J. Song, S. M. Mitrovic, and R. P. Lim, Linking fish tolerance to water quality criteria for the assessment of environmental flows: A practical method for streamflow regulation and pollution control, Water Research, 141, 96-108, doi:10.1016/j.watres.2018.05.025, 2018.

9. Operacz, A., A. Wałęga, A. Cupak, and B. Tomaszewska, The comparison of environmental flow assessment - The barrier for investment in Poland or river protection? Journal of Cleaner Production, 193, 575-592, doi:10.1016/j.jclepro.2018.05.098, 2018.

10. Książek, L., A. Woś, J. Florek, M. Wyrębek, D. Młyński, and A. Wałęga, Combined use of the hydraulic and hydrological methods to calculate the environmental flow: Wisloka river, Poland: case study, Environmental Monitoring and Assessment, 191:254, doi:10.1007/s10661-019-7402-7, 2019.

11. Shinozaki, Y., and N. Shirakawa, Current state of environmental flow methodologies: objectives, methods and their approaches, Journal of Japan Society of Civil Engineers – Ser. B1 (Hydraulic Engineering), 75(1), 15-30, doi:10.2208/jscejhe.75.15, 2019

D. Koutsoyiannis, N. Mamassis, and A. Tegos, *Logical and illogical exegeses of hydrometeorological phenomena in ancient Greece*, Water Science and Technology: Water Supply, 7 (1), 13–22, 2007

3-4), 731–750, doi:10.1080/02626667.2013.804625, 2014

Cited by:

1. Mays, L. W., Koutsoyiannis, D., & Angelakis, A. N. (2007). A brief history of urban water supply in antiquity. Water Science and Technology: Water Supply, 7(1), 1-12.

2. Koutsoyiannis, D. (2013). Hydrology and change. Hydrological Sciences Journal, 58(6), 1177-1197.

3. Mays, L. W. (2008). A very brief history of hydraulic technology during antiquity. Environmental Fluid Mechanics, 8(5-6), 471-484.

4. Koutsoyiannis, D. (2014). Reconciling hydrology with engineering. Hydrology Research, 45(1), 2-22.

5. Angelakis, A. N., & Spyridakis, D. S. (2010). A brief history of water supply and wastewater management in ancient Greece. Water Science and Technology: Water Supply, 10(4), 618-628.

6. Koutsoyiannis, D. (2007). A critical review of probability of extreme rainfall: principles and models. In Advances in Urban Flood Management (pp. 151-178). CRC Press.

7. Koutsoyiannis, D., Mamassis, N., Efstratiadis, A., Zarkadoulas, N., & Markonis, I. (2012). floods in Greece. Changes of flood risk in Europe, 238-256.

8. Koutsoyiannis, D., Kundzewicz, Z. W., Watkins, F., & Gardner, C. (2010). Something old, something new, something red, something blue.

9. Mamassis, N., & Koutsoyiannis, D. (2010). A web based information system for the inspection of the hydraulic works in Ancient Greece. In Ancient Water Technologies (pp. 103-114). Springer, Dordrecht.

10. Podimata, M. V., & Yannopoulos, P. C. (2015). Game theory application to reframe river myths. International Journal of Global Environmental Issues, 14(3-4), 238-255.

11. Angelakis, A. N., Dialynas, E. G., & Despotakis, V. (2012). Evolution of water supply technologies through the centuries in Crete, Greece. Evolution of Water Supply through the Millennia, 226-58.

Conference publications or book chapters with full evaluation

1. Ph.D related

Tegos, A. Efstratiadis, and D. Koutsoyiannis, *A parametric model for potential evapotranspiration estimation based on a simplified formulation of the Penman-Monteith equation*, Evapotranspiration - An Overview, edited by S. Alexandris, 143–165, doi:10.5772/52927, InTech, 2013.

Cited by:

1. Samaras, D. A., A. Reif and K. Theodoropoulos, Evaluation of radiation-based reference evapotranspiration models under different Mediterranean climates in Central Greece, Water Resources Management, 28 (1), 207-225, 2014.
2. Tabari, H., P. H. Talaee, P. Willems, and C. Martinez, Validation and calibration of solar radiation equations for estimating daily reference evapotranspiration at cool semi-arid and arid locations, Hydrological Sciences Journal, 61(3), 610-619, doi:10.1080/02626667.2014.947293, 2016.
3. Jaber, H. S., S. Mansor, B. Pradhan, and N. Ahmad, Evaluation of SEBAL model for evapotranspiration mapping in Iraq using remote sensing and GIS, International Journal of Applied Engineering Research, 11(6), 3950-3955, 2016.
4. Kumar, D., J. Adamowski, R. Suresh, and B. Ozga-Zielinski, Estimating evapotranspiration using an extreme learning machine model: case study in North Bihar, India, Journal of Irrigation and Drainage Engineering, 04016032, doi:10.1061/(ASCE)IR.1943-4774.0001044, 2016.
5. Djaman, K., D. Rudnick, V. C. Mel, and D. Mutiibwa, Evaluation of Valiantzas' simplified forms of the FAO-56 Penman-Monteith reference evapotranspiration model in a humid climate, Journal of Irrigation and Drainage Engineering, doi:10.1061/(ASCE)IR.1943-4774.0001191, 2017.
6. Norström, E., C. Katrantsiotis, R. H. Smittenberg, and K. Kouli, Chemotaxonomy in some Mediterranean plants and implications for fossil biomarker records, Geochimica et Cosmochimica Acta, 219, 96-110, doi:10.1016/j.gca.2017.09.029, 2017.
7. Hodam, S., S. Sarkar, A.G.R. Marak, A. Bandyopadhyay, and A. Bhadra, Spatial interpolation of reference evapotranspiration in India: Comparison of IDW and Kriging methods, Journal of The Institution of Engineers (India): Series A, doi:10.1007/s40030-017-0241-z, 2017.
8. Mentzafou, A., S. Wagner, and E. Dimitriou, Historical trends and the long-term changes of the hydrological cycle components in a Mediterranean river basin, Science of The Total Environment, 636, 558-568, doi:10.1016/j.scitotenv.2018.04.298, 2018.
9. Norström, E., C. Katrantsiotis, M. Finné, J. Risberg, R. H. Smittenberg, S. Bjursäter, Biomarker hydrogen isotope composition (δD) as proxy for Holocene hydroclimatic change and seismic activity in SW Peloponnese, Greece, Journal of Quaternary Science, 33(5), 563-574, doi:10.1002/jqs.3036, 2018.
10. Mengistu, B., and G. Amente, Three methods of estimating the power of maximum temperature in TM–ET estimation equation, SN Applied Sciences, 1:1403, doi:10.1007/s42452-019-1461-9, 2019
11. Mengistu, B., and G. Amente, Reformulating and testing Temesgen-Melesse's temperature-based evapotranspiration estimation method, Heliyon, 6(1), e02954, doi:10.1016/j.heliyon.2019.e02954, 2020

2. Other publications

Conference publications with evaluation of abstract

1. Ph.D related

N. Malamos, **A. Tegos**, I. L. Tsirogiannis, A. Christofides, and D. Koutsoyiannis, *Implementation of a regional parametric model for potential evapotranspiration assessment*, IrriMed 2015 – Modern technologies, strategies and tools for sustainable irrigation management and governance in Mediterranean agriculture, Bari, doi:10.13140/RG.2.1.3992.0725, 2015

A. Tegos, A. Efstratiadis, N. Malamos, N. Mamassis, and D. Koutsoyiannis, *Evaluation of a parametric approach for estimating potential evapotranspiration across different climates*, IRLA2014 – The Effects of Irrigation and Drainage on Rural and Urban Landscapes, Patras, doi:10.13140/RG.2.2.14004.24966, 2014.

N. Bountas, N. Boboti, E. Feloni, L. Zeikos, Y. Markonis, **A. Tegos**, N. Mamassis, and D. Koutsoyiannis, *Temperature variability over Greece: Links between space and time*, Facets of Uncertainty: 5th EGU Leonardo Conference – Hydrofractals 2013 – STAHY 2013, Kos Island, Greece, doi:10.13140/RG.2.2.17739.80164, European Geosciences Union, International Association of Hydrological Sciences, International Union of Geodesy and Geophysics, 2013

Cited by:

1. Kalamaras, N., Tzanis, C. G., Deligiorgi, D., Philippopoulos, K., & Koutsogiannis, I. (2019). Distribution of Air Temperature Multifractal Characteristics Over Greece. Atmosphere, 10(2), 45.
2. Philippopoulos, K., Kalamaras, N., Tzanis, C. G., Deligiorgi, D., & Koutsogiannis, I. (2019). Multifractal Detrended Fluctuation Analysis of Temperature Reanalysis Data over Greece. Atmosphere, 10(6), 336.

A. Tegos, N. Mamassis, and D. Koutsoyiannis, *Estimation of potential evapotranspiration with minimal data dependence*, European Geosciences Union General Assembly 2009, Geophysical Research Abstracts, Vol. 11, Vienna, 1937, doi:10.13140/RG.2.2.27222.86089, European Geosciences Union, 2009

Cited by:

1. Tabari, H., Hosseinzadehtalaei, P., Willems, P., & Martinez, C. (2016). Validation and calibration of solar radiation equations for estimating daily reference evapotranspiration at cool semi-arid and arid locations. Hydrological Sciences Journal, 61(3), 610-619.

2. Other publications

Koukouvinos, D. Nikolopoulos, A. Efstratiadis, **A. Tegos**, E. Rozos, S.M. Papalexiou, P. Dimitriadis, Y. Markonis, P. Kossieris, H. Tyralis, G. Karakatsanis, K. Tzouka, A. Christofides, G. Karavokiros, A. Siskos, N. Mamassis, and D. Koutsoyiannis, *Integrated water and renewable energy management: the Acheloos-Peneios region case study*, European Geosciences Union General Assembly 2015, Geophysical Research Abstracts, Vol. 17, Vienna, EGU2015-4912, doi:10.13140/RG.2.2.17726.69440, European Geosciences Union, 2015

Cited by:

1. Stamou, A. T., and P. Rutschmann, Pareto optimization of water resources using the nexus approach, Water Resources Management, doi:10.1007/s11269-018-2127-x, 2018

Efstratiadis, A. Koukouvinos, P. Dimitriadis, **A. Tegos**, N. Mamassis, and D. Koutsoyiannis, *A stochastic simulation framework for flood engineering*, Facets of Uncertainty: 5th EGU Leonardo Conference – Hydrofractals 2013 – STAHY 2013, Kos Island, Greece, doi:10.13140/RG.2.2.16848.51201, European Geosciences Union, International Association of Hydrological Sciences, International Union of Geodesy and Geophysics, 2013

V. Pagana, **A. Tegos**, P. Dimitriadis, A. Koukouvinos, P. Panagopoulos, and N. Mamassis, *Alternative methods in floodplain hydraulic simulation - Experiences and perspectives*, European Geosciences Union General Assembly 2013, Geophysical Research Abstracts, Vol. 15, Vienna, EGU2013-10283-2, European Geosciences Union, 2013.

Cited by:

1. #Μίχας, Σ. Ν., Κ. Ι. Νικολάου, Σ. Λ. Λαζαρίδου, και Μ. Ν. Πικούνης, Σύγκριση μαθηματικών ομοιωμάτων διόδευσης πλημμυρικού κύματος από υποθετική θραύσης φράγματος Αγιόκαμπου, Πρακτικά 2ου Πανελλήνιου Συνεδρίου Φραγμάτων και Ταμιευτήρων, Αθήνα, Αίγλη Ζαππείου, Ελληνική Επιτροπή Μεγάλων Φραγμάτων, 2013.

A. Oikonomou, P. Dimitriadis, A. Koukouvinos, **A. Tegos**, V. Pagana, P. Panagopoulos, N. Mamassis, and D. Koutsoyiannis, *Floodplain mapping via 1D and quasi-2D numerical models in the valley of Thessaly*, Greece, European Geosciences Union General Assembly 2013, Geophysical Research Abstracts, Vol. 15, Vienna, EGU2013-10366, doi:10.13140/RG.2.2.25165.03040, European Geosciences Union, 2013.

Cited by:

1. #Μίχας, Σ. Ν., Κ. Ι. Νικολάου, Σ. Λ. Λαζαρίδου, και Μ. Ν. Πικούνης, Σύγκριση μαθηματικών ομοιωμάτων διόδευσης πλημμυρικού κύματος από υποθετική θραύσης φράγματος Αγιόκαμπου, Πρακτικά 2ου Πανελλήνιου Συνεδρίου Φραγμάτων και Ταμιευτήρων, Αθήνα, Αίγλη Ζαππείου, Ελληνική Επιτροπή Μεγάλων Φραγμάτων, 2013.

A. Varveris, P. Panagopoulos, K. Triantafillou, **A. Tegos**, A. Efstratiadis, N. Mamassis, and D. Koutsoyiannis, *Assessment of environmental flows of Acheloos Delta*, European Geosciences Union General Assembly 2010, Geophysical Research Abstracts, Vol. 12, Vienna, 12046, doi:10.13140/RG.2.2.14849.66404, European Geosciences Union, 2010

Cited by:

1. #Fourniotis, N. T., M. Stavropoulou-Gatsi and I. K. Kalavrouziotis, Acheloos River: The timeless, and since ancient period, contribution to the development and environmental upgrading of Western Greece, Proceedings 3rd IWA Specialized Conference on Water & Wastewater Technologies in Ancient Civilizations, Istanbul-Turkey, 420-428, 2012.
2. Fourniotis, N. T., A proposal for impact evaluation of the diversion of the Acheloos River on the Acheloos estuary in Western Greece, International Journal of Engineering Science and Technology, 4(4), 1792-1802, 2012.

A. Efstratiadis, **A. Tegos**, I. Nalbantis, E. Rozos, A. Koukouvinos, N. Mamassis, S.M. Papalexiou, and D. Koutsoyiannis, *Hydrogeios, an integrated model for simulating complex hydrographic networks - A case study to West Thessaly region*, 7th Plinius Conference on Mediterranean Storms, Rethymnon, Crete, doi:10.13140/RG.2.2.25781.06881, European Geosciences Union, 2005